12-2018

HEME PEROXIDASE HPX-2 PROTECTS CAENORHABDITIS ELEGANS FROM PATHOGENS

Yi Liu

HEME PEROXIDASE HPX-2 PROTECTS *CAENORHABDITIS ELEGANS* FROM PATHOGENS

By

Yi Liu, M.S.

APPROVED:

_____

Danielle A. Garsin, Ph.D.

Advisory Professor,

_____

Ambro van Hoof, Ph.D.

_____

Swathi Arur, Ph.D.

_____

Hung Ton-that, Ph.D.

_____

Kevin Morano, Ph.D.

APPROVED:

_____

Dean, The University of Texas

MD Anderson Cancer Center UTHealth Graduate School of Biomedical Sciences

HEME PEROXIDASE HPX-2 PROTECTS *CAENORHABDITIS ELEGANS* FROM PATHOGENS

A

DISSERTATION

Presented to the Faculty of

The University of Texas

MD Anderson Cancer Center UTHealth

Graduate School of Biomedical Science

In Partial Fulfillment

of the Requirements

for the Degree of

DOCTOR OF PHILOSOPHY

by

Yi Liu, M.S.
Houston, Texas

December 2018

Dedication

To the memory of my father, Tiehui Liu, who always believed in me.

Acknowledgments

First, I would like to express my sincere gratitude to my mentor, Dr. Danielle Garsin, for her complete support and guidance. Dr. Garsin is most patient and sympathetic mentor I have ever had. She gave me the freedom and flexibility to explore my projects and offered tremendous help when needed. Her passion for science and her kindness for her trainees have inspired me to a become a better person not only in the scientific area but also in everyday life. I am lucky to be her student.

Second, I want to thank my advisory committee members, Drs. Kevin Morano, Ambro van Hoof, Hung ton-that, and Swathi Arur, for their guidance and feedback that helped me navigate through my project. I would especially like to thank Dr. Ambro van Hoof for his guidance and valuable insight for my RNAseq project. I would also like to thank Dr. David Reiner and his lab for their expert advice in worm biology.

Next, I would like to thank my current and past members of the Garsin Lab for their help and support. Specifically, Ms. Melissa Cruz, Dr. Karan Kaval and Dr. Ozgur Karakuzu for their help on my project. Dr. Clara Sinel for being a great lunch buddy and a good friend that always listens. Dr. Carrie Graham for the best companionship through the ups and downs during the graduate life. They have made the lab an amazingly collaborative and fun space to work in, an environment I will surely miss.

Last but not least, I would like to thank my family: my father, whose work ethic inspired me to push forward; my mother who raised me as an independent woman and provided me with unconditional support for all the decisions I have made throughout life; and my beloved husband and best friend, Ernie Lai, for his encouragement and comfort during difficult times. I could not complete this journey without them.

Heme Peroxidase HPX-2 Protects *Caenorhabditis elegans* from Pathogens

Yi Liu, M.S.

Advisory Professor: Danielle A. Garsin, Ph.D.

Heme-containing peroxidases are important components of innate immunity. Many of them functionally associate with NADPH oxidase (NOX)/dual oxidase (DUOX) enzymes by using the hydrogen peroxide they generate in downstream reactions. In *Caenorhabditis elegans,* a ShkT-containing peroxidase, SKPO-1, and the dual oxidase, BLI-3, contribute to resistance against the human pathogen *Enterococcus faecalis,* likely functioning in conjunction with each other. However, the exact mechanism(s) by which peroxidases and NOX/DUOXs contribute to pathogen resistance remain unclear. Here, we demonstrated that another peroxidase, HPX-2 (**H**eme-**P**ero**X**idase 2), is required for resistance against some, but not all pathogens. Tissue specific RNA interference (RNAi) revealed that HPX-2 functionally localizes to the hypodermis of the worm. In congruence with this observation, *hpx-2* mutant animals possessed a slightly weaker cuticle structure, indicated by higher permeability to a DNA dye, but exhibited no obvious morphological defects. In addition, fluorescent labeling of HPX-2 revealed its expression in the pharynx, an organ in which BLI-3 also resides. Interestingly, loss of HPX-2 increased intestinal colonization of *E. faecalis,* suggesting its role in the pharynx may limit intestinal colonization. Moreover, disruption of a catalytic residue in the peroxidase domain of HPX-2 resulted in decreased survival on *E. faecalis*, indicating its peroxidase activity is required for pathogen resistance. Finally, RNA-seq analysis of an *hpx-2* mutant revealed changes in genes encoding for cuticle structural components under the non-pathogenic conditions. Under pathogenic conditions, genes involved in infection response were differentially regulated to a greater degree, likely due to increased microbial burden. In conclusion, the characterization of

the heme-peroxidase, HPX-2, revealed that it contributes to *C. elegans* pathogen resistance through a role in generating cuticle material in the hypodermis and pharynx.

Table of contents

List of Figures

List of Tables

Chapter 1: Introduction

ROS in innate immunity

Reactive Oxygen Species (ROS) production is one of the first responses from host cells when infection occurs. After successful pathogen recognition, superoxide (O_2^-) and/or its dismutase product hydrogen peroxide (H_2O_2) are generated for two major purposes: 1) to serve as signal molecules and activate downstream immune factors and 2) to generate the oxidative burst and directly eliminate pathogens.

ROS as immune signals

The function of ROS as an indirect signal for activation of the immune response has been demonstrated in multiple organisms. In plants, ROS were shown to be involved in the hyper-sensitive response (HR) - a form of programmed cell death (PCD) in multiple species including *Arabidopsis thaliana*, *Glycine max* (soybean), and *Nicotiana tobacum* (tobacco) (1-4). Upon activation of the HR, ROS are produced by the plant NADPH oxidase respiratory burst oxidase homologue (RBOH) and glycolate oxidase (GOX) (1-4). ROBH generates O_2^- that can be converted into H_2O_2 by superoxide dismutase, whereas GOX directly produces H_2O_2 from the glyoxylate reaction. Once the level of H_2O_2 reaches the 6 mM threshold in the infected cells, HR-mediated PCD is triggered in a calcium-mediated fashion, resulting in the death of the infected cells and preventing the spread of the pathogen (3-5). In other instances, ROS associate with salicylic acid (SA), a plant signaling molecule involved in the defense response, to trigger the systematic acquired resistance (SAR) (6).

In *Drosophila melanogaster*, ROS play an important role as signal molecules for gut-to-fat body innate immune communication (7). Specifically, intestinal infection by enterobacteria *Erwinia carotovora carotovora 15* (Ecc15) in Drosophila larva results in localized ROS production in the intestine, which then induces nitric oxide (NO) production. The elevated NO level in the intestine triggers a global immune response in the fat body, a major immune organ

in insects, resulting in the production of an anti-microbial peptide (AMP) called diptericin. This process ensures the systematic control and confinement of the pathogen to the intestine (7, 8).

In zebrafish, ROS, specifically H_2O_2, serve as signal molecules for recruiting leukocytes to the wounded sites (9). Using a genetically encoded H_2O_2 reporter, it was shown that an increasing concentration gradient of H_2O_2 from the injured fish tail fin to the nearby areas leads to the rapid recruitment of leukocytes to the injured site (9). This process requires a dual oxidase (DUOX) and DUOX inhibition disrupts the gradient, abolishing leukocyte recruitment (9).

In humans, the signaling function of ROS was first illustrated through the discovery that micromolar concentrations of H_2O_2 activate the NF-κB transcription factor in T cells (10). More recently, it has been demonstrated that H_2O_2 produced by DUOX2 is involved in NOD2-dependent signal transduction resulting in protection against *Listeria monocytogenes* infection in epithelial cells (11).

ROS as antimicrobial effectors

Next, I will discuss how ROS serve as a direct antimicrobial reagent during infection with an emphasis on mammalian systems. While O_2^- and H_2O_2 are not considered strong microbicidal reagents, they can be converted into other oxidants that exhibit stronger antimicrobial activity. Peroxidases are the enzymes that carry out such reactions. A canonical example is the oxidative burst in macrophages and neutrophils, generated by formation of the potent bacterial cytotoxin hypochlorous acid (HOCl). Specifically, when bacteria are engulfed by neutrophils, H_2O_2 produced by an NADPH oxidase (NOX2, specifically, see next section) is subsequently converted into HOCl through a reaction with chloride ion catalyzed by myeloperoxidase (MPO) (reviewed in (12). HOCl generated in the phagolysome modifies tyrosine residues in the bacterial protein, forming 3-chlorotyrosine which serves as a marker for

bacterial killing (13, 14). Mutations in the NADPH oxidase or MPO results in decreased amounts of 3-chlorotyrosine bound bacterial protein and insufficient microbial clearance (12, 14).

Another example of ROS serving as direct effectors for pathogen elimination is the generation of the potent antimicrobial anion hypothiocyanite ($OSCN^-$) through the oxidation of thiocyanate (SCN^-) by lactoperoxidase (LPO) using H_2O_2 produced by dual oxidase (DUOX) as a substrate (15-18). During *Pseudomonas aeruginosa* infection of bronchial epithelial cells, the levels of H_2O_2 and subsequently $OSCN^-$ are increased, contributing to increased pathogen clearance (19). In addition to *P. aeruginosa* clearance, $OSCN^-$ is also involved in *Staphylococcus aureus* and *Burkholderia cepacia* clearance (19, 20). Disruption of the DUOX-LPO-SCN^- system would lead to a decrease in pathogen clearance efficiency. For example, inhibition of LPO activity leads to decreased pathogen clearance in sheep airways (15). Additionally, cystic fibrosis (CF) patients with mutated CF transmembrane conductance regulator (CFTR), which causes impaired transport of SCN^- to the apical membrane and decreased production of $OSCN^-$, cannot efficiently clear *P. aeruginosa* and *S. aureus* from their airways (19, 20).

NADPH Oxidases (NOXs), Dual Oxidases (DUOXs), and Peroxidases

As mentioned before, ROS serve as both signal molecules and microbicidal effectors in response to infection. NADPH oxidase (NOX) and dual oxidase (DUOX) produce ROS in the form of superoxide (O_2^-) and H_2O_2 whereas peroxidases can utilize the H_2O_2 to carry out further reactions such as generating a more potent anti-microbial oxidant.

NOX and DUOX

Five NOX (NOX1-5) and two DUOX (DUOX1 and 2) enzymes have been identified in mammalian cells (21). NOXs are transmembrane proteins that harbor the NADPH domain and flavin adenine dinucleotide (FAD)-binding domain, six transmembrane domains, and four evolutionally conserved histidine residues for heme-binding and catalytic activity (21). Expressed at different tissue/cellular locations, NOX/DUOX family members produce either superoxide or hydrogen peroxide that function in a variety of cellular processes including protein modification, redox signaling, apoptosis, and host defense (Table 1.1) (21, 22) (23). NOX2, or phagocytic NOX, was the first member discovered in the NOX/DUOX family and was characterized as generating the oxidative burst in macrophages and neutrophils for host defense (24). Mutations in NOX2 cause Chronic Granulomatous Diseases (CGD) with significant increased susceptibility to a variety of pathogen infections (24).

NOX/DUOX	Location	Function
NOX1	Colon	Host defense
NOX2 (phagocytic NOX)	Phagolysome of macrophage and neutrophil	Oxidative burst for host defense
NOX3	Inner ear	Otoconia morphogenesis
NOX4	Kidney, vascular cells, osteoclasts	unclear
NOX5	Lymphoid tissue and testis	Signaling process
DUOX1	Thyroid and respiratory epithelia	Thyroid hormone synthesis and epithelia host defense
DUOX2	Thyroid and gastrointestinal glandular epithelia	Thyroid hormone synthesis and epithelia host defense

Table 1.1 Localization and function of mammalian NOX/DUOX family. This table is a summary of a mini-review listed in the reference as (25).

DUOXs are structurally different from NOXs in that they possess an extracellular peroxidase-like domain at their N-terminus. Functionally, instead of producing O_2^-, DUOXs produce H_2O_2 through oxidation reactions. In addition to host defense function in mammals, DUOXs also play an important role in the stabilization of the extracellular matrix by crosslinking tyrosine in multiple organisms including Drosophila and *Anopheles gambiae* (26, 27).

In *C. elegans,* the only functional NOX/DUOX is BLI-3 (also known as Ce-DUOX1) was characterized for its role in maintaining extracellular matrix integrity, protecting worms from infection, and regulating the oxidative response. Similar to human DUOX1 and DUOX2, BLI-3 possesses a highly conserved NADPH and FAD binding domain at its C-terminus and an extracellular peroxidase domain at the N-terminus (28). Functionally, both its NADPH oxidase and peroxidase activity are important for cuticle crosslinking (28, 29). Cuticle is the collagenous extra cellular matrix that serves as the exoskeleton of the worm, providing structure and protection from the environment (30). RNAi knockdown of BLI-3 or mutations in either domain result in severe cuticle blistering due to the insufficient di- and tri- tyrosine crosslinking of collagen proteins (29). A heme peroxidase, MLT-7, is also involved in the tyrosine cross-linking process, presumably by utilizing the H_2O_2 generated by the BLI-3 NOX domain as a co-substrate (29). In addition to cuticle crosslinking, BLI-3 is also involved in pathogen resistance and the response to oxidative stress through the p38 MAPK and insulin signaling pathways (see the last section in this chapter for more detail).

Given the function of BLI-3 in cuticle cross-linking, innate immunity, and oxidative stress response, multiple internal and external signals can activate its expression and activity. The expression of BLI-3 peaks during the molting cycle, corresponding to cuticle biosynthesis. Additionally, environmental stress such as pathogen infection and oxidative stress stimulate its activity, resulting in an increased amount of ROS.

Peroxidases

Heme peroxidases catalyze a variety of oxidative reactions by utilizing H_2O_2 as an electron acceptor and heme as redox cofactor. The four families of peroxidases are 1) the catalase superfamily, aka bacterial, fungi, and plant peroxidase superfamily 2) the cyclooxygenase superfamily, aka animal peroxidase superfamily (although members of the this group include non-animal species) 3) the chlorite dismutase superfamily and (4) the peroxygenase superfamily (32). All the mammalian peroxidases belong to the cyclooxygenase super family (32). Some well-studied examples include eosinophil peroxidase (EPO), thyroid peroxidase (TPO), and previously mentioned MPO and LPO. Their differential expression, location and function are listed in Table 1.2.

Peroxidases in the cyclooxygenase family shares two conserved sequence signatures: -X-G-**Q**-X-X-**D**-**H**-**D**-X- and -X-**R**-X-X-**E**-X- (32). The first sequence is characterized by the distal catalytic histidine and two aspartates that are involved in heme-binding. The second conserved sequence includes a highly conserved catalytic arginine residue followed by a glutamate that is involved in forming an ester bond with heme (32). In human MPO, the crucial catalytic residues are Gln257, His261, and Arg405, with the function of forming the binding pockets for H_2O_2 (33). The latter two residues (His 261 and Arg 405) are also shown to be conserved in plant and yeast peroxidases (34, 35). In *C. elegans*, the distal histidine and arginine are present in all the peroxidases identified including MLT-7, SKPO-1, and HPX-2. The only exception is the peroxidase domain of the DUOX BLI-3, where the distal histidine has been replaced by a tyrosine residue (Tyr106) (Figure 4.9), which is believed to cause its slower turnover rate compared to other mammalian peroxidases (36). Functionally, mammalian heme peroxidases are capable of oxidizing small aromatic substrates as well as iodide (I-), thiocyanate (SCN^-), and bromide (Br^-), giving rise to their various functions in protein modification and generation of antimicrobial substances (33).

Peroxidase	Location	Function
MPO	Neutrophils and macrophages	Oxidative burst for host defense
LPO	Leukocytes in milk, tears, and saliva	Bactericidal compound production
EPO	Eosinophils	Bactericidal compound production
TPO	Thyroid gland	Thyroid hormone production

Table 1.2 Localization and function of some of the mammalian peroxidases. This table is a summary of a review listed in the reference as (33).

Mitochondrial ROS

In addition to NOX/DUOX enzymes, mitochondria are also a major source of ROS (mtROS). As a crucial cellular organelle, the most prominent function of mitochondrion is to generate ATP by a serious of oxidation reactions in the electron transport chain. mtROS are produced as a major by-product during the process. Although traditionally mtROS are viewed as destructive molecules that cause a variety types of cell damage, they are also involved in various metabolic and innate immunity signaling pathways that are beneficial and homeostatic (37, 38). Similar to the NADPH derived ROS, mtROS can function as a direct source of antimicrobial oxidants or as a signal to regulate innate immune responses in mammals (39). In *C. elegans*, although mtROS have been shown to function in promoting hypodermal wound healing and longevity under stress conditions, their roles in innate immunity have not been characterized (40, 41).

Complex I, the largest complex of the respiratory chain, is the major source of mtROS (39). During a bacterial infection, mtROS production is stimulated and mitochondria are directed towards newly formed phagosomes to join forces with NADPH-derived ROS for the bacteria eliminating oxidative burst (39). This process is regulated by multiple pathways starting from Pathogen Associated Molecular Pattern (PAMP) recognition by host cells. Upon successful recognition of pathogenic microbes, four distinct and partially overlapping signaling pathways are activated, resulting in: 1) NADPH oxidase activation and increased ROS production in the phagosome, 2) Proinflammatory cytokine production, 3) Release of the ubiquitin ligase TRAF6 from Rac-GDP which promotes TRAF6-ECSIT compound formation, and 4) Serine-threonine kinases Mst1/2 activation. These four pathways all have positive roles in reducing the oxidative phosphorylation in Complex I and increasing mtROS formation (42-44). Additionally, the TRAF6-ECSIT and Mst1/Mst2 pathways contribute to the movement of ROS-enriched

mitochondria towards the phagosome through the activation of F-actin assembly by the production of Rac-GTP (45, 46).

C. elegans as an infection model

C. elegans pathogens

C. elegans is a classic model organism in which fundamental biological processes, such as development and aging, have been studied since the 1970s (47-49). Only in the past two decades has it become a popular model for infectious diseases. Its simplified immune system and well-characterized biology make it ideal to study host-microbe interactions. As of today, a large number of pathogens, including fungi, bacteria, and even viruses of clinical relevance, have been demonstrated to effectively infect *C. elegans* (50). Generally speaking, there are two major modes by which microbes harm *C. elegans*: (1) secretion of toxins and (2) colonization and physical disruption of the worm body. These two mechanisms of causing disease in the worm apply to many pathogens, sometimes in a non-mutually exclusive way. In terms of the site of infection, the intestinal lumen and the hypodermis are the two major locations where infection starts. In this section, I will discuss some of the fungal and bacterial pathogens for which *C. elegans* is utilized as an infection model.

One of the well characterized fungal pathogens is *Candida albicans*, an opportunistic pathogen that can also be found as a commensal of the human microbiome. *C. albicans* can colonize the intestine of the worms, causing distal intestinal distention (51). Unlike live *C. albicans*, heat-killed *C. albicans* were avirulent, suggesting the pathogenesis is not mediated by toxins (51) . In contrast to *C. albicans*, another fungal pathogen, *Cryptococcus neoformans,* kills *C. elegans* independently of whether the microbe is alive, indicating that the mode of killing is through the production of toxin (52, 53) . In addition to intestinal colonization, some fungal species infect the worms through the cuticle. One example is *Drechmeria conisopora*, a natural pathogen of *C. elegans*. It utilizes its conidia to adhere to the head and vulva of the worm, then invades the worm body by penetrating the cuticle around the head and through the natural orifice around the vulva (54).

Pseudomonas aeruginosa is probably the most studied bacterial pathogen in *C. elegans* and indeed was the first pathogen ever reported to infect! Depending on the culture media conditions, *P. aeruginosa* utilizes either toxin-mediated killing or colonization of the intestine to kill *C. elegans* (55, 56). “Fast-killing” occurs when *P. aeruginosa* is grown under nutrient rich and high osmolarity conditions in which the bacteria secrete various toxins to mediate killing of the worms in a matter of hours. On the other hand, “slow-killing” is when bacteria are grown on minimal media, colonize the intestine, and kill the worms over the course of a few days. Slow-killing requires live bacteria whereas fast-killing does not. *P. aeruginosa* is not the only bacteria that secretes toxins/effectors that kill *C. elegans.* Many other bacteria have similar mechanisms of killing, although the effectors they produce varies. Some of the other toxin producing bacteria include *E. coli* EHEC (Shiga toxin) (57), *Baccillus thuringiensis* (pore-forming crystal protein) (58), *Staphylococcus aureus* (α-hemolysin) (59), and many Streptococcus species including *S. pyogenes* (hydrogen peroxide) (60).

Enterococcus faecalis is another important human pathogen that can be found in the gut flora of healthy individuals. This Gram-positive bacterium can cause a variety of diseases in immune compromised patients and is a leading cause of nosocomial infection. *E. faecalis* kills *C. elegans* by intestinal colonization and propagation with an LT_{50} of about 4 days (61). Transmission electron microscopy (TEM) revealed actively dividing bacteria in the intestine (72). *E. faecalis* also prevents *C. elegans* from propagating, although adults will lay eggs onto the bacteria lawn; none develop into adults. Consistent with other animal models, mutations in the major quorum sensing regulatory system, *fsr,* or in two extracellular protease encoding genes, *gelE* and/or *sprE*, attenuate killing (62, 63). In addition, production of cytolysin, a toxin that can lyse host cells, significantly increased the rate of killing (62, 64).

Kingdoms	Pathogens	Infection and Pathogenic Mode	Host Pathway and Response	References
Bacteria	*P. aeruginosa*	Feeding; slow killing by colonization; fast killing by toxin	PMK-1, ZIP-2, FSHR-1 dependent pathways	(55) (65, 66) (67)
	S. enterica	Feeding; killing by colonization; LPS as virulence factor	PMK-1-dependant programed cell death pathway	(68)
	S. aureus	Feeding, α-hemolysin as virulence factor	SEK-1 and NSY-1 dependent p38 MAP kinase pathway and TFEB mediated transcriptional response	(59, 69)
	C. diphtheriae	Feeding, diphtheriae toxin and pili as virulence factor	Not analyzed	(70)
	E. faecalis	Feeding, killing by colonization	p38 MAP kinase pathway	(62, 71)
	E. coli (EHEC)	Feeding, killing by colonization and toxins		
	S. pyogenes	Feeding; colonization; hydrogen peroxide as virulence factor	Not analyzed	(60)
Fungi	*C. albicans*	Feeding; colonization	PMK-1/p-38 MAPK pathways	(51)
	C. neoformans	Feeding; colonization; laccase; polysaccharide capsule and/or melanization as virulence factors	CED-1, C03F11.3 and ABL-1 dependent pathways	(52, 53)
	Drechmeria coinospora	Attachment and penetration through cuticle		(54)

Table 1.3 *C. elegans* pathogens. This table was adapted and modified from a previous publication and the article is listed for reference (50).

C. elegans innate immunity

Generally speaking, the Innate immune process consists of three steps: 1) Pathogen recognition by host receptors; 2) Signal transduction through phosphorylation and transcriptional regulation and 3) Production of effectors that achieve immunity. In this section, I will briefly discuss current knowledge of the components of the each of these steps.

Pathogen recognition

During microbial infection on start, host sense the infection through two major mechanisms: through the recognition of pathogen associated molecular patterns (PAMPs) (73), or though damage associated molecular patterns (DAMPs) (74, 75).

In C. elegans, the PAMP-associated pathogen recognition pathway has not been well defined, largely due to the lack of conserved pattern recognition receptor(s) (PRR) being identified in the *C. elegans* genome. The only Toll-like Receptor homologue, TOL-1, in *C. elegans* is not involved in direct pathogen recognition (76). In addition*, C. elegans* lacks the peptidoglycan receptors or the NOD-like receptors (77). However, studies have shown that both live and heat-killed pathogens, i.e. *C. albicans* and *E. faecium,* induced similar immune responses in *C. elegans*, suggesting there are mechanisms to recognize pathogen-associated patterns (78, 79). In the search for immune receptors, one candidate identified was the G protein-coupled receptor FSHR-1 (66). FSHR-1 is a surface protein containing evolutionary conserved extracellular leucine-rich repeat (LRR) domain that is present in many other pathogen receptors in animals and plants (66). However, it is unclear whether FSHR-1 directly recognizes infection and its pathogen ligand is yet to be identified (66, 80).

In addition to direct PAMP-recognizing mechanisms, *C. elegans* can also recognize pathogen induced damage and activate downstream immune responses. Examples include epidermis and cuticle disruption by physical force, causing activation of the PMK-1 pathway,

similar to epidermal fungal infection (81, 82), and pore-forming toxins causing activation of the PMK-1 pathway in the intestine (83). More recently, a G protein-coupled receptor (GPCR), DCAR-1, was identified as a potential sensor for fungal infection and cuticle defects (84). The endogenous ligand of DCAR-1 is thought to be the 4-hydroxyphenyllactic acid (HPLA), a tyrosine derivative that has increased presence during infection and cuticle alteration (84).

Signal transduction

In contrast with the uncertainty and speculation in the pathogen recognition research areas, signal transduction pathways in *C. elegans* are much more well-defined. Two major signaling pathways, the p38 MAPK pathway and the DAF-2/DAF-16 insulin signaling pathway, have been characterized for their functions during infection and many other stress-related responses.

The p38 MAPK pathway is an evolutionally conserved signaling pathway across diverse organisms, regulating not only innate immunity, but also stress responses. It has been well studied in yeast and mammals for its involvement in osmotic stress response (85), abiotic stress response, and innate immune response (86) (87). In *C. elegans*, the p38 MAPK pathway is activated in the intestine, hypodermis, and neurons during various infections. The core components include the MAPK, NSY-1, the MAPKK, SEK-1, and the MAPKKK, PMK-1. Loss of PMK-1 result in significant increases in susceptibility of *C. elegans* to multiple pathogens, including Gram-negative bacteria such as *P. aeruginosa* (71, 88) and *S. enterica* (68), Gram-positive bacteria such as *E. faecalis* (89) and *S. aureus* (59), and the fungal pathogen *C. albicans* (51). In addition, loss of the upstream components, NSY-1 and SEK-1, also result in enhanced killing during *P. aeruginosa* infection (71, 90).

The DAF-2/DAF-16 insulin signaling pathway regulates aging, metabolism, and development in *C. elegans* (91). It also plays an important role in innate immunity (61). DAF-2,

the insulin-like receptor, inhibits the activity of the downstream transcription factor DAF-16 through a cascade of phosphorylation of AGE-1, PDK-1, and AKT-1 (92). Constitutive activation of DAF-16 results from loss of function mutations in *daf-2* or *age-1* resulting in significantly increased resistance to multiple pathogens including *P. aeruginosa*, *S. aureus*, and *E. faecalis* (61).

Effector production

Antimicrobial effector secretion is a frequent result of innate immune signaling and plays an important role in pathogen clearance. In *C. elegans*, there are multiple types of effectors that have been demonstrated to have protective roles against pathogens. The saposin-like amoebapores (SPPs) and Anti-Microbial Peptides (AMPs) were the first ones to be discovered. *C. elegans* encodes a large number of SPPs that function in multiple tissues including the pharynx and the intestine to exert their antimicrobial function. Recombinant SSPs expressed in *E. coli* exhibited microbicidal activity (93). AMPs are antimicrobial peptides encoded by *abf-1* and *abf-2* genes (94). They are expressed in the pharynx and the intestine and experiments with recombinant protein showed strong antimicrobial activity against bacteria and fungi (94). Through expression profiling and sequence homology analysis, lysozymes, another family of immune effectors was identified (95). Overexpression of the *lys-1* gene increased *C. elegans* resistance to *Serratia marcescens* (95). Another important effector family is C-type lectins (CLEC), many of which are induced during infection and participate in immune defense (reviewed in (96) . For example, purified CLEC-39 and CLEC-49 bound to *S. marcesecens,* and mutations in the *clec-39* and *clec-49* genes resulted in increased susceptibly to this pathogen (95, 97).

Roles of DUOX and peroxidases in *C. elegans* innate immunity

As discussed in the beginning of this chapter, ROS production is one of the first innate immune responses upon successful pathogen recognition. In *C. elegans*, the NADPH dual oxidase ce-DUOX1(BLI-3) is the major source of ROS. BLI-3 was first discovered for its critical role in cuticle cross-linking and was found to be present in the hypodermis (28). Later, it was demonstrated that BLI-3 is responsible for the increased level of H_2O_2 observed when worms are infected by *E. faecalis*, and RNAi knockdown of BLI-3 result in a significant increase in pathogen sensitivity (98, 99). More recently, mCherry::BLI-3 transgene revealed that in addition to its hypodermis localization, BLI-3 was also produced in the pharynx and intestine (100). It is also shown that BLI-3 generated ROS activates the p38 MAPK pathway, resulting in the nuclear localization of stress response regulator SKN-1, a Nrf2 orthologue in mammalian system, and activation of detoxification genes (101). In the same study, it was established that SKN-1 is required for pathogen resistance. A model was proposed for BLI-3-mediated SKN-1 activation (103). Together, these findings implicated a role for ROS production in immune signaling. It also highlighted the significant cross-talk and overlap between stress response and innate immune pathways.

Interestingly, while the NADPH oxidase domain of BLI-3 is required for both pathogen resistance and cuticle cross-linking functions, the peroxidase domain is dispensable for pathogen resistance (99). This led to the speculation that a partner peroxidase might be involved. Indeed, a peroxidase, SKPO-1, which functions in pathogen resistance, was discovered (102). Loss of SKPO-1 not only resulted in incomplete penetration of dumpy phenotype, but also significantly increased *C. elegans* susceptibility to *E. faecalis*, suggesting that SKPO-1 plays a role in cuticle cross-linking and pathogen resistance (102). A *skpo-1* mutant produced an even higher level of H_2O_2 compared to N2 when exposed to pathogen, indicating a possible function in H_2O_2 consumption - perhaps modulating the levels of this

oxidant during infection (102). Furthermore, SKPO-1 localizes to the hypodermis of the worm, a tissue in which BLI-3 also resides (102). However, whether or not there is a physical interaction between BLI-3 and SKPO-1 is unknown.

Chapter 2 Materials and Methods

Strain Maintenance

C. elegans strains were grown and maintained as previously described (104). The *hpx-2* nonsense mutation strain VC20223 *hpx-2*(*gk252521*) was obtained from the *Caenorhabditis* Genetic Center and was backcrossed with N2 Bristol six times. *C. elegans* strains, bacterial strains, and fungal strains used in this study are listed in Supplemental Material, Table S5. For experiments requiring synchronized worms, L1 stage worms on starved plates were washed off, filtered through a 10μm filter (pluriSelect, pluriStrainer 10μm) spun down, transferred to seeded plates, and grown to the desired stage.

Strain Construction

To generate the *hpx-2(dg047)* CRISPR knock-out strain, single guide (sg) sequences were designed by WU CRISPR (http://crispr.wustl.edu) using the un-spliced sequence of the *hpx-2* gene. Four 18 bp sg sequences with WU score higher than 65 were selected and separately cloned into pJW1219 (105). A mixture of four plasmid constructs was injected into N2 worms at a concentration of 10 ng/μl each, and with 10 ng/μl of pJW1219-*dpy-10* as a co-CRISPR marker. Worms that displayed a roller or dumpy phenotype were then isolated for genotyping to test for insertions and/or deletions (INDEL) in the *hpx-2* gene. Verified *hpx-2* mutants were backcrossed with N2 to eliminate the *dpy-10* mutation.

The HPX-2 catalytic residue mutant (HPX-2-R372A), PHX782 *hpx-2(syb782*), was generated by Suny Biotech (http://www.sunybiotech.com) using CRISPR-Cas9. The mutant strain PHX782 *hpx-2(syb782)* was verified by PCR sequencing and the primers are listed in Table S6.

To generate the *hpx-2* complemented strains, a 12 kb DNA fragment containing the *hpx-2* gene and 5 kb of upstream and 4 kb of downstream sequences was amplified from the

genomic DNA of N2 worms. The PCR product was then purified and injected into *hpx-2(dg047)* and *hpx-2(gk252521)* at 20 ng/μl concentration with 50 ng/μl of EcoRV-digested genomic DNA from N2 worms. pCFJ90 (*pMyo2::mCherry*) was used as a fluorescent co-injection marker at a final concentration of 2 ng/μl.

To visualize *hpx-2* expression, the GF203 strain was generated by injecting the pPD95.75 (50 ng/μl) plasmid containing the 4 kb upstream of *hpx-2* and the first two exons fused to *gfp*, with 20 ng/μl pRF4 (*rol-6(su1006)*) as a roller co-injection marker. The obtained strains with extrachromosomal arrays were then exposed to trimethylpsoralen (TMP) with UV irradiation and back crossed six times to generate stable integrated transgenic lines using a previously described protocol (106). All the oligonucleotide primers used in this study are listed in Table S6.

Killing and Longevity Assays

Killing assays and longevity assays were conducted as previously described, with some slight modifications (61, 62, 107). All assays were done with 30 worms at the L4 stage worms on three replica plates (or 6-plate wells for the *C. albicans* assay) for a total of 90 animals and scored for survival over time. For plate preparation, *E. faecalis* OG1RF was grown in BHI for 5 hours and seeded onto BHI agar plates with 50 μg/ml of gentamycin and grown overnight at 37°C. *P. aeruginosa* PA14 was grown in LB broth overnight and seeded onto SK plates, incubated at 37°C for 24 hours, and then 25°C for another 24 hours. *S. enterica* SL1344 was grown in LB overnight and seeded onto SK plates and incubated at 37°C overnight. *S. aureus* NCTC8325, grown in TSB with 10 μg/ml nalidixic acid (Nal) overnight, was seeded to TSA+Nal plates and incubated at 37°C for 6 hours. *C. diphtheriae* NCTC13129 grown in BHI overnight was seeded onto BHI plates containing 25 μg/ml Nal and 50 μg/ml 5-fluoro-2-deoxyuridine

(FuDR) and incubated at 37°C for 24 hours. *C. albicans* strain SC5314 was grown overnight in BHI media and spotted onto solid BHI plates. L4 stage worms were exposed to *C. albicans* for 4 hours and were collected, washed, and transferred to six-well plates containing 20% BHI and 80% M9W, and scored for survival daily (108).

RNA interference

To knock down *hpx-2* gene expression, L1 to L4 stage larvae were exposed to *E. coli* HT115 containing the expression plasmid for double-stranded *hpx-2* previously constructed (109). L4 stage worms were then transferred to *E. faecalis* killing plates for the pathogen susceptibility assay.

Fluorescence microscopy

To visualize HPX-2::GFP expression, worms with the roller phenotype indicative of the co-injection marker were picked and anesthetized with 25 mM tetramisole and mounted on 2% agarose pads. The worms were then visualized and imaged using Olympus Fluoview FV3000.

To visualize intestinal colonization by *E. faecalis* and *P. aeruginosa*, *C. elegans* were exposed to these pathogens for 48 hours (*E. faecalis*) and 24 hours (*P. aeruginosa*) respectively on agar plates. They were then washed off the plates and washed four times with 1 ml of M9W. Following anesthesia with 25 mM tetramisole hydrochloride, the worms were mounted on 2% agarose pads for imaging.

Colony forming unit assay of intestinal colonization

To measure intestinal CFUs, animals were exposed to bacteria as described above and then washed off plates with M9W. They were then washed three times in 1 ml of M9W, then twice more with 1 ml of M9W containing 25 mM tetramisole hydrochloride. The worms were then treated with 500 μl M9W containing 25 mM tetramisole hydrochloride, 1 mg/ml of ampicillin, and 1 mg/ml kanamycin for 1 hour to kill all surface bacteria. The treated worms were washed twice more with 1 ml of M9W containing 25 mM tetramisole hydrochloride, transferred to an Eppendorf tube containing 100 μl of M9 (one worm per tube), and disrupted using a motorized pestle (Kontes cordless pestle (cat# K749540-0000) and pestles (cat# K749521-1590) for 1 min. The solution was then serially diluted in M9 and spotted on agar plates for CFU counting.

Hoechst staining

Hoechst staining of the worms was performed as previously described (110). Specifically, worms were washed off plates with M9W buffer, and then incubated in M9W containing 1 mg/ml Hoechst 33258 dye (Sigma) at room temperature for 20 minutes with gentle shaking, followed by three more washes with M9W before imaging. Hoechst-positive worms were scored based on staining of the epithelial cell nuclei, which is indicative of cuticle penetration.

RNA isolation and qRT-PCR analysis

L4 animals were exposed for 16 hours to the condition of interest and total RNA was extracted using Trizol (Invitrogen) according to the manufacturer's instructions. RNA samples were treated with Turbo DNA free kit (Applied Biosystems) to eliminate DNA contamination.

qRT-PCR was performed as previously described (101). The actin gene was used as an internal control. Primers used in qRT-PCR are listed in Table S7.

RNA sequencing

L4 stage worms were exposed to *E. faecalis* or *E. coli* for 16 hours and total RNA was extracted for 5 biological replicates. Illumina Hiseq 4000 sequencer with 75 nt pair-ended read format was used to conduct the sequencing. The sequencing reads (ranging from 20 million to 37 million per biological replicate) were quality and adaptor trimmed and mapped to the reference genome (version WBcel235 downloaded from http://ensemblgenomes.org) using Tophat (111). The expression level (RPKM) of annotated genes was measured using Cufflink (112), and differential expression analysis was conducted using Cuffcompare and Cuffdiff (112) using the gene annotation (Caenorhabditis_elegans.WBcel235.37.gff3 downloaded from http://ensemblgenomes.org). Gene Ontology analysis was carried out by using DAVID (the Database for Annotation, Visualization, and Integrated Discovery) 6.8 (113). Gene enrichment with a Benjamini adjusted $P < 0.05$ is listed. Genes that were differentially regulated under different conditions are listed in Table S1-4.

Amplex Red Assay

To measure H_2O_2 concentration of the worms, the Amplex red assay was performed as previously described (109) using the Amplex Red hydrogen peroxide/peroxidase kit (Invitrogen Molecular Probes, Eugene, OR) with the following modifications: L4 worms were exposed to a bacterial strain for 16 hours and transferred to 96 well plates with 30 worms in each well. A total of 80 mM diphenyleneiodinium chloride (DPI) (TCI, Tokyo) was added to some wells and

allowed to incubate for 15 minutes prior to addition of Amplex Reagents. After 1 hour of incubation, fluorescence was measured at 540/590 nm excitation and emission, respectively.

Pharyngeal pumping Rate

To measure the pharyngeal pumping rate of the worms, contractions of the posterior pharyngeal bulb were observed and counted over a 10 second interval for 15 adult animals under a 20X magnification stereo microscope.

Brood size

To measure the brood size of the worms, 9 L4 stage worms were singled on NGM plates, allowed to lay eggs and transferred to a new plate each day until no more eggs were produced. The offspring on the plates were counted to calculate brood size.

Statistical Analysis

Survival, longevity assays, qRT-PCR, intestinal CFU, and Hoechst staining data were analyzed using GraphPad Prism version 5.0 (GraphPad Software, San Diego). Kaplan-Meier log rank analysis was used to compare longevity and survival curves. An unpaired Student's t-test was used to determine the statistical significance of the intestinal CFU and Hoechst staining data. In all the experiments, P-values < 0.05 were considered to be significant and are noted in the figures with one asterisk indicating $P < 0.05$, two indicating $P < 0.01$, three indicating $P < 0.001$ and four indicating $P < 0.0001$.

Strains	Description	References
Enterococcus faecalis		
OG1RF	Wild-type strain, Fa^R, Rf^R	(114)
OG1RF-GFP		(115)
Pseudomonas aeruginosa		
PA14	Wild-type strain	(116)
PA14-dsRed	Expresses dsRed	(117)
Escherichia coli		
OP50	Wild-type strain, Str^R	(49)
HT115(DE3)	Used to express dsRNA for RNAi in *C. elegans*, Amp^R, Tet^R	(71)
EHEC O157:H7	Outbreak strain	(118, 119)
Candida albicans		
SC5314	Wild-type prototrophic strain	(120)
Staphylococcus aureus		
NCTC 8325	Prototypical strain	(121)
Salmonella enterica		
SL1344		(122)
Corynebacterium diphtheriae		
NCTC 13129		(123)
Caenorhabditis elegans		
N2	Wild-type	(49)
Hypodermal RNAi strain	Tissue-specific RNAi strain, *rde-1*(*ne129*); *Is*[*wrt-2prom::RDE-1::unc-54 3' utr; myo2p::RFP3*]	(124) (124)
Intestinal RNAi strain	Tissue-specific RNAi strain, *sid-1*(*qt9*); *Is*[*vha-6::sid-1*]	(124) (124)
GF200	*hpx-2* nonsense mutation strain, *hpx-2 (gk252521) V backcrossed 6 time from* VC20223	This study
GF201	*hpx-2* CRISPR/Cas9 knockout strain, *hpx-2*(*dg047) V*	This study
GF202	*hpx-2::gfp expression strain, dgIs049* [*hpx-2p::gfp; rol-6(su1006)]*	This study
GF203	*hpx-2 complementation strain, hpx-2 (dg047) V; dgEx050 [hpx-2p::hpx-2; myo-2p::mCherry]*	This study
GF204	*hpx-2 complementation strain, hpx-2 (gk252521) V; dgEx050 [hpx-2p::hpx-2; myo-2p::mCherry]*	This study

GF205	*hpx-2 overexpression strain, hpx-2 (dg047) V; dgEx050 [hpx-2p::hpx-2; myo-2p::mCherry]*	This study
GF206	*hpx-2 overexpression strain, hpx-2 (gk252521) V; dgEx050 [hpx-2p::hpx-2; myo-2p::mCherry]*	This study
PHX782	*hpx-2(syb782)*	This study

Table 2.1 Strains used in this study.

Ss#	Oligo name	Oligo sequence	Purpose
40	P1-sg1-pJW1219-F	cct cct att gcg aga tgt ctt g CCA ATG AAG TCA TTG AAA GA gtt taa gag cta tgc tgg aaa c	Clone hpx-2 single guide sequence #1 to pJW1219
41	P1-sg1-pJW1219-R	gtt tcc agc ata gct ctt aaa c TCT TTC AAT GAC TTC ATT GG caa gac atc tcg caa tag gag g	
42	P1-sg2-pJW1219-F	cct cct att gcg aga tgt ctt g CGG TTA TTG CAG TTA ATT GG gtt taa gag cta tgc tgg aaa c	Clone hpx-2 single guide sequence #2 to pJW1219
43	P1-sg2-pJW1219-R	gtt tcc agc ata gct ctt aaa c CC AAT TAA CTG CAA TAA CCG c aag aca tct cgc aat agg agg	
44	P1-sg3-pJW1219-F	cct cct att gcg aga tgt ctt g CTT CGA TTC GAT CAA TCA CA gtt taa gag cta tgc tgg aaa c	Clone hpx-2 single guide sequence #3 to pJW1219
45	P1-sg3-pJW1219-R	gtt tcc agc ata gct ctt aaa c TG TGA TTG ATC GAA TCG AAG c aag aca tct cgc aat agg agg	
46	P1-sg4-pJW1219-F	cct cct att gcg aga tgt ctt g ATG CAG CTC CCA GAA TTC GG gtt taa gag cta tgc tgg aaa c	Clone hpx-2 single guide sequence #4 to pJW1219
47	P1-sg4-pJW1219-R	gtt tcc agc ata gct ctt aaa c CC GAA TTC TGG GAG CTG CAT c aag aca tct cgc aat agg agg	
205	pHPX2-4kb-9567-F	GCCTGCAGGTCGACTtacttcttttgtaaattctcctgtatg aacttttgtg	Clone 4kb promoter region of hpx-2(plus first 5 aa) into pPD95.67
206	pHPX2-4kb-9567-R	CCGGGGATCCTCTAGcggtttcaaattcatatttcaaaa tgaattctaaataatcgg	
212	HPX2-12KB-pBluescript-F	cactagttctagagcggaagtcattgatcaacccgtgag	Gibson assembly of 10KB HPX-2 fragment into pBluescript
213	HPX2-12KB-pBluescript-R	accgcggtggcggcccttgtgtgctcttgtaaaatcgcaagc	
257	YL01-seq-s	AACTACCGTCTGCTAGGCTA	PCR and sequencing primers for HPX-2-R372A (*syb482*)
258	YL01-seq-a1	TAGATGGATCTACACTGGTAC	

Table 2.2 Oligonucleotides used in this study.

act-1 F	ACC ATG TAC CCA GGA ATT GC
act-1 R	TGG AAG GTG GAG AGG GAA G
lys-1 F	CCACAGGACAACTTCGAAGTGACT
lys-1 R	TGTCTTGAGGCAGTTCATTTGAGAAACT
lys-2 F	CGCTTCAATGGGAAATGCTGTCG
lys-2 R	CCAACACAATTTGAATCAAAAGCTCCATTT
lys-3 F	CTCTATTACATTGTGCTACTCTTTCC
lys-3 R	TCATCATATGGAATTGCTGGAGC
lys-7 F	TGCATACAACCCAGCAGG
lys-7 R	ATGATCTCATCCAACTGTTGGT
spp-20 F	CATATTTGCCAGCTTGCTCC
spp-20 R	CAACAAATTGAGAGACGAGTACAC
f53a9.8 F	GTCGCACCAAGAACACGGAC
f53a9.8 R	GCCTGATGGTTGCCCCC
pmk-2 F	GGCGATTCAGCCAGCATTCCCG
pmk-2 R	CTCCATACGCTCCTTCTCCTAGAGGC
col-20 F	CTATCATTGCCGTGCCAATG
col-20 R	GATCAGAAACAGCGTTAGATCG
col-88 F	TGATGCCTGGAGATCCATG
col-88 R	GGTCCTGGTGGTCCG
hsp12.3 F	CTGGACTACGAAGACCATTTC
hsp12.3 R	AATACTGCGGGTGATAGATCC

Table 2.3 Primers used in qRT-PCR

Chapter 3 HPX-2 contributes to pathogen resistance in *C. elegans*

Introduction

When exposed to pathogen, production of Reactive Oxygen Species (ROS) is one of the first innate immune responses initiated by the host. ROS can exert immune-protective effects by acting directly as an antimicrobial, serving as a signal to activate downstream responses, and/or contributing to the generation of physical barriers. There are two major groups of enzymes involved in this process – the ROS producing NADPH oxidases/Dual-oxidases (NOX/DUOX) and the ROS utilizing, heme-containing peroxidase (reviewed by 22, 125)). In many cases, these enzymes are functionally, and sometimes physically linked to contribute to innate immunity against pathogen. The most canonical case studied in mammalian systems is that of myeloperoxidase (MPO), which resides in the phagolysosome of macrophages and utilizes the superoxide produced by NOX2 to generate the powerful oxidant HOCl during the oxidative burst that occurs as a result of microbial engulfment (reviewed by (126)). Additionally, it has been shown that lactoperoxidase (LPO) coupled with DUOX2, is responsible for the generation of the antibiotic oxidant hypothiocyanite (OSCN-) from H_2O_2 and thiocyanate (SCN-) on mucosal surfaces (16, 18, 127). These responses are not limited to animals; plants also employ peroxidases and NADPH oxidases as part of their antimicrobial arsenal (reviewed in (128)).

In *C. elegans*, the one functional NOX/DUOX encoded by the genome is BLI-3, a dual oxidase that produces H_2O_2 when animals are exposed to pathogen (28, 98, 99, 129). Like all dual oxidases, BLI-3 consists of an NADPH oxidase domain and a heme peroxidase domain (28). The production of H_2O_2 from the NADPH oxidase domain of BLI-3 is required for pathogen resistance and point mutants that affect this domain significantly increase pathogen susceptibility (99, 100). In addition to its role during infection, BLI-3 is crucial for cuticle development. The peroxidase domain uses the H_2O_2 produced by the NADPH oxidase domain to cross-link collagen proteins (28). Another independent heme-binding peroxidase, MLT-7, additionally contributes to this process (29). Mutations in the peroxidase domains of BLI-3 and

MLT-7 that impair activity result in a blistered phenotype. However, these mutations do not affect pathogen susceptibility (102).

Given that NOX/DUOX enzymes and heme-containing peroxidases often functionally partner, we hypothesized that there might be DUOX-Peroxidase systems in *C. elegans* that contribute to pathogen resistance. To test this hypothesis, a previous graduate student in our lab, Dr. George Tiller, conducted a RNAi screen where he knocked down each of all the putative peroxidases encoded in *C. elegans* genome and tested their susceptibility to *E. faecalis* (102). He found three putative peroxidases that when knocked down significantly increase pathogen susceptibility. One, which he named SKPO-1, was characterized in detail in his Ph.D. dissertation (102). He showed that a *skpo-1* mutant was more susceptible to *E. faecalis* compared to the N2 reference strain. In addition to pathogen sensitivity, the *skpo-1* mutant also had an incomplete penetrance of dumpy phenotype, suggesting a potential role in the process of cuticle bio-generation. Interestingly, SKPO-1 localized to the hypodermis of the worm, a tissue where BLI-3 also resides, indicating a potential physical interaction between the two (102). Despite the functional and spatial overlap of the DUOX BLI-3 and the heme-peroxidase SKPO-1, questions remain regarding how this peroxidase and others function in a protective role against pathogens.

Here, I characterized the other two immune-protective peroxidases, F09F3.5 and F08F11.7, which I named HPX-2 and HPX-3 respectively for **H**eme **P**eroxidase 2 and 3. Using a combination of RNA interference (RNAi) and CRISPR-Cas9 mediated gene inactivation approcaches, I demonstrated that HPX-2 is important for protecting *C. elegans* against some, but not all, pathogens.

Results

RNAi of the putative peroxidases results in susceptibility to *E. faecalis*

To verify the protective role of the putative peroxidases against pathogen, I utilized RNA interference experiments to knock down HPX-2 and HPX-3. The RNAi constructs were available in the RNAi library (130), (131). The RNAi-treated animals were exposed to *E. faecalis* and scored for survival over time. Consistent with previous findings, reduced expression of *hpx-2* and *hpx-3* resulted in a significant increase in pathogen susceptibility (Figure 3.1) (102).

Generation of CPRSR/Cas9 mutants of the putative peroxidases

To further study the function of the two putative peroxidases, I generated the truncated mutant alleles of *hpx-2* and *hpx-3* through CRISPR-Cas9 mediated gene editing (Figure 3.2). After PCR and sequencing for verification, one allele was obtained for each gene: *hpx-2(dg047)* and *hpx-3(dg048)*. The changes in DNA sequence are listed in Figure 3.3. Both alleles had insertions and deletions (INDELS) at the 5' end of the genes, resulting in the translated product missing most of the predicted peroxidase domain and are therefore predicted loss-of-function mutants (Figure 3.4). In addition to the CRISPR mutant, I was also able to obtain a nonsense mutant allele of *hpx-2 (hpx-2(gk252521)*) from the Caenorhabditis Genetic Center (GCG) (Figure 3.4). The EMS-generated mutant was backcrossed with the N2 strain six times to eliminate background mutations.

After exposure to *E. faecalis*, I observed significant increases in the susceptibility of both *hpx-2* mutants *(hpx-2(dg047)* and *hpx-2(gk252521))* to the pathogen which were more dramatic than the RNAi-treated strain (Figure 3.6). However, in contrast with the RNAi result, no significant changes in pathogen susceptibility from *hpx-3(dg048)* was observed (Figure 3.7). To independently verify this result, I constructed one more allele of *hpx-3* (*hpx-3(dg049))* and tested the strain's pathogen sensitivity by exposing it to *E. faecalis* (Figure 3.5). The newly

generated mutant allele of *hpx-3* also did not exhibit pathogen sensitivity compared to the N2 strain (Figure 3.7). I hypothesized that the RNAi construct of *hpx-3* used in the previous experiments might have off-target effects, resulting in a false pathogen sensitivity phenotype. Indeed, close examination of the sequence of the RNA construct revealed significant sequence homology to the hpx-2 gene. It is likely that the *hpx-3* RNAi construct had an off-target effect on the *hpx-2* gene causing a false positive result. Hence, I focused my project solely on HPX-2.

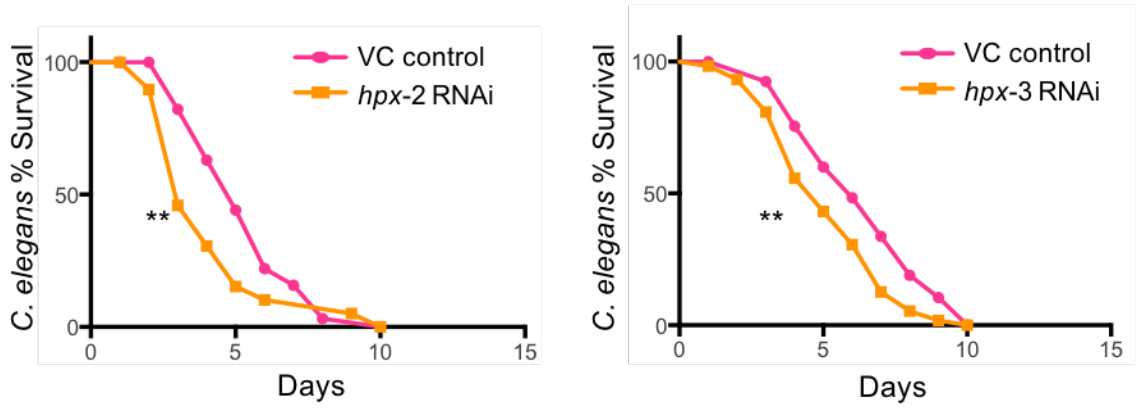

Figure 3.1 Survival of worms on E. faecalis OG1RF following exposure to vector control (VC) RNAi, (A) hpx-2 RNAi and (B) hpx-3 RNAi. Representative results from one experiment with an n of approximately 90 worms for each condition are shown. Median survival and P-values are listed in Table 3.1 as experiment No.1 along with other biological replicates.

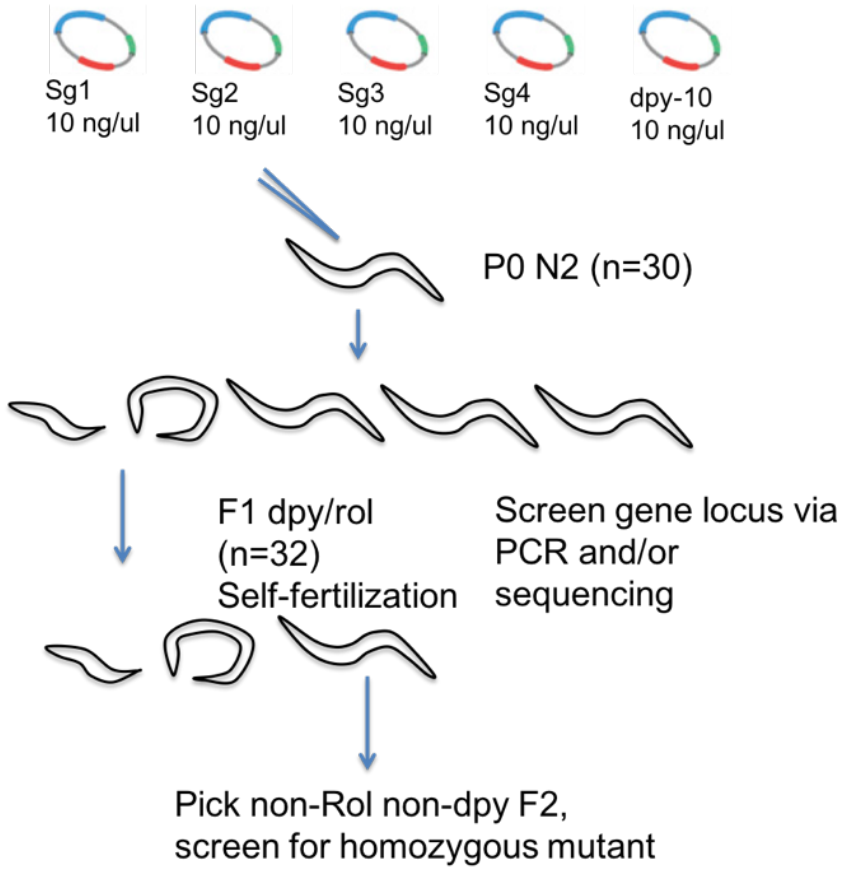

Figure 3.2 Microinjection and screen for CRISPR mutants. Four single guide (sg) sequences designed by WU CRISPR (http://crispr.wustl.edu) using the un-spliced sequence of the *hpx-2 or hpx-3* gene were cloned into pJW1219 (105). A mixture of four plasmid constructs were injected into N2 worms at a concentration of 10 ng/μl each, and with 10 ng/μl of pJW1219-*dpy-10* as a co-CRISPR marker. Worms that displayed a roller or dumpy phenotype were then isolated for genotyping to test for insertions and/or deletions (INDELs) in the targeted genes. Verified CRISPR mutants were backcrossed with N2 to get rid of the *dpy-10* mutation.

Figure 3.3 DNA sequence of HPX-2 and HPX-3 CRISPR mutants. Blue letters indicate single guide sequences, Grey and underlined letters indicate PAM sequences, red indicates the changed sequence in the mutants.

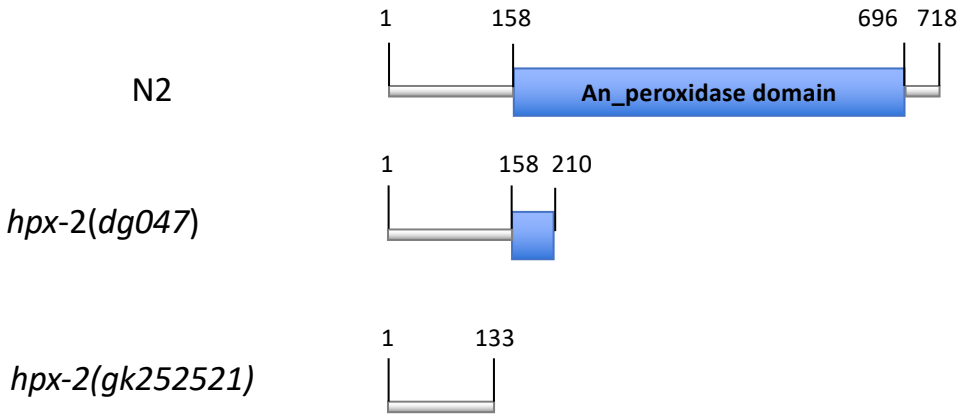

Figure 3.4 Schematic representation of HPX-2 mutants. Wilde-type HPX-2 protein is composed of 718 amino acids, with the predicted peroxidase domain at the C-terminus. *hpx-2(dg047)* allele harbors an INDEL mutation at its N-terminus, resulting in a frameshift and premature stop for protein translation. The predicted protein length is 210 amino acids. The *hpx-2(gk252521)* allele has an amber mutation at its N-terminus, resulting in a truncated 133 amino acid protein.

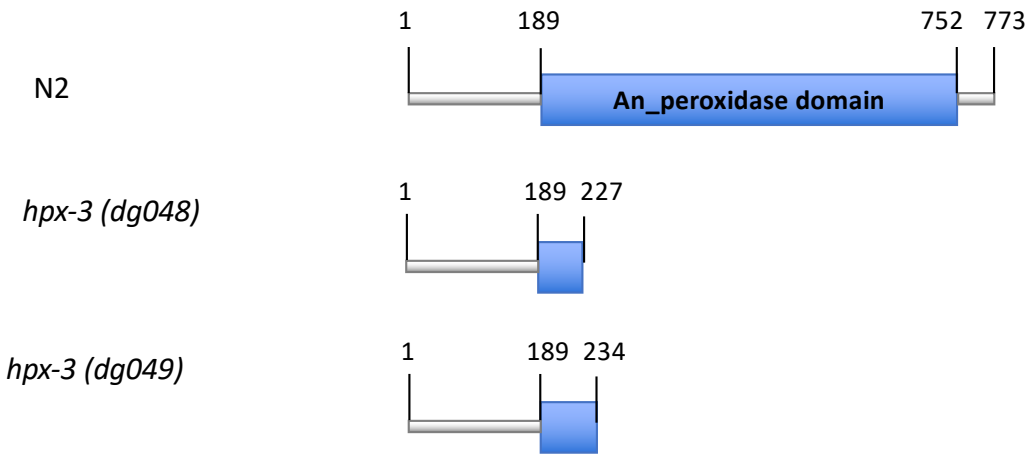

Figure 3.5 Schematic representation of HPX-3 mutants. Wild-type HPX-3 protein is composed of 773 amino acids, with the predicted peroxidase domain at the C-terminus. *hpx-3(dg048)* allele harbors an INDEL mutation at its N-terminus, resulting in a frameshift and premature stop for the translated protein. The predicted protein length is 227 amino acids. The *hpx-3(dg049)* allele has an has an INDEL mutation at its N-terminus, resulting in a frameshift and premature stop for the translated protein. The predicted protein length is 234 amino acids.

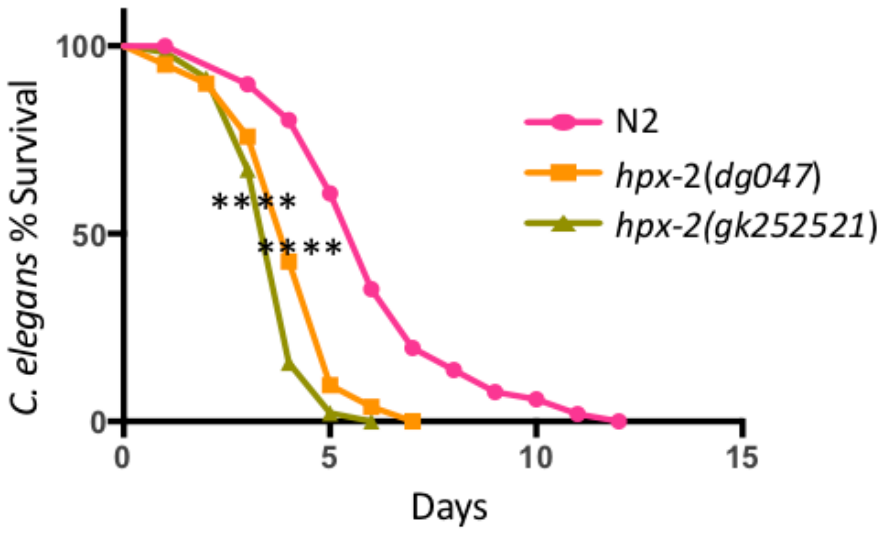

Figure 3.6 Survival of *hpx-2* mutants on *E. faecalis*. Results from one representative experiment with an n of approximately 90 worms for each condition are shown. Median survival and P-values are listed in Table 3.1 as experiment No.1 along with other biological replicates.

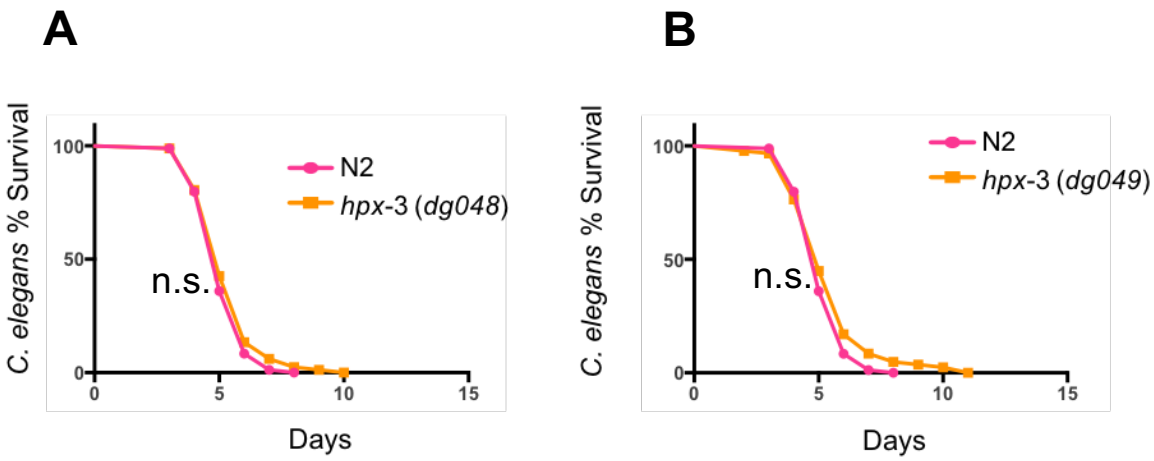

Figure 3.7 Survival of *hpx-3* mutants on *E. faecalis*. Results from one representative experiment with an n of approximately 90 worms for each condition are shown. Median survival and P-values are listed in Table 3.1 as experiment No.1 along with other biological replicates.

Hpx-2 mutants showed no general fitness defects

To ensure that the pathogen sensitivity phenotype of *hpx-2* mutants was not due to an impairment in general fitness of the worms, the mutants were tested for general defects in fitness by measuring their longevity on live (Figure 3.8A) and heat-killed *E. coli* OP50 (Figure 3.8B). While both mutants showed slight longevity defects compared with the N2 strain on live *E. coli,* there was no significant difference on heat-killed *E. coli*. The minor longevity defect of the mutants on live *E. coli* OP50 might result from the slight pathogenicity of OP50 towards worms as they age (132). Next, the mutants were tested on vancomycin inactivated *E. faecalis* for survival. Although both mutant alleles showed significantly decreased survival on live *E. faecalis* compared to N2 worms (Figure 3.6), the difference disappeared when worms were exposed to *E. faecalis* inactivated by vancomycin treatment (Figure 3.9), suggesting live bacteria were required for killing, and again indicating that the animals do not have a general fitness defect.

In addition to wild-type survival rates on non-pathogenic bacteria, the *hpx-2* mutants also exhibited normal morphology and brood size compared to N2 wild type (Figure 3.10 and 3.11). Overall, these data suggest that the loss of HPX-2 does not dramatically affect the fitness of the worms.

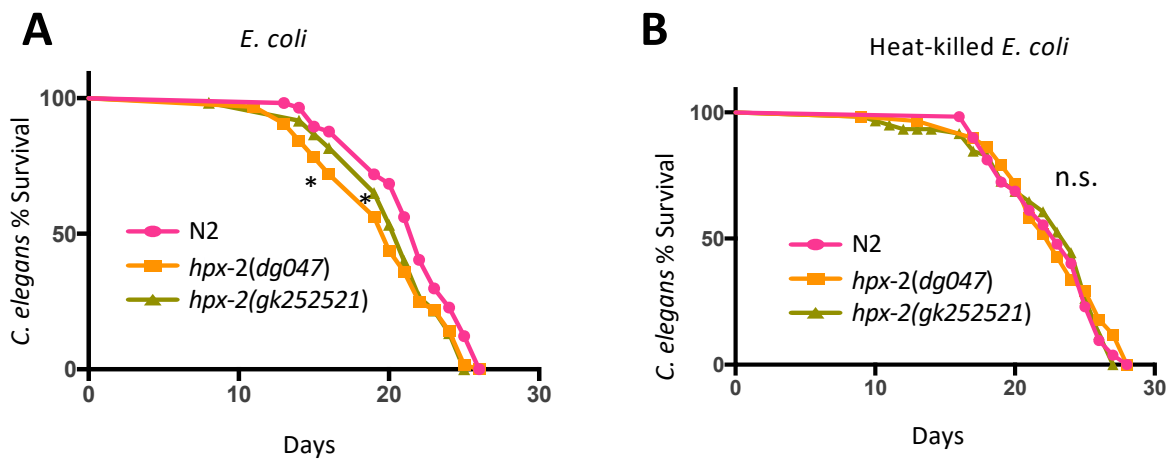

Figure 3.8 HPX-2 does not contribute to the overall fitness of the worm on *E. coli.* Survival of N2 and *hpx-2* mutants on (A) *E. coli* OP50 and (B) heat-killed *E. coli* OP50. Results from one representative experiment with an n of approximately 90 worms for each condition are shown. Median survival and P-values are listed in Table 3.1 as experiment No.1 along with other biological replicates.

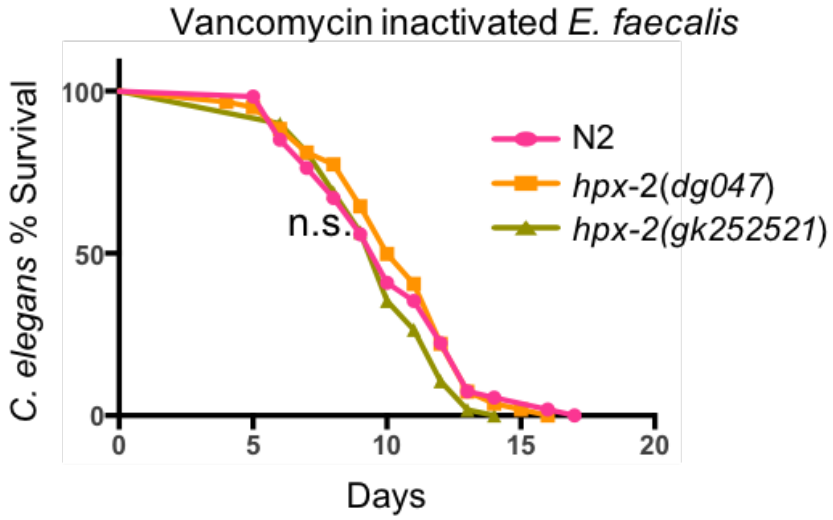

Figure 3.9 HPX-2 does not contribute to the overall fitness of the worm on vancomycin inactivated *E. faecalis*. Results from one representative experiment with an n of approximately 90 worms for each condition are shown. Median survival and P-values are listed in Table 3.1 as experiment No.1 along with other biological replicates.

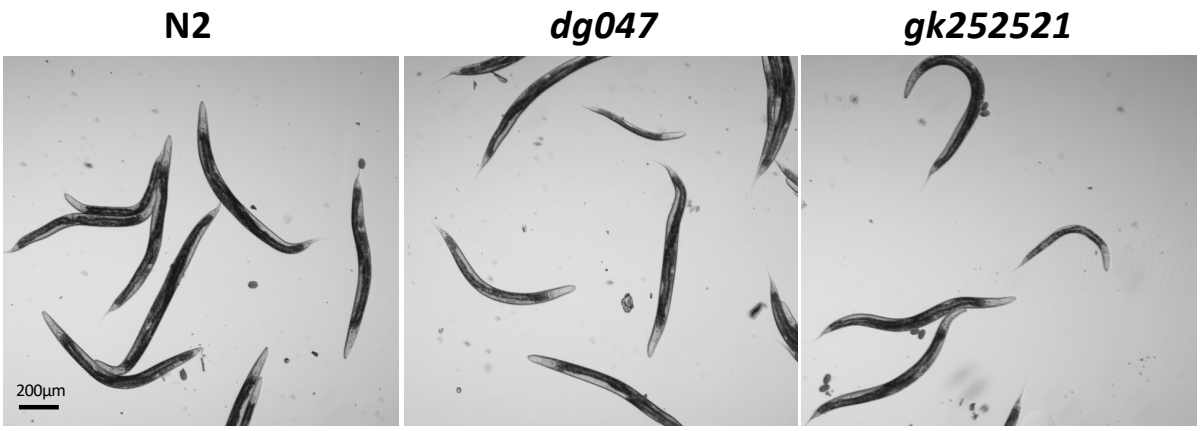

Figure 3.10 *hpx-2* mutant adults exhibit the same average size and morphology of N2 worms. Young adult worms of N2, *hpx-2(dg047),* and *hpx-2 (gk252521*) were collected and observed under the light microscopy. Images are representative of >100 worms observed.

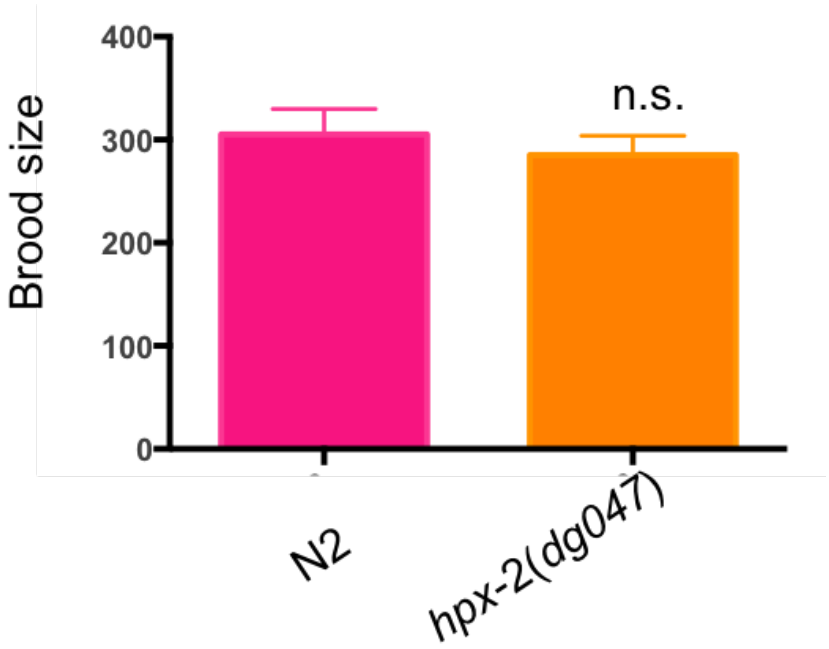

Figure 3.11 *hpx-2* mutants have comparable brood sizes compared to N2 worms. $P_{hpx\text{-}2(dg047)}$ =0.2430, n = 9. Error bars represent the SEM, and P-values were calculated via Student's paired t-test. Data are representative of three independent replicates.

HPX-2 protects *C. elegans* from some but not all pathogens

To test if the pathogen susceptibility of the *hpx-2* mutants is pathogen-specific, I exposed them to multiple human pathogens including the fungal pathogen *Candida albicans* SC5314 (Figure 3.12 A), Gram-positive pathogens *Staphylococcus aureus* NCTC8325 (Figure 3.12 B) and *Corynebacterium diphtheriae* NCTC12129 (Figure 3.12 C), and finally Gram-negative pathogens *Pseudomonas aeruginosa* PA14 (Figure 3.12 D), *Escherichia coli* O157:H7 Sakai (EHEC; Figure 3.12 E), and *Salmonella enterica* SL1344 (Figure 3.12 G). Interestingly, *hpx-2* mutants showed susceptibility to all the microbial pathogens tested except for the Gram-negative bacteria, raising the possibility that differences in microbial cell wall structure might impact the phenotype observed with loss of *hpx-2* (see Discussion).

***hpx-2* mutants can be complemented with genomic DNA containing *hpx-2* gene**

To verify that HPX-2 is required for pathogen resistance, I complemented the mutant strains with DNA containing the *hpx-2* gene and subjected the animals to *E. faecalis* exposure. Specifically, a 12-kb DNA fragment was PCR amplified from the genomic DNA of N2 worms. The fragment was purified and injected into both mutant alleles at a concentration of 20 ng/μl with P*myo-2*::mcherry (2 ng/μl) as a co-injection marker. When exposed to *E. faecalis*, the complemented strains showed a significant increase in pathogen tolerance compared to the parental strains, reaching a level of resistance similar to N2 (Figure 3.13 A and B). These data collectively suggest that HPX-2 is required for resistance to many, but not all, pathogens capable of infecting *C. elegans*.

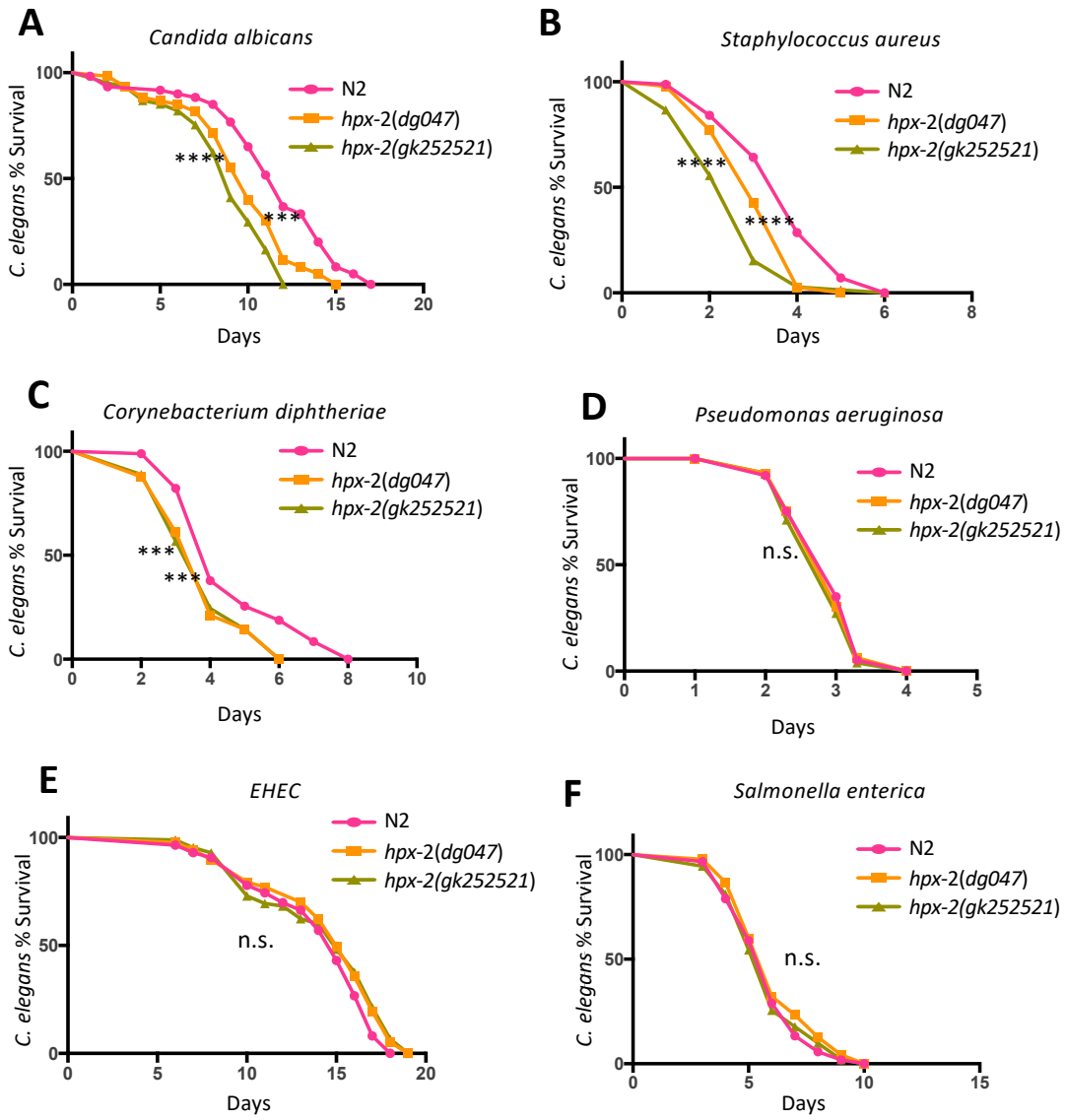

Figure 3.12 HPX-2 contributes to *C. elegans* resistance to some pathogens. Survival of N2 and *hpx-2* mutants on (A) *Candida albicans* SC5314, (B) *Staphylococcus aureus* NCTC8325, (C) *Corynebacterium diphtheriae* NCTC12129, (D) *Pseudomonas aeruginosa* PA14, (E) *Escherichia coli* O157:H7 Sakai (EHEC), and (F) *Salmonella enterica* SL1344. Results from one representative experiment with an n of approximately 90 worms for each condition are shown. Median survival and P-values are listed in Table 3.1 as experiment No.1 along with other biological replicates.

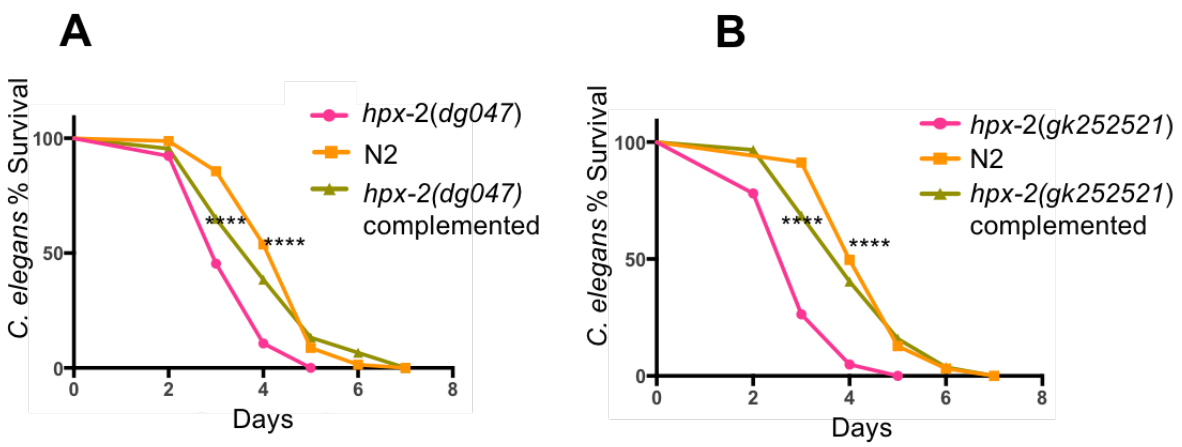

Figure 3.13 Genomic *hpx-2* complementation rescues the susceptibility to *E. faecalis.* (A) Survival of N2, *hpx-2(dg047)* mutant, and its complemented strain on *E. faecalis.* (B) Survival of N2, *hpx-2(gk252521)* mutant, and its complemented strain on *E. faecalis*. The *hpx-2* mutants are set as control. Results from one representative experiment with an n of approximately 90 worms for each condition are shown. Median survival and P-values are listed in Table 3.1 as experiment No.1 along with other biological replicates.

Figure number	Experiment number	Strain	Exposure conditions	Median survival (days)	P-value
3.1 A	1	N2 VC RNAi	*E. faecalis*	5	C
		N2 *hpx-2* RNAi	*E. faecalis*	3	0.0029
	2	N2 VC RNAi	*E. faecalis*	5	C
		N2 *hpx-2* RNAi	*E. faecalis*	4	0.007
3.1 B	1	N2 VC RNAi	*E. faecalis*	6	
		N2 *hpx-3* RNAi	*E. faecalis*	5	0.0042
	2	N2 VC RNAi	*E. faecalis*	7	
		N2 *hpx-3* RNAi	*E. faecalis*	6	0.0233
3.6	1	N2	*E. faecalis*	6	Control (C)
		hpx2 (dg047)	*E. faecalis*	4	<0.0001
		hpx-2 (gk252521)	*E. faecalis*	4	<0.0001
	2	N2	*E. faecalis*	5	C
		hpx2 (dg047)	*E. faecalis*	4	0.0036
		hpx-2 (gk252521)	*E. faecalis*	4	0.0016
3.7 A	1	N2	*E. faecalis*	5	C
		hpx-3(dg048)	*E. faecalis*	5	0.1834
	2	N2	*E. faecalis*	5	C
		hpx-3(dg048)	*E. faecalis*	5	0.8783
3.7 B	1	N2	*E. faecalis*	5	C
		hpx-3(dg049)	*E. faecalis*	5	0.1093
	2	N2	*E. faecalis*	5	C
		hpx-3(dg049)	*E. faecalis*	5	0.5014
3.8 A	1	N2	*E. coli*	22	C
		hpx2 (dg047)	*E. coli*	20	0.0257
		hpx-2 (gk252521)	*E. coli*	21	0.0115
	2	N2	*E. coli*	22	C
		hpx2 (dg047)	*E. coli*	20	0.014
		hpx-2 (gk252521)	*E. coli*	20	0.026
3.8 B	1	N2	Inactivated *E. coli*	23	C
		hpx2 (dg047)	Inactivated *E. coli*	23	0.4918
		hpx-2 (gk252521)	Inactivated *E. coli*	24	0.8962
	2	N2	Inactivated *E. coli*	21	C
		hpx2 (dg047)	Inactivated *E. coli*	21	0.4737
		hpx-2 (gk252521)	Inactivated *E. coli*	21	0.9988
3.9	1	N2	Inactivated *E. faecalis*	10	C
		hpx2 (dg047)	Inactivated *E. faecalis*	10	0.2266
		hpx-2 (gk252521)	Inactivated *E. faecalis*	10	0.8574
	2	N2	Inactivated *E. faecalis*	10	C
		hpx2 (dg047)	Inactivated *E. faecalis*	10	0.3007
		hpx-2 (gk252521)	Inactivated *E. faecalis*	11	0.1732

3.12 A	1	N2	*C. albican*	12	C
		hpx2 (dg047)	*C. albican*	10	0.0004
		hpx-2 (gk252521)	*C. albican*	9	<0.0001
	2	N2	*C. albican*	10	C
		hpx2 (dg047)	*C. albican*	8	0.0089
		hpx-2 (gk252521)	*C. albican*	8	0.0029
3.12 B	1	N2	*S. aureus*	4	C
		hpx2 (dg047)	*S. aureus*	3	<0.0001
		hpx-2 (gk252521)	*S. aureus*	3	<0.0001
	2	N2	*S. aureus*	4	C
		hpx2 (dg047)	*S. aureus*	3	0.008
		hpx-2 (gk252521)	*S. aureus*	3	<0.0001
3.12 C	1	N2	*C. diphtheriae*	4	C
		hpx2 (dg047)	*C. diphtheriae*	4	0.0004
		hpx-2 (gk252521)	*C. diphtheriae*	4	0.001
	2	N2	*C. diphtheriae*	4	C
		hpx2 (dg047)	*C. diphtheriae*	4	0.0003
		hpx-2 (gk252521)	*C. diphtheriae*	4	0.0007
3.12 D	1	N2	*P. aeruginosa*	3	C
		hpx2 (dg047)	*P. aeruginosa*	3	0.8260
		hpx-2 (gk252521)	*P. aeruginosa*	3	0.3605
	2	N2	*P. aeruginosa*	2	C
		hpx2 (dg047)	*P. aeruginosa*	2	0.9207
		hpx-2 (gk252521)	*P. aeruginosa*	2	0.9896
3.12 E	1	N2	*EHEC*	15	C
		hpx2 (dg047)	*EHEC*	15	0.0586
		hpx-2 (gk252521)	*EHEC*	15	0.0516
	2	N2	*EHEC*	15	C
		hpx2 (dg047)	*EHEC*	15	0.9479
		hpx-2 (gk252521)	*EHEC*	15	0.4300
3.12 F	1	N2	*S. enterica*	6	C
		hpx2 (dg047)	*S. enterica*	6	0.1765
		hpx-2 (gk252521)	*S. enterica*	6	0.8918
	2	N2	*S. enterica*	6	C
		hpx2 (dg047)	*S. enterica*	6	0.2610
		hpx-2 (gk252521)	*S. enterica*	6	0.4413
3.13 A	1	*hpx-2 (dg047)*	*E. faecalis*	3	C
		N2	*E. faecalis*	5	<0.0001
		hpx2 (dg047) complemented	*E. faecalis*	4	<0.0001
	2	*hpx-2 (dg047)*	*E. faecalis*	3	C
		N2	*E. faecalis*	4	<0.0001
		hpx2 (dg047) complemented	*E. faecalis*	4	0.0012
3.13 B	1	*hpx-2 (gk252521)*	*E. faecalis*	3	C
		N2	*E. faecalis*	4	<0.0001
		hpx2 (gk252521) complemented	*E. faecalis*	4	<0.0001
	2	*hpx-2 (gk252521)*	*E. faecalis*	3	C

		N2	*E. faecalis*	4	<0.0001
		hpx2 (gk252521) complemented	*E. faecalis*	3	<0.0001

Table 3.1 Median survival and P-values in killing assays

Discussion

In this chapter, I characterized a putative heme peroxidase, HPX-2, that contributes to resistance to multiple pathogens in *C. elegans.* Base on previous work from our lab, I started my investigation examining two putative peroxidases (HPX-2 and HPX-3) in *C.elegans* genome that when knocked-down by RNAi render *C. elegans* susceptible to *E. faecalis* (102). Upon the generation of CRISPR knockout mutants of these two peroxidases, I found that one of them, HPX-3, does not contribute to pathogen resistance, and the RNAi results were likely due to off-target effect. Hence, I have focused the remainder of my dissertation on HPX-2.

I first demonstrated that loss of HPX-2 did not affect the overall fitness of the worms as reflected by the normal overall morphology, brood size, and survival rate on *E. coli* compared to N2 strain. In contrast, the two previously identified peroxidases, SKPO-1 and MLT-7, both had impacts on the morphology of *C. elegans* when knocked down or mutated (29, 102). Specifically, the SKPO-1 mutant exhibited an incomplete penetration of dumpy phenotype (102). It also exhibited a significantly smaller brood size and slower growth compared to the N2 strain (102) (unpublished data). MLT-7, on the other hand, exhibits a severe blistered phenotype when mutated because of its essential role in cuticle cross-linking (29). Overall, the data suggest that HPX-2 is not likely to be heavily involved in the morphogenesis of the worm cuticle (discussed in more detail in Chapters 4 and 5).

Next, I showed that HPX-2 protects worms from Gram-positive bacteria and fungi, but not Gram-negative bacteria. The pathogens I tested included *C. albicans* SC5314, *Staphylococcus aureus* NCTC8325, *Corynebacterium diphtheriae* NCTC12129, *Pseudomonas aeruginosa* PA14, *Escherichia coli* O157:H7 Sakai (EHEC), and *Salmonella enterica* SL1344. The reasons I chose those microbes are as follows: First, they represent a wild-range of pathogenic microbes spanning from prokaryotes to eukaryotes. Second, they are all well characterized human pathogens with important clinical relevance. Last but not least, they have

been shown to be pathogenic to *C. elegans* following colonization of the intestines. As to why *hpx-2 mutants* were more susceptible to fungal and Gram-positive pathogen but not the Gram-negative, I hypothesize that it is because of the difference in their cell wall structure. Yeast and Gram-positive bacteria have thick and hard to disrupt cell walls compared to Gram-negatives. As mentioned in the introductory chapter, the pharyngeal grinder of the worm disrupts most bacteria through chemical and physical mechanisms, serving as the first defense against intestinal colonization. Given the fact that HPX-2 is produced in the pharynx of the worm (see next chapter for detail), it might play an important role in assisting the pharyngeal disruption of microbial cell wall during feeding. It could also be that different pathogens have different modes of killing, and the mechanism of HPX-2 action might be protective against some modes but not others. To lessen this possibility, I made sure that I was using pathogens with similar infection sequelae. For all these pathogens, intestinal colonization is a prerequisite for infection. Specifically, I used the slow-killing assay to assess *P. aeruginosa* pathogenesis, which has been shown to require intestinal colonization as compared to fast-killing, which is toxin mediated. Additionally, I used the shiga toxin-negative strain of EHEC to infect *C. elegans*, which also requires intestinal colonization for killing.

In conclusion, I report a putative peroxidase, HPX-2, protects *C. elegans* from fungal and Gram-positive pathogen infection, and that loss of HPX-2 does not affect overall fitness of the worm. This highlights the immune-specific function of peroxidases in the worm.

Chapter 4: HPX-2 functions in pharynx and hypodermis as a putative peroxidase for pathogen resistance

Introduction

In Chapter 3, I showed that HPX-2 provides protection from many, but not all pathogen infections. In order to further study the function of HPX-2 in innate immune protection, I decided to investigate its localization and enzymatic function.

The only functional NOX/DUOX, BLI-3, was first shown to be localized to the hypodermis using immune-staining, which is consistent with its function in cuticle cross-linking (28). Later, a study from our lab showed that BLI-3 might also be present in the intestine and involved in pathogen resistance since intestinal-specific RNAi knockdown of BLI-3 resulted in increased susceptibility to *E. faecalis* (99). More recently, through the construction of a BLI-3::mCherry transgene, BLI-3 was localized to the pharynx in addition to the intestine and the hypodermis (100). It was also shown that BLI-3 is involved in protecting worms from *C. albicans* infection in addition to *E. faecalis* infection, although the amount and pattern of BLI-3 localization did not change upon exposure to these pathogens (101).

Given that DUOXs often pair with peroxidases for their function, I postulated that peroxidases that functionally interact with BLI-3 are likely to be in one or more of the tissues that harbor BLI-3. Indeed, a previous study from our lab demonstrated that SKPO-1, another immune-protective peroxidase, localizes to the hypodermis (102). Considering that HPX-2 is also likely to functionally interact with BLI-3, I tested the hypothesis that it has a similar expression/ localization pattern and is likely to be found in pharynx, gut and/or hypodermis.

Results

HPX-2 localizes to pharynx and hypodermis of the worms

To functionally localize HPX-2, I conducted tissue-specific RNAi to knock down *hpx-2* in the intestine or hypodermis and measured the worms' susceptibility to *E. faecalis*. I observed that intestinal RNAi did not affect pathogen susceptibility, whereas hypodermal RNAi resulted in a slight but significant decrease, suggesting that HPX-2 might be present in the hypodermis and contribute to pathogen resistance in this tissue (Figure 4.2 A and B).

To directly visualize the expression of HPX-2, I created a partial translational fusion of HPX-2 to GFP. Specifically, a 4-kb region containing the upstream sequence and the first two exons of the *hpx-2* gene was cloned to generate a fusion with GFP (Figure 4.3 A). The construct was injected into the worms at a concentration of 50 ng/μl with pRF4 (20 ng/μl) as a co-injection marker (133). The resulting extrachromosomal array was then integrated into the chromosome by the TMP/UV method (106). I initially looked at the stable transgenic worms at different development stages but did not observe GFP expression in the majority. Occasionally (in about ~1% of the worms), I observed a green fluorescent stripe extending from the distal bulb of the pharynx to the anterior of the buccal cavity (Figure 4.3 B). I postulated that the expression level might be too low to detect. In fact, expression data from Wormbase and our RNA-seq data (see below) indicate that the overall expression level of *hpx-2* gene is extremely low at the whole worm level but increases significantly upon entry into dauer. When I subsequently analyzed dauer animals using confocal microscopy, I observed weak expression of *hpx-2*::GFP in the distal bulb of the pharynx in nearly all the animals (Figure 4.3 C). At higher magnification, the localization pattern was most consistent with expression in the gland cells (Figure 4.3 D) (134). Again, around 1% of the worms showed the striped expression pattern, resembling the structure called the "process" that extends from the dorsal g1 gland cell to the anterior of the buccal cavity

(Figure 4.3 E). Interestingly, the process functions in transporting excreted material from the gland cell to the pharyngeal lumen (135, 136). Overall, these results indicate that *hpx-2* is expressed in the epidermis and pharynx.

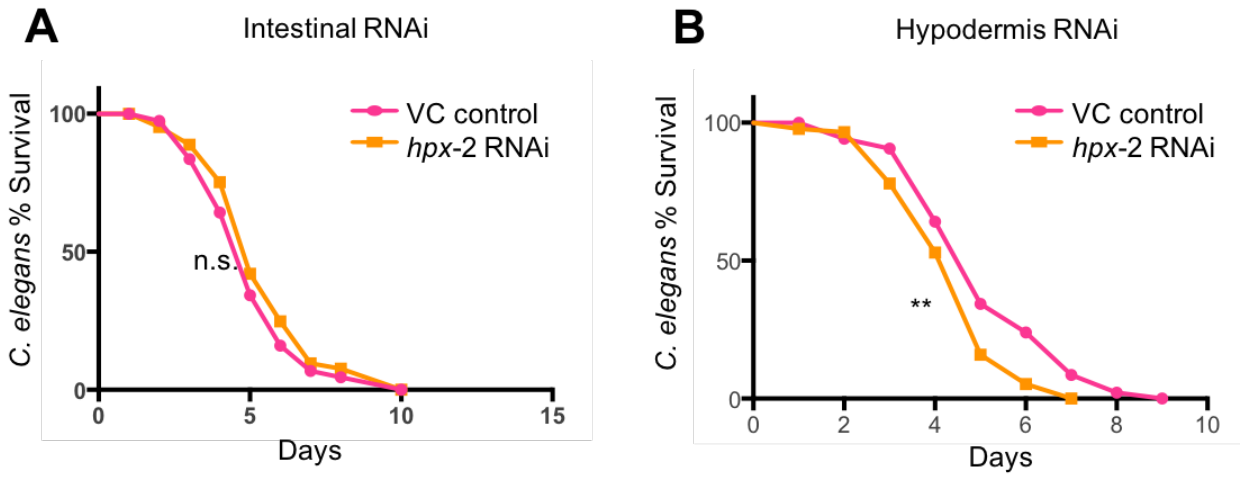

Figure 4.2. HPX-2 functionally localizes to the hypodermis of the worm. (A) Survival of the intestinal RNAi strain on *E. faecalis* following exposure to of *hpx-2* or VC control RNAi. (B) Survival of the hypodermal RNAi strain on *E. faecalis* following exposure to *hpx-2* or VC control RNAi. Representative results from single experiments with an n of approximately 90 worms for each condition are shown. Median survival and P-values along with replicates are listed in S8 Table as experiment No.1.

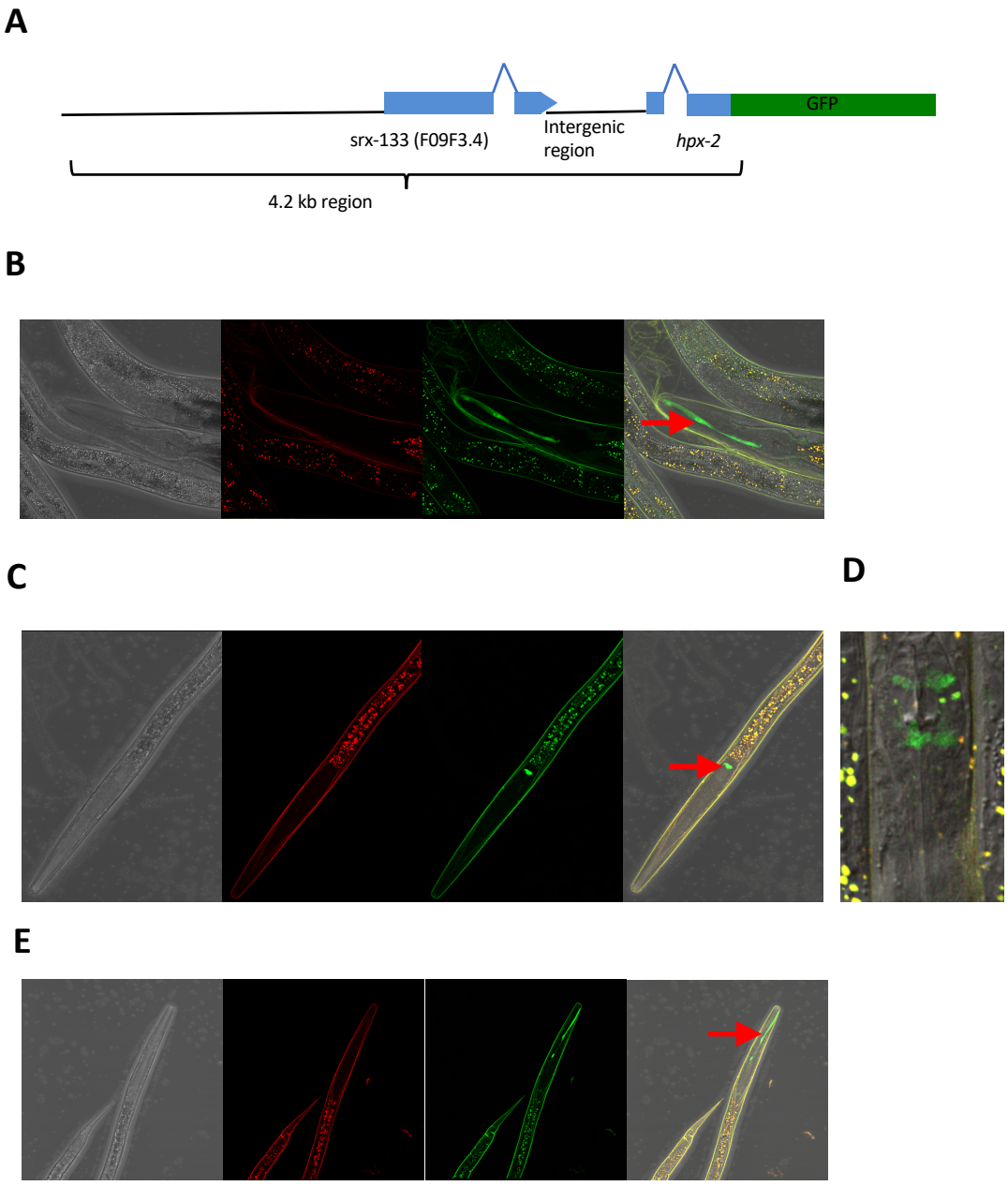

Figure 4.3. *hpx-2* is expressed in the pharynx. (A) Illustration of upstream region and the first two exons of the *hpx-2* gene that are fused to *gfp*. The expression pattern of *hpx-2*::*gfp* under the confocal microscope in (D) young-adult worms and (E-G) dauer worms. Red arrow head indicates the pharyngeal expression of *hpx-2*. (F) Higher magnification showing the pharyngeal expression pattern of *hpx-2*::*gfp*.

HPX-2 contributes to cuticle integrity

A functional role in cuticle biogenesis was demonstrated for some of the previously studied heme peroxidases and loss-of-function mutations sometimes caused abnormal cuticle morphology. For example, MLT-7, was shown to function in conjunction with BLI-3 to cross-link the cuticular collagens during the molting process. Loss of MLT-7 resulted in a blistered phenotype due to incomplete cross-linking of these extracellular matrix proteins (29). Another immune protective peroxidase previously studied by our lab, SKPO-1, has an incomplete penetrance of dumpy phenotype when mutated, again suggesting a role in cuticle generation (102).

Given the pathogen sensitivity phenotype that resulted from hypodermal-specific RNAi (Figure 4.2 B), I postulated that HPX-2 might play a role in the generation and/or structural integrity of the cuticle. However, unlike the *mlt-7* or *skpo-1* mutants, the *hpx-2* animals displayed normal morphology as observed under the dissecting microscope (Figure 3.10). To test for more subtle defects, cuticle integrity was measured by testing how permeable the animals were to a DNA dye (137). Specifically, I exposed the worms to the DNA staining agent Hoechst 33258 and scored how many exhibited nuclear staining of their hypodermal cells, evidence of dye penetration (Figure 4.4 A). While about 15% of N2 animals showed evidence of nuclear staining, 25-30% of the HPX-2 mutants displayed this phenotype, indicative of some loss of cuticle integrity (Figure 4.4 B).

Even though the loss of HPX-2 did not affect the low-resolution morphology of the worm, I observed that some of the strains generated by injection of higher amounts of the *hpx-2* complementation construct displayed a slightly dumpy or partial roller phenotype. These animals were also more sensitive to *E. faecalis* than wild-type or *hpx-2* mutant animals (Figure 4.5 A and B). I hypothesized that overexpression of *hpx-2* might be contributing to these phenotypes. The level of *hpx-2* expression in the different strain backgrounds was measured,

showing a correlation between higher mRNA levels and hyper-sensitivity to *E. faecalis* (Figure 4.4 C). The results indicate that too much as well as too little HPX-2 cause cuticle defects and sensitivity to the pathogen.

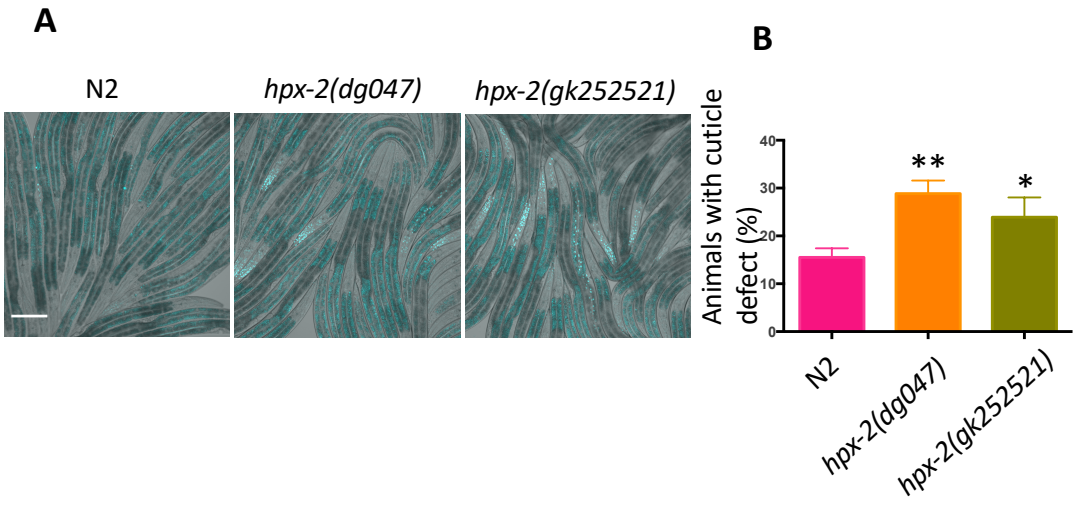

Figure 4.4. The cuticle defect of *hpx-2* mutants. (A) Hoechst staining of N2, *hpx-2(dg047)* and *hpx-2(gk252521)* worms. Worms with stained nuclei were scored as positive. Images presented are representative of ~300 worms observed. (B) Quantification of Hoechst positive worms in N2, *hpx-2(dg047)* and *hpx-2(gk252521)* worms. Compared with N2, both mutants had significant higher level of Hoechst staining ($P_{hpx\text{-}2(dg047)}$=0.0022, $P_{hpx\text{-}2(gk252521)}$=0.033). The graph was generated from 3 independent experiments (n=30). Error bars represent SEM.

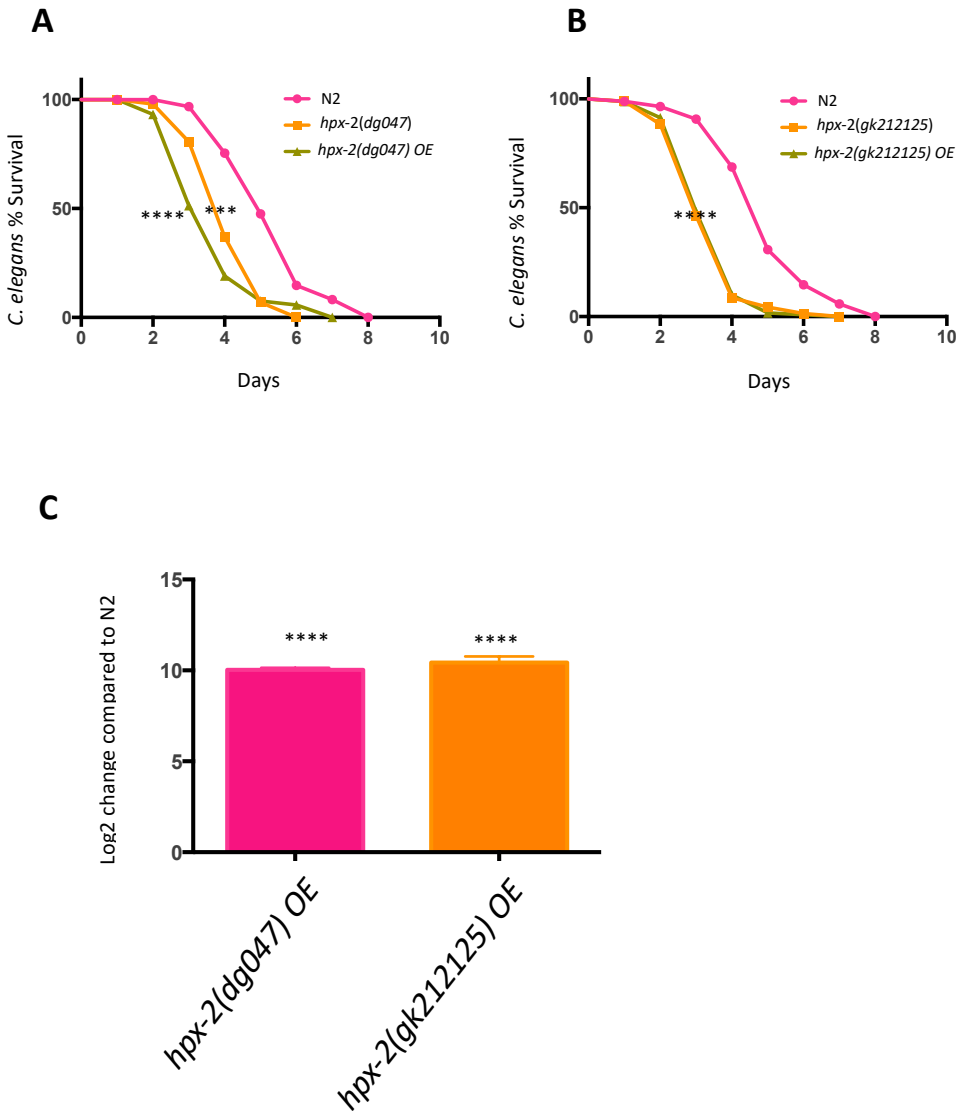

Figure 4.5. Overexpression of HPX-2 results in susceptibility to *E. faecalis.* (A) Survival of N2, *hpx-2(dg047),* and the strain overexpressing *hpx-2* in *hpx-2(dg047)* background on *E. faecalis* OG1RF. (B) Survival of N2*, hpx-2(gk252521*), and the strain overexpressing *hpx-2* in *hpx-2(gk252521*) background on *E. faecalis* OG1RF. (C) qRT PCR showing the relative $\log_2$ (fold change) of *hpx-2* gene expression level in *hpx-2(dg047)* overexpression (OE) and *hpx-2 (gk252521)* OE strains compared to N2. The average gene expression of biological triplicates is shown, and the error bars represent SEM.

HPX-2 limits colonization by *E. faecalis*, but has no effect on *P. aeruginosa*

I next examined the functional relevance of the pharyngeal presence of HPX-2, predicting it might contribute to this organ's structural integrity. The apical surface of the pharyngeal lumen is lined with cuticle, which connects to the cuticle of the epidermis. Specialized projections of the pharyngeal cuticle can form structures, such as the teeth-like formations found in the terminal bulb (grinder) that are thought to contribute to mechanical microbial disruption (135). HPX-2 was found to be expressed in the gland cells of the pharynx (Figure 4.3 B-E), and one hypothesis for its function is aiding cuticle development/remodeling of this organ following excretion into the pharyngeal lumen. I hypothesized that loss of *hpx-2* might weaken the pharynx, resulting in less disruption of ingested bacteria and increased intestinal colonization by pathogens. To test this hypothesis, I exposed L4 worms to a strain of *E. faecalis* OG1RF that constitutively expresses GFP and measured the level of intestinal colonization by both fluorescence microscopy and CFU plating (115). At Day 2 of infection, I observed a higher level of intestinal colonization in the *hpx-2* mutant strains, indicated by higher fluorescent intensity and CFU counts (Figure 4.6 A and B). In contrast, when I exposed worms to a *P. aeruginosa* PA14 strain expressing dsRed (117), I did not observe any significant differences between the N2 strain and the mutants in either fluorescent intensity or CFUs (Figure 4.6 C and D), which is consistent with the observation that N2 and *hpx-2* mutants are equally susceptible to *P. aeruginosa* (Figure 3.12 D). Although the *hpx-2* mutant might have impaired grinding capability, no obvious structural abnormalities of the pharynx were observed when examined by light microscopy (Figure 4.7 A). In addition, the pumping rate of the worms was not significantly affected (Figure 4.7 B). Together, these results suggest that HPX-2 functions in the pharynx to reduce intestinal colonization by some pathogens, possibility through the structural reinforcement of the grinder or other parts of the pharyngeal cuticle.

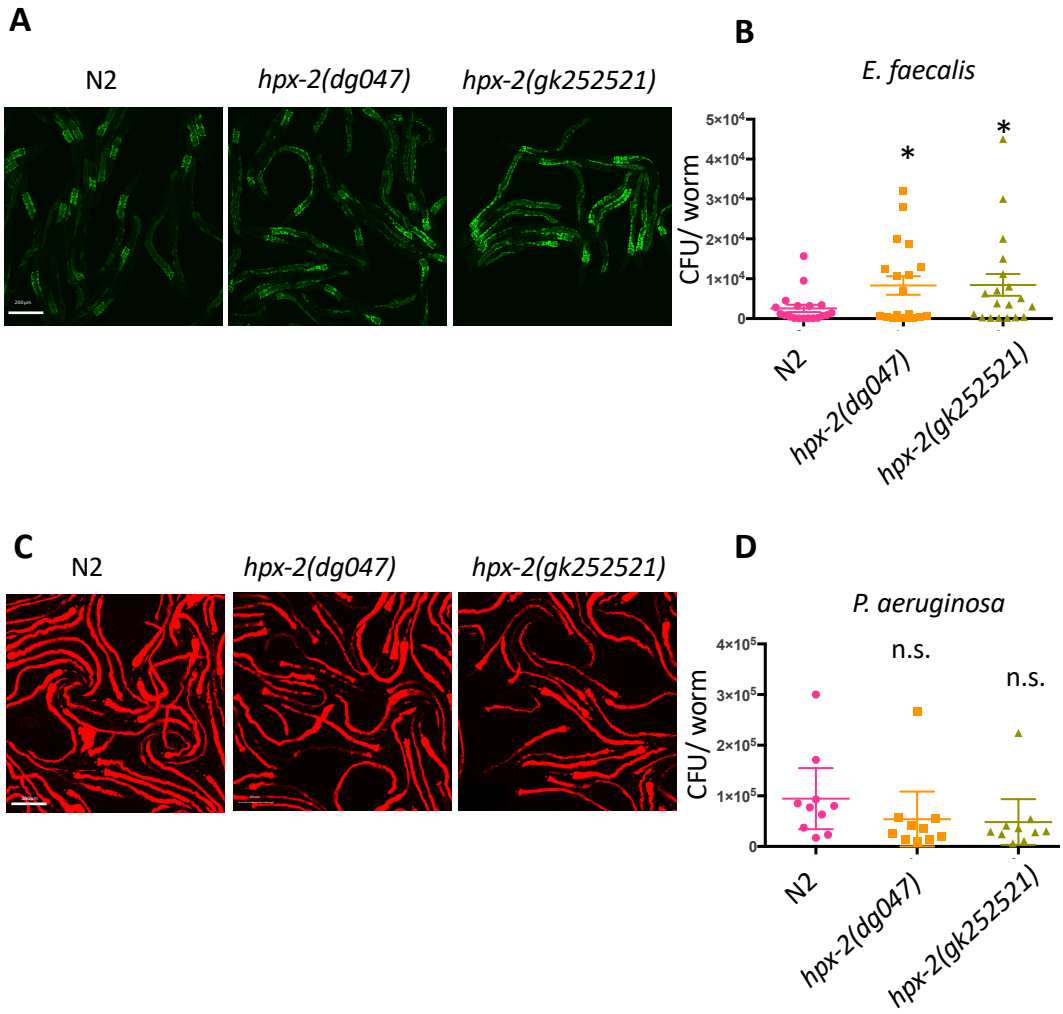

Figure 4.6. Intestinal colonization of *hpx-2* mutants by pathogens. Colonization of (A) GFP-labeled *E. faecalis* OG1RF and (C) dsRed labeled *P. aeruginosa* PA14 in N2, *hpx-2(dg047)* and *hpx-2(gk252521)* worms at day two and day one of infection, respectively. (B) *E. faecalis* CFU counts per worm ($P_{hpx\text{-}2(dg047)}$ = 0.0471, $P_{hpx\text{-}2(gk252521)}$ =0.0275, n=19 (combined from 3 independent experiments)). (D) *E. faecalis* CFU counts per worm ($P_{hpx\text{-}2(dg047)}$ =0.1833, $P_{hpx\text{-}2(gk252521)}$ =0.2724, n =19 (combined from 3 independent experiments)). Error bars represent SEM.

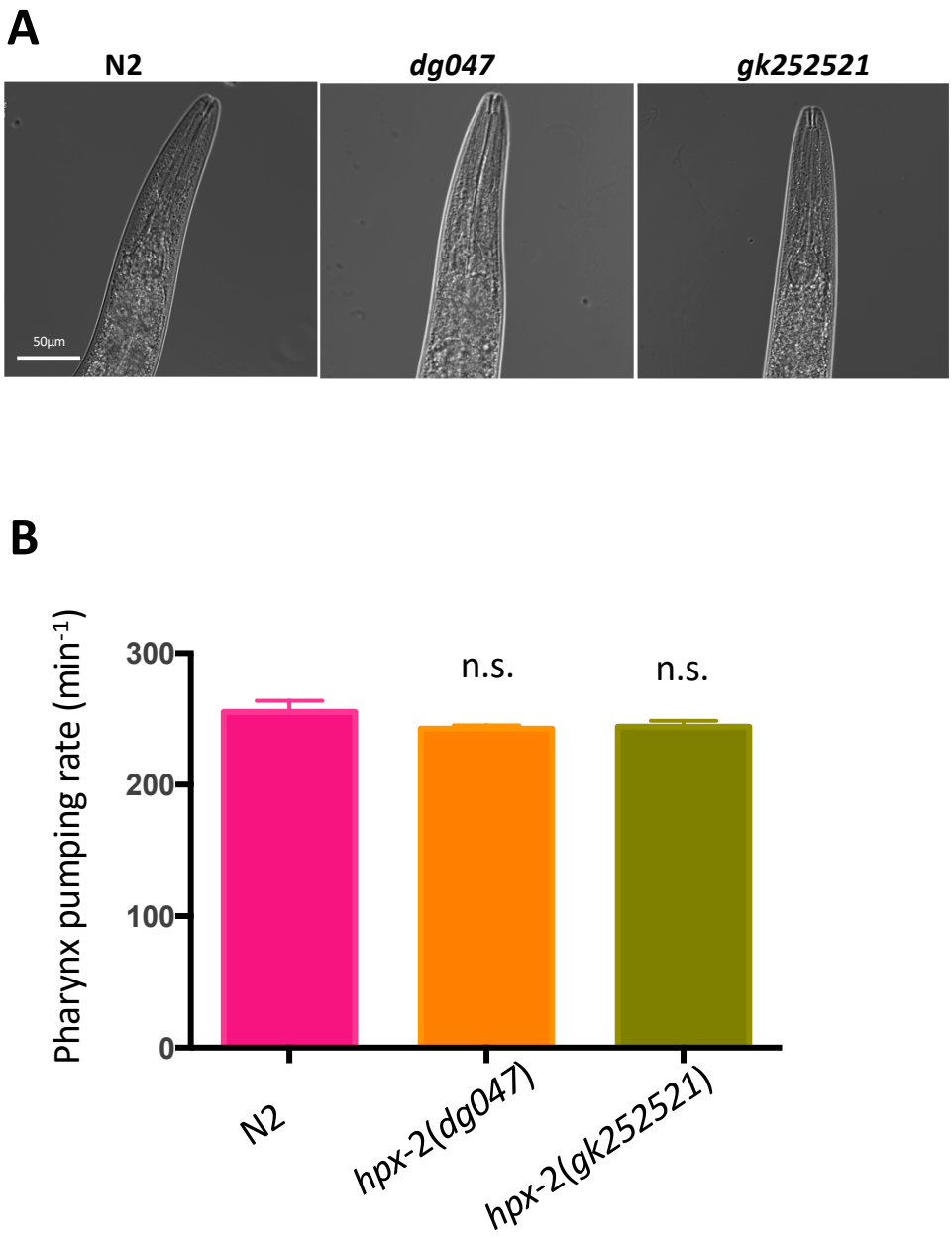

Figure 4.7. *hpx-2* mutants exhibit normal pharyngeal traits. (A) *hpx-2* mutants have normal pharynx structure compared to N2 worms. Images are representative of >100 N2, *hpx-2(dg047), hpx-2(gk252521)* worms observed, respectively (C) *hpx-2* mutants have comparable pumping rates compared to N2 worms. $P_{hpx\text{-}2(dg047)}$ =0.071, $P_{hpx\text{-}2(gk252521)}$ =0.1147, n =15

The catalytic activity of HPX-2 is required for resistance to pathogens

Sequence comparison of HPX-2 to other peroxidases indicates that HPX-2 possesses all the conserved residues required for peroxidase catalytic activity, including the distal histidine (H^{240}), the catalytic arginine (R^{372}), and the proximal histidine (H^{240}) (reviewed by (138)). On the other hand, similar to BLI-3 and MLT-7, HPX-2 lacks the covalent heme-binding residues that are conserved in mammalian peroxidases (138). However, this does not rule out the possibility of non-covalent heme binding since both human DUOX1 and DUOX2 lack the conserved residues but still bind heme weakly (139, 140). Thus, I hypothesize HPX-2 has peroxidase activity.

To test this hypothesis, I used an Amplex red assay that measures pathogen-stimulated H_2O_2 release in the *hpx-2* mutant strain *hpx-2(dg047)* (99) (98). In previous work, a *skpo-1* mutant was characterized as releasing more H_2O_2 than N2 when exposed to the pathogen *E. faecalis*, presumably because less H_2O_2 was being consumed (102). In contrast, I found H_2O_2 levels generated by the *hpx-2(dg047)* mutant were comparable to N2 following exposure to *E. faecalis* (Figure 4.8). While this could be because HPX-2 possesses little peroxidase activity, it also could be due to its low expression level or a lack of activity under these conditions.

To directly test the activity of HPX-2 using in vitro assays, I attempted to express the HPX-2 recombinant protein in *E. coli* expression system. Specifically, the cDNA of *hpx-2* encoding full-length protein excluding the signal peptide of HPX-2 was cloned into expression vector pET-29b (+) and transformed into in *E. coli* BL21 (DE3). Unfortunately, upon induction, I could not detect any expression of the recombinant protein through SDS-PAGE and Coomassie staining. Although a weak band can be detected by Western blotting using anti-His antibody, the amount was too little to be used in any biochemical assays.

To further examine the possible contribution of HPX-2's peroxidase activity to pathogen resistance, I analyzed a strain harboring a single amino acid mutation that changes an active

site residue of the peroxidase domain. Specifically, the catalytic arginine residue was substituted to alanine through CRISPR-Cas9 mediated mutagenesis (Figure 4.9 A). The catalytic arginine is conserved throughout peroxidase–cyclooxygenase superfamily, and the substitution of the arginine to alanine abolishes peroxidase activity (141, 142). Like the *hpx-2* deletion mutants, this point mutant exhibited increased sensitivity to *E. faecalis*, suggesting that the catalytic activity of the peroxidase active site of HPX-2 is required for the pathogen resistance phenotype (Figure 4.9 B).

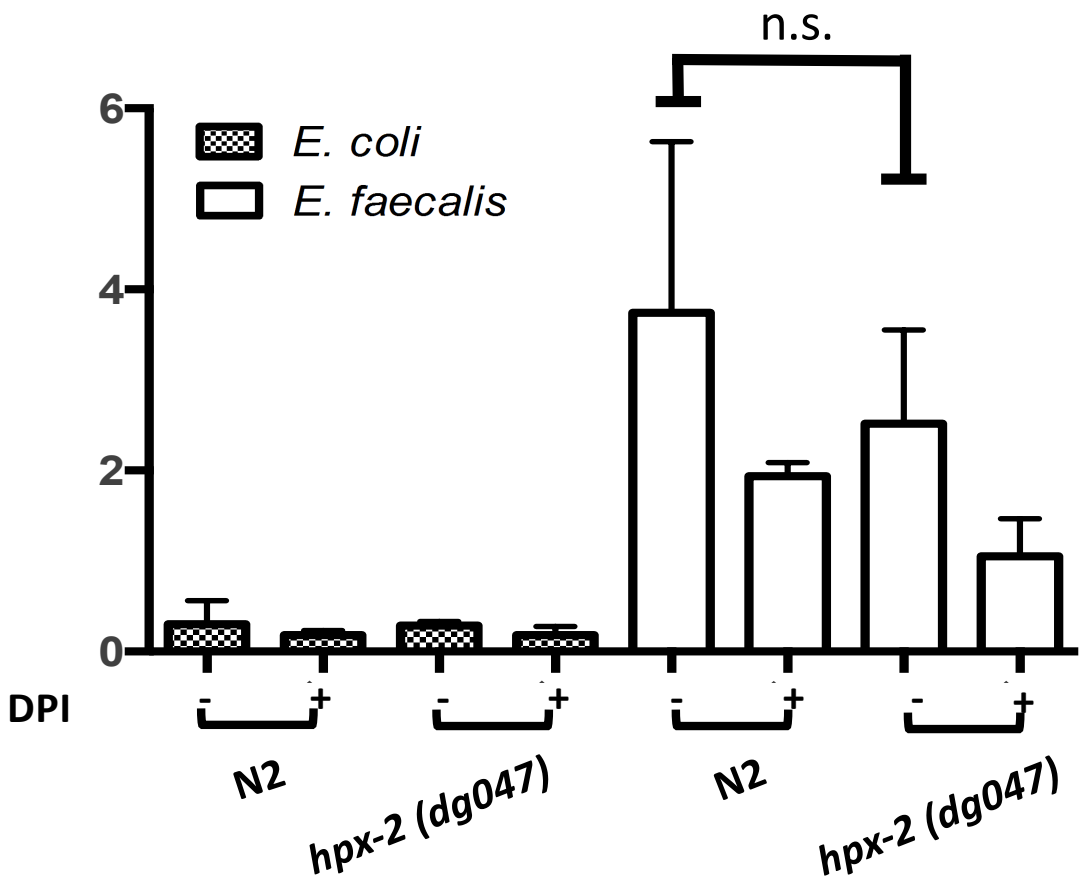

Figure 4.8 Amplex red assay of N2 and *hpx-2(dg047)* mutant. Worms were grown to L4 stage and exposed to *E. coli* OP50 or *E. faecalis* OG1RF for 16 hours at 25°C. The amount of H_2O_2 was then measured with or without exposure to 80mM diphenyleneiodinium chloride (DPI). Error bars represent the SEM and P values were calculated via Student's paired t-test. Data is representative of three independent replicates.

A

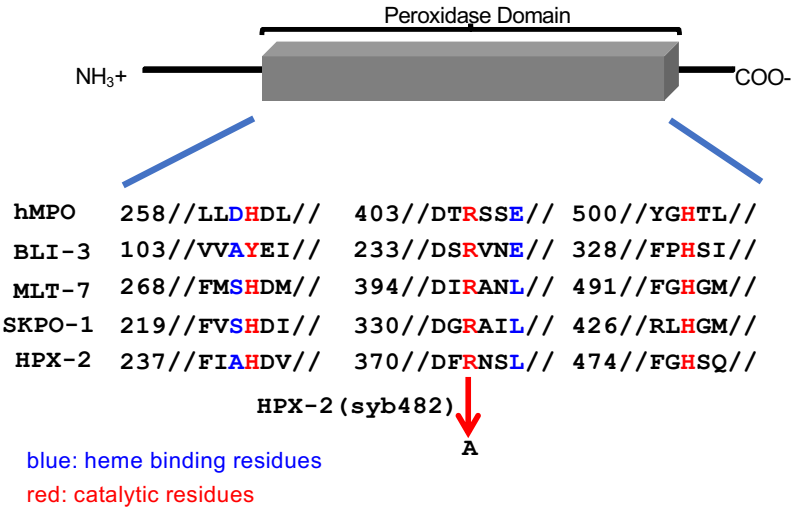

B

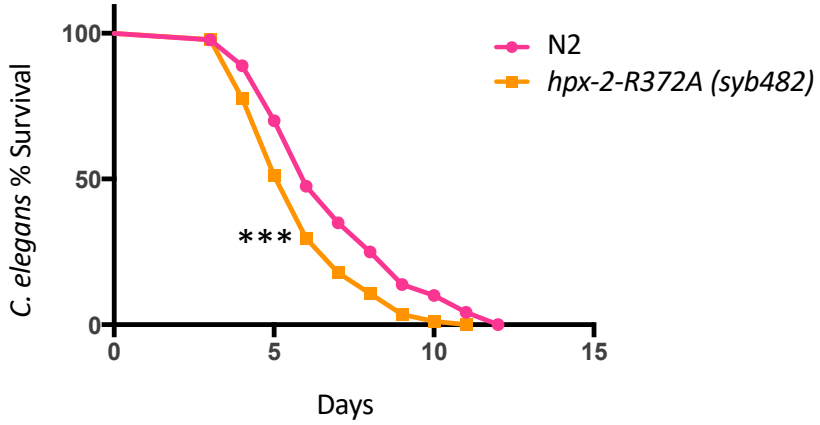

Figure 4.9. HPX-2 peroxidase activity is required for pathogen resistance. (A) Sequence alignment of the peroxidase domain of HPX-2 and HPX-2 site-directed (SD) mutant to other peroxidases and DUOX. hMPO, human myeloperoxidase. (B) The survival of N2 and HPX-2-SD strain *(hpx-2 (syb238)*) on *E. faecalis*. Results from one representative experiment with an n of approximately 90 worms for each condition are shown. Median survival and P-values are listed in Table 4.1 as experiment No.1 along with other biological replicates.

Figure number	Experiment number	Strain	Exposure conditions	Median survival (days)	P-value
3A	1	*vha-2* VC RNAi	*E. faecalis*	5	C
		vha-2 hpx-2 RNAi	*E. faecalis*	5	0.8339
	2	*vha-2* VC RNAi	*E. faecalis*	5	C
		vha-2 hpx-2 RNAi	*E. faecalis*	3	0.9548
3B	1	*wrt-2* VC RNAi	*E. faecalis*	5	C
		wrt-2 hpx-2 RNAi	*E. faecalis*	5	0.0022
	2	*wrt-2* VC RNAi	*E. faecalis*	5	C
		wrt-2 hpx-2 RNAi	*E. faecalis*	3	0.0029
	3	*wrt-2* VC RNAi	*E. faecalis*	5	C
		wrt-2 hpx-2 RNAi	*E. faecalis*	4	0.0005
4.8 B	1	N2	*E. faecalis*	6	C
		hpx-2(syb482)	*E. faecalis*	6	0.0005
	2	N2	*E. faecalis*	4	C
		hpx-2(syb482)	*E. faecalis*	4	0.0145

Table 4.1 Median survival and P-values in killing assays

Discussion

In this chapter, I demonstrated that HPX-2 is produced in the pharynx and hypodermis of the worms, as well as its function in cuticle strengthening and pathogen resistance.

Pharyngeal function of HPX-2

In the pharynx, the expression pattern of *hpx-2::GFP* resembles that of the gland cell reporter gene B02807::GFP (143, 144), with expression being observed in the process that extends from the terminal bulb to the posterior end of the buccal cavity. There are two groups of gland cells, three g1 cells and two g2 cells, located at the distal bulb of the pharynx. The gland cells are thought to secrete vesicles containing enzymes that function in the digestion of microbial food and aid in cuticle formation during the molting process (136). Specifically, during the feeding process, small vesicles are transported from the g1 cells through the process to the secretory ducts to aid digestion. During molting, much larger vesicles are transported through the process and the enzymes they contain are thought to be involved in the tearing down and building up of the cuticle, a critical remodeling process (136).

I postulate that HPX-2 is protective by virtue of it being secreted into the pharyngeal lumen by gland cells to aid in cuticle remodeling of the pharynx during development. A properly developed pharyngeal cuticle is likely necessary for effective disruption of microbes during the digestive process. Because Gram-positive bacteria and fungi like *C. albicans* have thicker, harder-to-disrupt cell walls, this model could explain why the *hpx-2* mutants were colonized more efficiently by, and were more susceptible to, these pathogens compared to Gram-negative bacteria (Figures 3.12). The cell envelope of Gram-negatives is comprised of two membranes, but only a thin layer of peptidoglycan, rendering these organisms easier to disrupt by mechanical means (Reviewed in (145)), and may explain why the *hpx-2* mutants were not more susceptible to them.

In previous studies examining staged animals, significant levels of *hpx-2* expression were only observed during dauer (146). Using lines expressing an HPX-2::GFP fusion, I also detected expression during dauer in most animals examined (Figure 4.3). However, I did not observe GFP expression in the vast majority of animals at other stages (L1-L4 and adult) and during pathogen exposure. Using the HPX-2::GFP line, I occasionally saw expression in the pharynx of animals examined at the L4 to young adult stages and speculate that they might be animals undergoing molting. Based on all these observations, I speculate that *hpx-2* is expressed during times of cuticle remodeling, including the larval molts and dauer formation. Additionally, HPX-2 may be subject to mechanisms of post-transcriptional regulation that would not necessarily be elucidated by these approaches focused on transcriptional regulation.

Hypodermal function of HPX-2

Peroxidases play important roles in cuticle bio-generation process and loss-of-function mutants frequently exhibit morphological defects. Mutations in MLT-7 or the peroxidase domain of BLI-3 result in severe blister phenotypes (29, 147). *skpo-1* mutants have a partially penetrant dumpy phenotype (102). Loss of HPX-2 did not result in a morphological phenotype observable by light-microscopy. However, the increase in cuticle permeability, as evidenced by Hoechst staining, indicates some perturbation of the cuticle. Additionally, overexpression of *hpx-2,* by injection of higher concentrations of the transgene, resulted in some *dpy* and *rol* animals, again indicative of HPX-2 playing a role cuticle biogenesis. Tissue-specific RNAi knock-down of *hpx-2* in the hypodermis resulted in a weak susceptibility phenotype. Collectively, these data suggest that *hpx-2* is expressed and plays an infection-protective role in the hypodermis, though expression of our HPX-2::GFP transgene was not detectable in this tissue.

How might a cuticle impaired by lack of HPX-2 translate into susceptibility to pathogen? First of all, it is important to note that not all cuticle defects alter sensitivity. For example, *mlt-7*

mutations and *bli-3* peroxidase domain mutations result in severe blistered phenotypes, with no concomitant increase in pathogen susceptibility (99, 102) Interestingly, a recent study showed that disruption of some, but not all, aspects of cuticle structure triggers the activation of multiple stress response pathways (148). Specifically, it was discovered that disruption of the annular furrows activates detoxification, osmolyte, and most importantly, antimicrobial responses. In regard to HPX-2, I hypothesize that structural disturbance of the hypodermal cuticle perturbs signal transduction related to innate immune and/or stress responses. However, a precise understanding will require more detailed knowledge of exactly how HPX-2 modulates cuticle structure.

In conclusion, I report the characterization of a peroxidase, HPX-2, that functions protectively against multiple pathogen infections in *C. elegans*. The data suggest that HPX-2 contributes in a peroxidase-dependent manner either directly, by modulating the cuticular structure, and/or indirectly, by affecting downstream innate immune and/or stress responses pathways. While further investigations will be required to elucidate the precise mechanism, our findings highlight the complexity and multiple factors involved in pathogen defense.

Chapter 5 Transcriptome analysis reveals that hpx-2 mutant misregulates genes for cuticle synthesis and has a stronger response to infection.

Introduction

In the last two chapters, I demonstrated that HPX-2 is expressed in the pharynx and hypodermis of the worm and functions in pathogen resistance. More specifically, it reduced intestinal colonization of Gram-positive bacteria. I also showed that over-expression of HPX-2 not only resulted in pathogen susceptibility comparable to *hpx-2* mutants, but also caused abnormal body morphology, i.e. occasional dumpy and roller phenotypes. These findings strongly suggest that HPX-2 plays roles in pathogen resistance and cuticle biogenesis. However, the exact mechanisms and the pathways by which HPX-2 operates in these two processes are not clear. Furthermore, the loss of HPX-2 did not result in any physiological changes in the animal under non-pathogenic conditions, making it hard to pin-point the functions of HPX-2 during normal development of the worms. Thus, I decided to utilize RNAseq analysis as an un-biased and highly sensitive method to measure the changes in gene expression profile, which reflects the overall physiology of the animal. I also decided to examine *hpx-2* animals exposed to the pathogen *E. faecalis* to determine if the innate immune response was significantly different than that of the N2 reference strain. I believe that investigating the global transcriptional changes in both the *hpx-2* mutant and the N2 wild-type, under non-pathogenic and pathogenic conditions might uncover some insights into the mechanisms and pathways by which HPX-2 influences pathogen susceptibility and cuticle development.

Results

Transcriptome analysis reveals that *hpx-2* mutant misregulates genes for cuticle syntheses.

To better understand how the loss of HPX-2 affected the global gene profile of the worm, I examined the differences in gene expression of a *hpx-2* mutant (*hpx-2(dg047))* compared to the N2 reference strain under both non-pathogenic (exposed to *E. coli* OP50) and pathogenic (exposed to *E. faecalis* OG1RF) conditions.

First, under the non-pathogenic condition (exposed to *E. coli* OP50), there were a total of 69 genes that were significantly differentially expressed in the mutant, with 34 genes up-regulated and 35 down-regulated. 21 of the affected genes encode structural constituents of the cuticle, including 17 *col* genes, 3 *dpy* genes (*dpy-3, dpy-4,* and *dpy-5*), and 2 *rol* genes (*rol-1* and *rol-6*). GO term analysis further revealed an enrichment of genes that are involved. All of them are downregulated, suggesting a perturbed cuticle biogeneration process upon the loss of HPX-2 (Table 5.1). In addition, genes involved in locomotion are also affected, which could explain the partial roller and dumpy phenotype in the HPX-2 overexpression strains examined in chapter 4 (Table 5.1).

hpx-2(dg047) on OP50 vs. N2 on OP50				
Category	**Term**	**Count**	**Fold Enrichment**	**P-value**
BP	body morphogenesis	32	6.6	8.30E-18
BP	locomotion	39	3.5	5.30E-13
BP	collagen and cuticulin-based cuticle development	11	12.4	1.50E-08
BP	molting cycle, collagen and cuticulin-based cuticle	14	6	4.80E-07
BP	cellular response to osmotic stress	5	42.6	4.30E-06
BP	UV protection	5	39.9	5.70E-06
BP	single-organism transport	4	73	1.50E-05
BP	molting cycle process	4	30.1	2.80E-04
BP	cuticle development	4	26.9	4.00E-04
BP	epithelial cell development	4	21.3	8.10E-04
BP	intein-mediated protein splicing	3	42.6	2.10E-03
BP	cuticle development involved in collagen and cuticulin-based cuticle molting cycle	3	42.6	2.10E-03
BP	response to osmotic stress	3	38.3	2.60E-03
BP	response to oxidative stress	5	8.5	2.70E-03
BP	cell-cell signaling	3	34.8	3.10E-03
BP	nematode larval development	27	1.7	3.80E-03
BP	MAPK cascade	3	16.7	1.30E-02
BP	defense response	5	5.3	1.40E-02
BP	regulation of multicellular organism growth	3	13.7	2.00E-02
BP	nematode male tail tip morphogenesis	4	6.6	2.20E-02
BP	segment polarity determination	2	63.9	3.10E-02
BP	protein catabolic process	5	4.1	3.30E-02
CC	collagen trimer	35	26	5.50E-40
CC	cell periphery	6	32.3	8.80E-07
CC	collagen and cuticulin-based cuticle extracellular matrix	5	58.7	1.00E-06
CC	extracellular region	10	3.9	9.40E-04
MF	structural constituent of cuticle	41	30	2.30E-51
MF	structural constituent of collagen and cuticulin-based cuticle	7	39.2	1.50E-08
MF	MAP kinase activity	3	28.4	4.70E-03
MF	hydrolase activity, acting on carbon-nitrogen (but not peptide) bonds	2	18.9	9.90E-02

Table 5.1: GO Term analysis of genes that changed upon loss of HPX-2 (hpx-2(dg047)) compared to N2, when exposed to E. coli OP50. Genes that are involved in cuticle generation and body morphogenesis are enriched in the *hpx-2* mutant. BP: Biological Processes; MF: Molecular Functions. CC: Cellular Component.

I next analyzed gene expression changes in a *hpx-2* mutant after 16 hours of exposure to *E. faecalis* OG1RF compared to N2 strain. I chose this early time point because the worms show limited damage and thus the indirect effects should be smaller than later during infection. Under these conditions, there were a total of 125 genes that were differentially expressed in the mutant (72 up-regulated and 53 down-regulated) with 106 of them unique to the pathogenic condition. Interestingly, genes involved in cuticle generation were again significantly altered, and with a greater enrichment score (Table 5.2). Compared to the 21 genes under nonpathogenic conditions, a total of 41 cuticle genes were affected and up-regulated. In addition to the increased changes in cuticle structural genes, there was an enrichment of genes encoding proteins involved in defense response to Gram-positive bacteria (Table 5.2). These include 4 out of 10 lysozyme genes (*lys-1, lys-2, lys-3,* and *lys-7), and f53a9.8,* which is involved in defense response against Gram-positive bacteria and expressed in the intestine (144, 149, 150). Additionally, genes that are involved in general innate immune response, response to Gram-negative, and xenobiotic stress response were also enriched, although there was some overlap of genes in those groups (Table 5.2).

In order to verify the RNAseq result, I performed qRT-PCR on 10 genes that are changed in expression in the *hpx-2* mutant compared to N2 under the pathogenic condition. The $\log_2$ change in gene expression from qRT data was then plotted against the RNAseq data to evaluate their correlation (Figure 5.1). Trend line analysis revealed that $R^2 > 0.9$, suggesting consistency between the RNAseq data and the qRT-PCR data.

Finally, in order to compare the genes that were differentially expressed under the non-pathogenic compared to the pathogenic condition, I plotted the gene lists against each other (Figure 5.2). In general, there was a close correlation between the two conditions, meaning genes that were differentially expressed under one condition were also changed in the other,

although the degree of changes was sometimes different. In addition, the degree of fold-change was quite small with majority of the $\log_2$ changes less than 2 (Figure 5.2).

hpx-2(dg047) on OG1RF vs. N2 on OG1RF				
Category	**Term**	**Count**	**Fold Enrichment**	**P-value**
BP	innate immune response	21	5.7	4.80E-10
BP	metabolic process	32	2.6	8.00E-07
BP	response to xenobiotic stimulus	5	54.2	1.10E-06
BP	defense response to Gram-negative bacterium	9	9.3	5.00E-06
BP	defense response	10	7.2	9.80E-06
BP	defense response to Gram-positive bacterium	6	13	8.70E-05
BP	response to nematicide	4	31.6	2.30E-04
BP	flavonoid glucuronidation	6	7.3	1.30E-03
BP	flavonoid biosynthetic process	6	7.3	1.30E-03
BP	MAPK cascade	4	15.1	2.20E-03
BP	response to osmotic stress	3	26	5.50E-03
BP	transmembrane transport	11	2.3	2.00E-02
BP	proteolysis involved in cellular protein catabolic process	4	6	2.90E-02
BP	oxidation-reduction process	11	1.8	7.60E-02
BP	monocarboxylic acid transport	2	21.7	8.80E-02
BP	response to gamma radiation	2	19.3	9.80E-02
CC	intracellular membrane-bounded organelle	7	6.1	9.40E-04
CC	extracellular region	11	3.4	1.50E-03
CC	lysosome	5	6.9	5.90E-03
CC	collagen trimer	7	4.1	7.10E-03
CC	membrane raft	4	5.6	3.30E-02
MF	ATPase activity, coupled to transmembrane movement of substances	7	7	6.00E-05
MF	iron ion binding	8	8	6.50E-04
MF	steroid hydroxylase activity	5	5	1.30E-03
MF	carbohydrate binding	12	12	1.50E-03
MF	ATPase activity	7	7	1.70E-03
MF	efflux transmembrane transporter activity	3	3	2.30E-03
MF	heme binding	8	8	3.50E-03
MF	transferase activity, transferring hexosyl groups	6	6	4.10E-03
MF	oxidoreductase activity, acting on paired donors, with incorporation or reduction of molecular oxygen	6	6	4.50E-03
MF	structural constituent of cuticle	8	8	5.60E-03
MF	monooxygenase activity	6	6	7.30E-03
MF	glucuronosyltransferase activity	5	5	9.90E-03
MF	MAP kinase activity	3	3	1.10E-02
MF	ATP binding	20	20	3.20E-02
MF	oxidoreductase activity	11	11	4.30E-02
MF	nutrient reservoir activity	2	2	7.40E-02
MF	protein serine/threonine kinase activity	8	8	7.90E-02
MF	cysteine-type endopeptidase activity	3	3	9.20E-02

MF	monocarboxylic acid transmembrane transporter activity	2	2	9.80E-02

Table 5.2: GO Term analysis of genes that changed upon loss of HPX-2 (hpx-2(dg047)) compared to N2, when exposed to E. faecalis OG1RF. Genes that are involved in cuticle generation and body morphogenesis are further enriched in the *hpx-2* mutant. Additionally, defense response genes are enriched as well. BP: Biological Processes; MF: Molecular Functions. CC: Cellular Component.

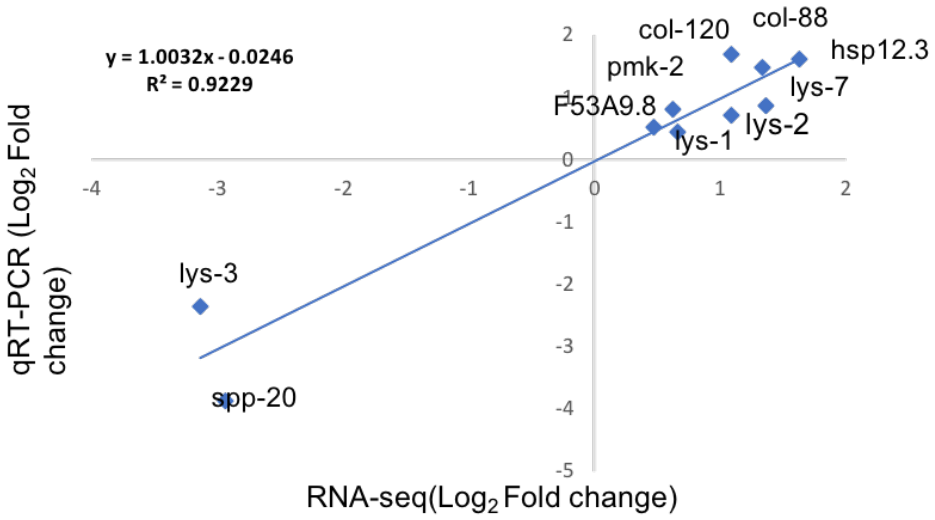

Figure 5.1 qRT-PCR validation of 10 selected genes differentially expressed in the RNA-seq analysis of *hpx-2(dg047)* to N2 on *E. faecalis*. Mean $\log_2$ (fold change) determined in three independent qRT-PCR were plotted against the $\log_2$ (fold change) from the RNAseq experiments.

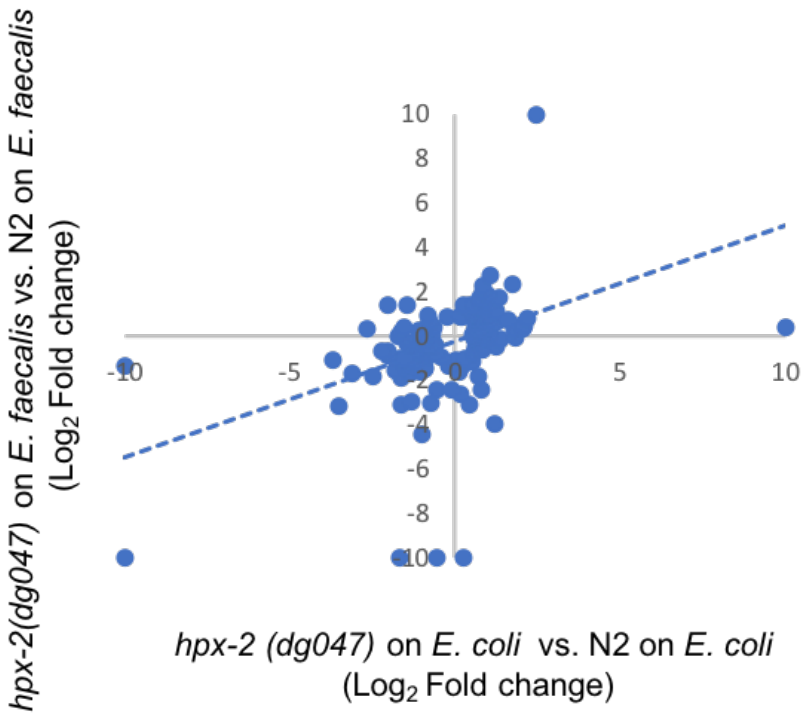

Figure 5.2. Scatter plot of genes changed in *hpx-2(dg047)* animals, as compared to N2 animals, when either exposed to *E. coli* (x-axis) or *E. faecalis* (y-axis). Values of 10 or -10 indicate expression level under one condition was 0 RPKM.

Transcriptome analysis reveals a stronger response in *hpx-2* mutant upon infection.

To understand the general response of the worms when exposed to *E. faecalis,* I examined the gene profiles of animals exposed to *E. faecalis* as compared to those exposed to OP50. Not surprisingly, there were a great number of genes that were differentially expressed when exposed to pathogen, suggesting a global reaction that involves in host defense. In N2, a total of 4217 genes (2560 up-regulated and 1657 down-regulated) were significantly differentially expressed, many of which were consistent with previously published data (79). GO term analysis revealed a long list of genes that are involved in multiple physiological process, with innate immune response being the most significant one (Table 5.3). In the *hpx-2* mutant, however, an even larger number of genes were significantly differentially expressed: 8313 genes in total with 4255 of them up-regulated and 4058 down-regulated (Table 5.4). To examine the relationship between the two sets of genes, genes that were significantly expressed under at least one condition were plotted (Figure 5.3). Compared to the N2 strain, the *hpx-2* mutant had similar, but stronger responses to the pathogen, contributing to the larger number of genes with significant changes in expression under the pathogenic condition. In summary, we conclude that the loss of *hpx-2* results in a stronger response to infection, perhaps reflecting the increased microbial load experienced by this strain during *E. faecalis* infection (Figure 4.6 A and B).

N2 on OP50 vs. N2 on OG1RF				
Category	**Term**	**Count**	**Fold Enrichment**	**P-value**
BP	innate immune response	70	3.3	3.30E-19
BP	oxidation-reduction process	74	2.1	7.40E-10
BP	metabolic process	120	1.7	4.90E-09
BP	flavonoid glucuronidation	21	4.4	2.00E-08
BP	flavonoid biosynthetic process	21	4.4	2.00E-08
BP	cell projection organization	10	8.3	6.80E-07
BP	nonmotile primary cilium assembly	11	5	3.60E-05
BP	defense response to Gram-negative bacterium	17	3	1.10E-04
BP	cilium assembly	10	4.8	1.30E-04
BP	dauer entry	12	3.7	3.00E-04
BP	steroid hormone mediated signaling pathway	35	1.9	5.00E-04
BP	single-organism transport	5	10.7	5.80E-04
BP	fatty acid metabolic process	11	3.5	8.70E-04
BP	defense response to Gram-positive bacterium	10	3.8	1.00E-03
BP	response to xenobiotic stimulus	5	9.4	1.10E-03
BP	lipid metabolic process	26	1.9	3.50E-03
BP	epithelial cell development	7	4.4	4.00E-03
BP	defense response	17	2.1	6.30E-03
BP	transcription, DNA-templated	54	1.4	9.80E-03
BP	transmembrane transport	41	1.5	1.10E-02
BP	fatty acid beta-oxidation	6	4.3	1.10E-02
BP	positive regulation of transcription from RNA polymerase II promoter	20	1.9	1.10E-02
BP	homophilic cell adhesion via plasma membrane adhesion molecules	5	5.4	1.10E-02
BP	cell-matrix adhesion	4	7.5	1.30E-02
BP	regulation of transcription, DNA-templated	67	1.3	1.40E-02
BP	negative regulation of transcription from RNA polymerase II promoter	13	2.2	1.40E-02
BP	carbohydrate metabolic process	19	1.8	1.60E-02
BP	collagen and cuticulin-based cuticle development	15	2	1.70E-02
BP	neuron differentiation	5	4.7	1.90E-02
BP	molting cycle process	5	4.4	2.30E-02
BP	regulation of neuron differentiation	4	5.5	3.20E-02
BP	response to nematicide	4	5.5	3.20E-02
BP	cuticle development	5	4	3.40E-02
BP	vulval location	5	4	3.40E-02
BP	heme transport	3	9	3.90E-02
BP	interneuron axon guidance	3	9	3.90E-02
BP	nervous system development	11	2.1	3.90E-02
BP	one-carbon metabolic process	4	4.6	5.10E-02
BP	intraciliary transport	4	4.6	5.10E-02
BP	sphingolipid metabolic process	6	2.9	5.20E-02

BP	anion transport	9	2.2	5.20E-02
BP	macromolecule glycosylation	5	3.4	5.40E-02
BP	MAPK cascade	5	3.3	6.30E-02
BP	lipid storage	56	1.2	6.80E-02
BP	dephosphorylation	8	2.2	7.10E-02
BP	fatty acid beta-oxidation using acyl-CoA dehydrogenase	5	3.1	7.10E-02
BP	cell wall macromolecule catabolic process	3	6.4	7.40E-02
BP	proteolysis involved in cellular protein catabolic process	8	2.1	8.90E-02
BP	protein localization to ciliary transition zone	3	5.6	9.50E-02
BP	unsaturated fatty acid biosynthetic process	3	5.6	9.50E-02
BP	intraciliary retrograde transport	3	5.6	9.50E-02
BP	regulation of backward locomotion	3	5.6	9.50E-02
CC	collagen trimer	40	3.6	3.40E-12
CC	intracellular membrane-bounded organelle	27	3.6	1.40E-08
CC	extracellular region	49	2.3	7.70E-08
CC	membrane raft	20	4.3	8.10E-08
CC	ciliary basal body	9	6.7	2.70E-05
CC	extracellular space	35	2.1	4.80E-05
CC	BBSome	5	11.1	5.00E-04
CC	cilium	10	3.2	3.10E-03
CC	lysosome	12	2.5	7.20E-03
CC	cell projection	13	2	3.00E-02
CC	gut granule membrane	3	9.3	3.60E-02
CC	intraciliary transport particle B	4	5.2	3.70E-02
CC	apical plasma membrane	9	2.2	4.70E-02
CC	proteinaceous extracellular matrix	6	2.9	5.10E-02
CC	nonmotile primary cilium	9	2	8.40E-02
CC	peroxisome	6	2.5	9.40E-02
MF	structural constituent of cuticle	40	3.3	2.40E-11
MF	monooxygenase activity	28	4.1	2.30E-10
MF	iron ion binding	31	3.8	2.40E-10
MF	oxidoreductase activity, acting on paired donors, with incorporation or reduction of molecular oxygen	26	4.3	4.90E-10
MF	oxidoreductase activity	63	2.1	2.50E-08
MF	heme binding	33	3	2.70E-08
MF	transferase activity, transferring hexosyl groups	23	3.9	4.50E-08
MF	steroid hydroxylase activity	14	5.2	1.10E-06
MF	glucuronosyltransferase activity	18	3.8	2.40E-06
MF	sequence-specific DNA binding	57	1.7	4.40E-05
MF	cholinesterase activity	11	4.5	8.60E-05
MF	carbohydrate binding	38	1.8	6.90E-04
MF	transcription factor activity, sequence-specific DNA binding	55	1.6	9.30E-04
MF	RNA polymerase II regulatory region sequence-specific DNA binding	16	2.4	2.00E-03

MF	transmembrane transporter activity	18	2.3	2.30E-03
MF	lysozyme activity	5	7	3.80E-03
MF	UDP-glycosyltransferase activity	7	4.3	4.50E-03
MF	metal ion binding	132	1.2	4.80E-03
MF	efflux transmembrane transporter activity	4	9.3	6.10E-03
MF	hydrolase activity, acting on ester bonds	8	3.1	1.20E-02
MF	transferase activity, transferring glycosyl groups	20	1.8	1.60E-02
MF	RNA polymerase II transcription factor activity, sequence-specific DNA binding	10	2.4	2.10E-02
MF	carboxylic ester hydrolase activity	6	3.7	2.10E-02
MF	ATPase activity, coupled to transmembrane movement of substances	9	2.3	3.60E-02
MF	transcriptional activator activity, RNA polymerase II core promoter proximal region sequence-specific binding	4	5.1	3.90E-02
MF	heme transporter activity	3	8.4	4.40E-02
MF	ATPase activity	13	1.8	5.10E-02
MF	MAP kinase activity	4	4.3	6.00E-02
MF	stearoyl-CoA 9-desaturase activity	3	7	6.30E-02
MF	acid phosphatase activity	6	2.7	6.60E-02
MF	acyl-CoA dehydrogenase activity	5	3	7.70E-02
MF	acyl-CoA oxidase activity	3	6	8.40E-02
MF	oxidoreductase activity, acting on the CH-CH group of donors, with a flavin as acceptor	5	2.9	8.70E-02
MF	DNA binding	68	1.2	9.30E-02

Table 5.3: GO Term analysis of genes that changed in N2 strain under pathogenic conditions (exposed to E. faecalis OG1RF) compared to non-pathogenic conditions (exposed to E. coli OP50). BP: Biological Processes; MF: Molecular Functions. CC: Cellular Component.

hpx-2(dg047) on OP50 vs. *hpx-2(dg047)* on OG1RF				
Category	**Term**	**Count**	**Fold Enrichment**	**P-value**
BP	protein dephosphorylation	71	3.3	3.00E-21
BP	peptidyl-tyrosine dephosphorylation	50	3.7	1.70E-17
BP	innate immune response	83	2.2	6.20E-12
BP	regulation of cell shape	39	3.3	1.10E-11
BP	peptidyl-serine phosphorylation	38	2.4	3.90E-07
BP	epithelial cell development	13	4.5	6.00E-06
BP	metabolic process	175	1.4	7.40E-06
BP	nonmotile primary cilium assembly	15	3.8	1.10E-05
BP	protein phosphorylation	83	1.6	1.60E-05
BP	peptidyl-tyrosine autophosphorylation	17	3.3	2.00E-05
BP	molting cycle process	10	4.9	5.10E-05
BP	homophilic cell adhesion via plasma membrane adhesion molecules	9	5.3	6.70E-05
BP	cell projection organization	10	4.6	9.10E-05
BP	transmembrane receptor protein tyrosine kinase signaling pathway	18	2.8	9.80E-05
BP	cuticle development	10	4.4	1.50E-04
BP	intraciliary transport	8	5.1	3.20E-04
BP	single-organism transport	6	7.1	4.30E-04
BP	oxidation-reduction process	87	1.4	1.40E-03
BP	negative regulation of endopeptidase activity	16	2.4	2.00E-03
BP	cell differentiation	36	1.7	2.20E-03
BP	defense response	27	1.9	2.20E-03
BP	cilium assembly	11	2.9	2.50E-03
BP	flavonoid biosynthetic process	18	2.1	3.80E-03
BP	flavonoid glucuronidation	18	2.1	3.80E-03
BP	nematode male tail tip morphogenesis	19	2	3.90E-03
BP	defense response to Gram-negative bacterium	20	2	4.50E-03
BP	detection of stimulus involved in sensory perception	4	8.3	6.30E-03
BP	sperm motility	4	8.3	6.30E-03
BP	cell-matrix adhesion	5	5.2	9.80E-03
BP	positive regulation of transcription from RNA polymerase II promoter	31	1.6	1.00E-02
BP	hyperosmotic response	8	2.9	1.60E-02
BP	proteolysis	59	1.3	2.00E-02
BP	carbohydrate metabolic process	29	1.5	2.10E-02
BP	chemotaxis	14	2	2.10E-02
BP	mesodermal cell migration	5	4.1	2.40E-02
BP	dorsal/ventral axon guidance	7	2.9	2.60E-02
BP	collagen and cuticulin-based cuticle development	22	1.6	2.80E-02
BP	dauer entry	12	2	2.90E-02
BP	regulation of neuron differentiation	5	3.8	3.40E-02

BP	cell-cell signaling	5	3.8	3.40E-02
BP	fatty acid alpha-oxidation	3	8.3	4.00E-02
BP	defense response to Gram-positive bacterium	10	2.1	4.50E-02
BP	spermatid development	5	3.5	4.70E-02
BP	spermatogenesis	12	1.9	4.80E-02
BP	fatty acid metabolic process	11	1.9	5.00E-02
BP	3'-UTR-mediated mRNA destabilization	6	2.8	5.60E-02
BP	multicellular organism development	61	1.2	5.70E-02
BP	response to xenobiotic stimulus	4	4.1	6.10E-02
BP	protein localization to ciliary transition zone	4	4.1	6.10E-02
BP	regulation of backward locomotion	4	4.1	6.10E-02
BP	anterior/posterior pattern specification	5	3.2	6.10E-02
BP	chitin metabolic process	5	3.2	6.10E-02
BP	one-carbon metabolic process	5	3.2	6.10E-02
BP	lipid metabolic process	34	1.3	6.90E-02
BP	male meiosis chromosome segregation	3	6.2	7.40E-02
BP	Roundabout signaling pathway	3	6.2	7.40E-02
BP	cell fate specification involved in pattern specification	3	6.2	7.40E-02
BP	regulation of axonogenesis	3	6.2	7.40E-02
BP	S-adenosylmethionine biosynthetic process	3	6.2	7.40E-02
BP	response to gamma radiation	4	3.7	8.40E-02
BP	peptidyl-tyrosine phosphorylation	10	1.8	8.50E-02
BP	response to stimulus	5	2.8	9.70E-02
BP	L-amino acid transport	5	2.8	9.70E-02
BP	oxygen transport	6	2.4	9.90E-02
CC	collagen trimer	64	3.1	6.60E-17
CC	extracellular region	84	2.1	2.40E-11
CC	membrane raft	23	2.7	2.30E-05
CC	extrinsic component of cytoplasmic side of plasma membrane	17	3.2	2.70E-05
CC	intracellular membrane-bounded organelle	29	2.1	2.10E-04
CC	ciliary basal body	10	4	3.90E-04
CC	cilium	15	2.6	1.10E-03
CC	integral component of membrane	779	1.1	1.30E-03
CC	intraciliary transport particle B	7	4.8	1.50E-03
CC	membrane	788	1.1	1.50E-03
CC	neuron projection	18	2	5.90E-03
CC	axoneme	6	4.5	6.20E-03
CC	proteinaceous extracellular matrix	10	2.6	1.10E-02
CC	cell projection	21	1.7	1.80E-02
CC	nonmotile primary cilium	16	1.9	2.00E-02
CC	axonemal microtubule	3	8.3	4.00E-02
CC	motile cilium	4	4.7	4.20E-02
CC	BBSome	4	4.7	4.20E-02
CC	chromatin	7	2.3	7.10E-02
CC	cytoskeleton	36	1.3	7.30E-02
CC	dendrite	15	1.6	7.40E-02
CC	extracellular space	40	1.3	7.70E-02

MF	structural constituent of cuticle	67	3.1	1.60E-18
MF	protein tyrosine phosphatase activity	51	3.5	7.20E-17
MF	phosphoprotein phosphatase activity	42	3.1	7.90E-12
MF	receptor binding	27	3.1	8.90E-08
MF	heme binding	43	2.2	8.90E-07
MF	monooxygenase activity	31	2.6	1.20E-06
MF	iron ion binding	34	2.3	3.90E-06
MF	protein kinase activity	84	1.6	7.10E-06
MF	oxidoreductase activity, acting on paired donors, with incorporation or reduction of molecular oxygen	27	2.5	1.20E-05
MF	non-membrane spanning protein tyrosine kinase activity	19	3	1.60E-05
MF	protein tyrosine kinase activity	26	2.5	1.80E-05
MF	hydrolase activity	133	1.3	5.30E-04
MF	steroid hydroxylase activity	14	2.9	5.50E-04
MF	serine-type endopeptidase inhibitor activity	16	2.6	6.30E-04
MF	oxidoreductase activity	75	1.4	2.40E-03
MF	metallopeptidase activity	30	1.8	2.70E-03
MF	transferase activity, transferring hexosyl groups	21	2	3.30E-03
MF	protein serine/threonine kinase activity	54	1.5	4.20E-03
MF	Roundabout binding	4	7.8	7.50E-03
MF	transcriptional activator activity, RNA polymerase II core promoter proximal region sequence-specific binding	6	4.3	8.00E-03
MF	chitin binding	13	2.2	1.30E-02
MF	RNA polymerase II regulatory region sequence-specific DNA binding	20	1.7	2.20E-02
MF	metalloendopeptidase activity	23	1.6	2.20E-02
MF	lysozyme activity	5	3.9	2.90E-02
MF	glucuronosyltransferase activity	15	1.8	3.60E-02
MF	transmembrane transporter activity	22	1.5	4.40E-02
MF	phytanoyl-CoA dioxygenase activity	3	7.8	4.50E-02
MF	structural constituent of collagen and cuticulin-based cuticle	7	2.5	5.20E-02
MF	transporter activity	21	1.5	5.80E-02
MF	calcium ion binding	34	1.4	6.00E-02
MF	UDP-glycosyltransferase activity	7	2.4	6.30E-02
MF	oxidoreductase activity, acting on single donors with incorporation of molecular oxygen, incorporation of two atoms of oxygen	4	3.9	7.10E-02
MF	ATPase activity, coupled to transmembrane movement of substances	12	1.7	7.60E-02
MF	methionine adenosyltransferase activity	3	5.9	8.20E-02
MF	acid phosphatase activity	8	2	9.10E-02

Table 5.3: GO Term analysis of genes that changed in hpx-2 mutant strain under pathogenic conditions (exposed to E. faecalis OG1RF) compared to non-pathogenic conditions (exposed to E. coli OP50). BP: Biological Processes; MF: Molecular Functions. CC: Cellular Component.

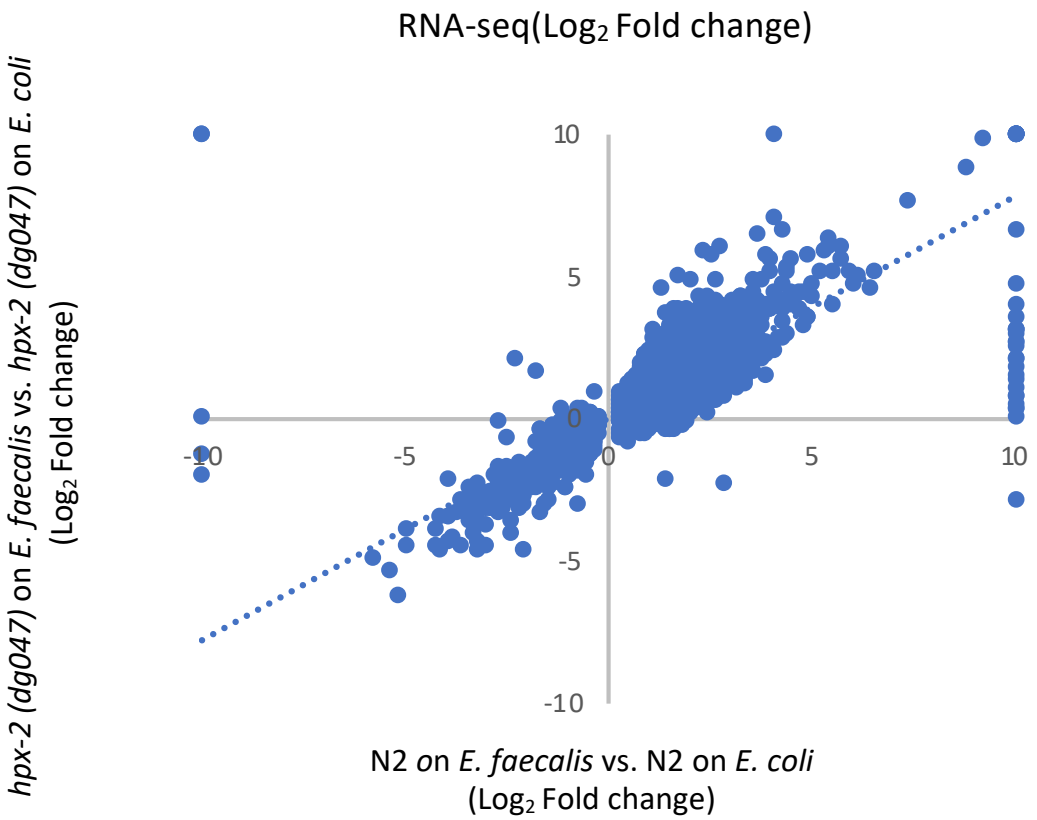

Figure 5.3. Scatter plot of genes changed under pathogenic conditions, as compared to non-pathogenic conditions, in either N2 strain (x-axis) or *hpx-2* mutant (y-axis). Values of 10 or -10 indicate expression level under one condition was 0 RPKM.

Discussion

In this chapter, RNASeq revealed that loss of *hpx-2* modestly impacts the expression of genes that are involved in cuticle generation, body morphogenesis, and immune defense against pathogenic bacteria, indicating HPX-2 may be influencing these processes. This observation is consistent with the weaker cuticle structure and increased susceptibility to pathogens (Figure 3.12 and Figure 4.4).

Although the transcriptome changes detected in the worms were modest, both in the number of genes affected and the amplitude of the effect, several observations suggest these reflect the biological effect of HPX-2. First, *hpx-2* gene expression is restricted to a few cells, and thus we would not expect large transcriptome effects that are averaged over the whole animal. Second, we performed five biological replicates of RNAseq and the differences were highly reproducible. Third, the affected genes are enriched for cuticle biogenesis, which correlates well with the known requirement for peroxidases in cuticle cross-linking. Fourth, although the overlap in genes that were significantly affected in *hpx-2* mutant under the two conditions is modest, in most cases genes that were significantly affected in one direction under the *E. coli* condition were affected in the same direction under the *E. faecalis* condition and vice versa, even if the effect reached significance only in one comparison (Figure 5.3). Finally, I used qRT-PCR to validate ten genes that were changed in the *hpx-2* mutant compared to N2 under pathogenic conditions. These qRT-PCR experiments were performed on RNA isolated from three biological replicates that were independent of the RNAseq RNA samples, yet there was a strong correlation between the results (Figure 5.1; R^2=0.92 between fold change by RNAseq and qRT-PCR). Therefore, I believe that there were modest but significant effects on the transcriptome that implicate HPX-2 in cuticle biogenesis and defense against Gram-positive bacteria.

Through the RNAseq analysis, we were able to evaluate several subtle changes in global transcription compared to the N2 strain. First, when worms were under non-pathogenic conditions, no obvious physiological abnormalities was observed in the *hpx-2* mutant. However, a large number of genes involved in cuticle biogenesis were differentially expressed according to RNAseq result, which explains the subtle increase in cuticle permeability phenotype observed in the *hpx-2* mutant. Secondly, genes that are involved in locomotion were differentially expressed in the *hpx-2* mutant under non-pathogenic conditions, suggesting a potential role for HPX-2 in regulating this process. Indeed, when *hpx-2* was overexpressed in the worm, occasional dumpy and roller phenotypes were observed. Lastly, several components of the p38 MAPK pathway were slightly induced in *hpx-2* mutant, consistent with the overall increase in the innate response observed in the *hpx-2* mutant.

When comparing the pathogenic condition with the non-pathogenic, it was not surprising that a much larger set of genes were affected. Although the overall gene expression profile was not that different between N2 and *hpx-2* when exposed to pathogen, a much stronger response was observed in the *hpx-2* mutant, possibility due to the already disturbed physiological state in *hpx-2* mutant. The increased microbial load of *E. faecalis* in *hpx-2* mutant could also explain why the transcriptional response was stronger compared to N2. Interestingly, the *hpx-2* transcript was not detectable in the N2 strain under non-pathogenic conditions, and was not induced following pathogen exposure. This again, highlights the specific expression pattern and tight regulation of *hpx-2* (Table S3). Other genes encoding proteins involved in cuticle development like *mlt-7* are expressed at intervals corresponding to the larval molts (29), and were not affected by the loss of HPX-2.

In conclusion, RNAseq analysis revealed an altered gene expression profile in *hpx-2* mutant, consistent with a role in body morphogenesis, locomotion, and cuticle biogenesis. When exposed to the pathogen *E. faecalis*, loss *hpx-2* resulted a stronger immune response

compared to N2 strain likely due to the more aggressive colonization by the pathogen that occurs in this background.

Chapter 6 Conclusions and Perspectives

Summary

In this work, I characterized a putative peroxidase, HPX-2, for its immuno-protective role in *C. elegans* against multiple pathogens. Based on the expression pattern of HPX-2 and the tissue specific RNAi, I suspect HPX-2 functions in two major tissues, the pharynx and the hypodermis, for its function in preventing infections.

In the pharynx, the HPX-2::GFP expression pattern revealed that HPX-2 is likely to be expressed in the gland cells located at the distal bulb of the pharynx. Gland cells function in secreting vesicles through the process into the pharyngeal lumen and aiding cuticle remodeling during the developmental process. Accordingly, loss of HPX-2 resulted in increased susceptibility to and intestinal colonization by the Gram-positive bacterium *E. faecalis* but not Gram-negative *P. aeruginosa*. The protective role of HPX-2 only applies to Gram-positive bacterial and fungal species, but not to Gram-negative bacteria, suggesting the thick outer layer of these pathogens could be the reason for this phenotype.

In terms of hypodermis function, I first showed that tissue-specific knock down of HPX-2 in the hypodermis significantly increased the susceptibility of worms to *E. faecalis*. Loss of HPX-2 also resulted in a less intact cuticle as measured by a permeable DNA dye, suggesting again the role of HPX-2 in pathogen resistance is a function of cuticle reinforcement.

Finally, I utilized RNAseq analysis as an un-biased and highly sensitive measurement of global transcriptomic changes upon the loss of HPX-2. The RNAseq results provided insight into the potential physiological processes HPX-2 is involved in. Under non-pathogenic conditions, loss of *hpx-2* resulted in a subtle but significant change in genes involved in cuticle biogenesis, locomotion, and molting, confirming the role of HPX-2 in cuticle biogenesis during development. Under pathogenic conditions, in addition to the enrichment of cuticle genes, there was significant induction of genes involved in innate immunity, suggesting a stronger immune response compared to N2 strain. Surprisingly, the expression level of *hpx-2* is extremely low on

the organismal level resulting in *hpx-2* gene reads being undetectable through RNAseq. However, the fact that loss of HPX-2 still results in dramatically increased sensitivity to the pathogen *E. faecalis* highlights its importance in innate immunity.

In conclusion, I showed that HPX-2 is expressed in the pharynx and hypodermis of the worm strengthening the cuticle lining these organs and resulting in less colonization and multiplication of the pathogen in the intestine.

Discussions and future directions

Cuticle reinforcement role of HPX-2

Cuticle is the very outside layer that covers the worm body, and functions in protecting the worm from environmental insult, supporting the body structure, and facilitating locomotion through attachment with the underlying muscles (151-153). The body cuticle is secreted by the underlying hypodermal cells and has distinct layers and structures. The very outside layer of body cuticle is the surface coat majorly consisting of glycoproteins, whereas the remaining four layers underneath contain cross-linked collagens and cutlins proteins (30). So far, a wide range of cuticle defective mutants have been identified and studied, which cause a variety of phenotypes, from altered body morphology, abnormal surface appearance, to pathogen resistance (30).

In addition to the worm body, the four major openings of the worm (pharynx, vulva, anus, and excretory pore) are also covered with cuticle. However, unlike the body cuticle, opening-lining cuticle lacks complex layers, and is mainly composed of soluble collagen proteins and insoluble cutlin proteins (30).

As the major component of the cuticle, collagen proteins encompass up to 80% of the soluble proteins in the extracellular matrix. The *C. elegans* genome encodes for over 170 collagen proteins (30). Thus far, 21 collagen-encoding genes have been shown to be involved in worm morphology (30). Mutation of these genes results in a variety of phenotypes including Dumpy (Dpy), Roller (rol), Blister (bli), and Squat (Sqt). Surprisingly, 10 out of those 21 genes were significantly altered in *hpx-2* mutant according to the RNAseq analysis, providing a strong indication that the loss of HPX-2 affects the overall cuticle structure and morphology of the worm. However, like the other genes that were differentially expressed in the *hpx-2* mutant, the log2 fold-changes were not dramatic, most of them falling between one and two, suggesting a

subtle change. This could also explain why there were no visible morphology defects; only the Hoescht dye assay indicated a small disturbance in cuticle integrity (See chapter 4 for more detail).

The cuticle is also the site of first contact between the worms and some pathogenic microbes that rely on the attachment and penetration of worm's surface for their pathogenicity. Some components of the cuticle such as the carbohydrate-rich surface coat serve as a protective shield from pathogen attachment, and mutations in genes that are involved in production and secretion of these components result in increased pathogen susceptibility (50, 154). For example, loss of function mutations in bacterially Un-Swollen genes *bus-2*, *bus-4*, *bus-12,* and *bus-17* increases attachment of the fungal pathogen *Drechmeria coniospora* spores to the cuticle (155), *Microbacterium nematophilum* to the rectal epithelia (156-159) and *Yersinia pseudotuberculosis* to the head (160, 161). For the pathogens tested in this study, the site of infection was the intestine. It would be interesting to test the susceptibility of the *hpx-2* mutant to cuticle pathogens, and such an investigation might provide more insight into HPX-2's function in hypodermal immunity.

While the body cuticle serves as the very first line of defense against environmental and microbial insult, the pharynx, especially the grinder, has a similar function against potential pathogens that are ingested. Studies have shown that mutants that have defective grinding function had increased uptake of intact microbes, resulting in higher susceptibility to pathogens (71, 162).

In terms of the pharyngeal function of HPX-2, it is very likely that it plays the same role in hypodermis, specifically cuticle cross-linking, since the pharyngeal lumen including the grinder is lined with cuticle and it is connected to the cuticle of the hypodermis (30). By physical strengthening of the pharyngeal grinder, HPX-2 functions in pathogen resistance. Alternatively, HPX-2 could serve as a secreted peroxidase in the gland cells located in the distal bulb of the

pharynx for cuticle grinder strengthening or aiding digestion of the microbe. While the cell body of the gland cells are embedded within the muscle cell epithelium at the distal bulb of the pharynx, there are structures, named processes, that protrude from the cell body and open into the pharyngeal lumen (135). During the molting process, the gland cells excrete vesicles that contains enzymes that aid in the tearing down of the old cuticle lining inside the pharynx and around the worm body (135, 136). When feeding on bacteria, a different kind of vesicle is secreted to aid in digesting food (135). In chapter 4, I showed that the expression of HPX-2::GFP in pharynx, specifically, the expression pattern resemble the gland cells in the pharynx in dauer worms and occasionally a protruding structure extending from the posterior bulb to the buccal cavity of the worms. It could be that HPX-2 is being produced in the gland cells located at the distal bulb and being secreted during molting and/or feeding.

To further investigate whether HPX-2 is functioning in the physical reinforcement of the pharyngeal grinder or chemically aiding the digestion of microbes, it would be interesting to feed the worms with fluorescently-labeled beads that would normally be disrupted by a healthy grinder. If the intestinal fluorescence is stronger in *hpx-2* mutant compared to N2 strain, it would indicate a less intact grinder in HPX-2 mutant. Alternatively, we could cross *hpx-2* lines with those with known pharyngeal defects, i.e. the *eat* mutants, to see if there is an additive affect in pathogen susceptibility.

The peroxidase activity of HPX-2

In order to understand the mechanism of protection of HPX-2 in innate immunity, it is crucial to understand its enzymatic activity as a heme-peroxidase, specifically, the ability to utilize H_2O_2 as a substrate to carry out oxidation reactions. I first utilized Amplex Red Assay as a measurement for the level of H_2O_2 during infection. Previous studies showed that when exposed to pathogen, *C. elegans* produces elevated level of H_2O_2, and the deletion of a major

peroxidase could further increase H_2O_2 level (99, 102). However, the Amplex Red Assay did not reveal an increased level of H_2O_2 in *hpx-2* mutants when exposed to pathogen, suggesting HPX-2 is not a major consumer of H_2O_2 (Figure 4.8). On the other hand, the immune protective peroxidase previously identified in our lab, SKPO-1, was demonstrated to utilize H_2O_2 when worms where exposed to pathogen, because the level of H_2O_2 drastically increases in the *skpo-1* mutant. There are a couple of possible explanations for the fact that I did not detect changes in the H_2O_2 levels in the *hpx-2* mutant. It could be because HPX-2 possesses little peroxidase activity under the conditions tested. It also could be due to low levels of HPX-2 such that the Amplex Red Assay was not sensitive enough to detect a change. Also, along the same line of reasoning, the fact that SKPO-1 is a major consumer of H_2O_2 during infection could mask the contribution of HPX-2's peroxidase activity. Last but not least, it's likely that HPX-2 role happens early during development and it is not active in the adult animal.

To test whether HPX-2's peroxidase activity is required for pathogen resistance, a point mutation was generated in the *hpx-2* gene through CRIPSR-cas9 mediated mutagenesis. Specifically, the catalytic arginine residue that is highly conserved throughout peroxidase-cyclooxygenase superfamily was substituted with Alanine in HPX-2, resulting in a mutant protein in which peroxidase activity is expected to be lost (141, 163). Worms harboring the mutated version of HPX-2 exhibited increased susceptibility to pathogens (Figure 4. 9), indicating the peroxidase activity is required for HPX-2' s immune protective role (see Chapter 4 for more detail)

The natural next step in exploring the activity of HPX-2 is through in-vitro purification and enzymatic analysis of the protein. Historically, using a baculovirus system in eukaryotic cells, multiple human peroxidases including MPO and LPO have been expressed (139). On the other hand, some studies showed that the peroxidase domain-containing proteins BLI-3 and MLT-7 can be expressed and purified from an *E. coli* expression system with the peroxidase activity

intact (28), (29). Given the lack of expertise in viral-mediated protein expression, I decided to try the *E. coli* expression system first. Unfortunately, my attempt at purifying the recombinant HPX-2 was not successful. One explanation for lack of good expression could be the differences in codon preference in *E. coli* versus *C. elegans*. To address this problem, we could order artificially synthesized, codon-optimized DNA, encoding HPX-2. Another potential problem with using the *E. coli* system is that peroxidases are usually heavily glycosylated during the post-translational process, and the modifications can be crucial for their full activity. In that case, a eukaryotic expression system may be the better choice for the expression and purification of fully active peroxidase.

Potential involvement of HPX-2 in innate immune pathways

Given the cuticle reinforcement function and potential peroxidase activity of HPX-2, there might be two non-mutually exclusive ways HPX-2 is involved in innate immunity. The first possibility is through the disturbed hypodermis and downstream signal pathway to activate the immune effectors. One example of this is the activation of AMP genes by the disruption of the hypodermis. Specifically, disruption of the hypodermis by fungal pathogen or in *dpy-9* and *dpy-10* mutants results in an increased level of a tyrosine derivative 4-hydrophenyllactic acid (HPLA), which then activates its cognate G protein-coupled receptor (GPCR) DCAR-1 (84). The activation of DCAR-1 then triggers the expression of AMPs through p38 MAPK pathway and via the release of a negative regulator STA-2 (84, 164). Another example is from a recent study showing that disruption of specific structures of the cuticle triggers the activation of multiple stress response and innate immunity pathways (148). Specifically, disruption of the annular furrows by knocking down *dpy-2*, *dpy-3, dpy-7*, and *dyp-10* genes activates detoxification, osmolyte resistance, and most importantly, antimicrobial responses in *C. elegans* (148). It was also discovered that multiple transcription factors act downstream of this process with

overlapping functions: i.e SKN-1/Nrf and ELT-3/GATA for detoxification, STA-2/stat and ELT-3/GATA for antimicrobial gene expression (148).

Intriguingly, one important observation from the RNAseq analysis is that the key player in the p38 MAPK, *pmk-1,* was induced upon the loss of HPX-2 under non-pathogenic conditions. In addition to *pmk-1*, genes that encode for the other two MAPK kinases, *pmk-2* and *pmk-3*, were also upregulated 2 to 6-fold in the *hpx-2* mutant compared to the N2 reference strain under the same conditions. This suggests that loss of HPX-2 had subtle but significant effects on the major immune signaling pathway. However, the physiological relevance of this effect requires further investigation.

The other possible role for HPX-2 in innate immunity that I explored is production of an immune effector for pathogen elimination, in this case, a strong oxidant that could be derived from an oxidation reaction using H_2O_2 as a substrate. As discussed in section 6.1 of this chapter, HPX-2 pharyngeal localization and the requirement of its catalytic residue for pathogen resistance indicate that HPX-2 might be serving as a catalytic enzyme aiding the digestion/ elimination of ingested pathogens. One way to further test this hypothesis is to purify HPX-2 and assay for its enzymatic activity against different substrates.

Interactions with BLI-3

To explore the possibility of physical interactions between BLI-3 and HPX-2, I first tried the yeast-two-hybrid method, in which I cloned the full-length HPX-2 and the peroxidase domain of BLI-3 into the yeast two hybrid vectors. However, I was not able to detect any interaction between BLI-3/SKPO-1 and BLI-3/HPX-2 (Figure 6.1 A and B). I reasoned that since BLI-3 and the peroxidases all have a predicted secretion signal peptide at their N terminus, they could be excreted out from yeast cells during production, contributing to a lack of detectable interactions. Hence, I cloned those genes without the signal peptide sequence into the yeast 2-hybrid

plasmids and tested their interactions. However, there was still no interaction detected (Figure 6.1 C). it could be that DUOXs are usually extensively glycosylated during protein synthesis and such modifications are critical for their cell surface expression activity such that the yeast 2-hybrid system is not suitable (140). An alternative assay that could be used to explore this question further and has the advantage of being in vivo is the bimolecular fluorescence complementation (Bi-FC) assay (165). Specifically, the BLI-3 peroxidase domain and its potential interacting peroxidases could be fused to two non-fluorescent fragments derived from a fluorescent protein. The constructs would then be delivered into *C. elegans* through microinjection. Fluorescent signals can be detected if there is an interaction between BLI-3 and the peroxidases. Last but not least, co-immunoprecipitation (co-IP) could be applied to investigate direct interaction between BLI-3 and HPX-2. It has been previously demonstrated that the peroxidase domain of hDUOX1 may mediate protein-protein interaction through its cysteine residues (166). Given its significant sequence homology with BLI-3, it is postulated the protein-protein interaction function of hDUOX1 might be conserved in BLI-3. A potential problem with this approach is that the extremely low expression of HPX-2 on the whole organism level will make the detection of an IP-ed product difficult.

Although it is postulated that there might be direct interactions between BLI-3 and H_2O_2 utilizing peroxidases, it could also be that direct physical interaction is not required for the function of peroxidases for the following reasons: First, H_2O_2 is a diffusible molecule that moves freely intracellularly and extracellularly following the concentration gradient. This makes H_2O_2 easily accessible to peroxidases in proximity. Second, although BLI-3 is a membrane anchored protein, many peroxidases are secreted. Through temporal and spatial control of the peroxidases, a close proximity could be created between the two.

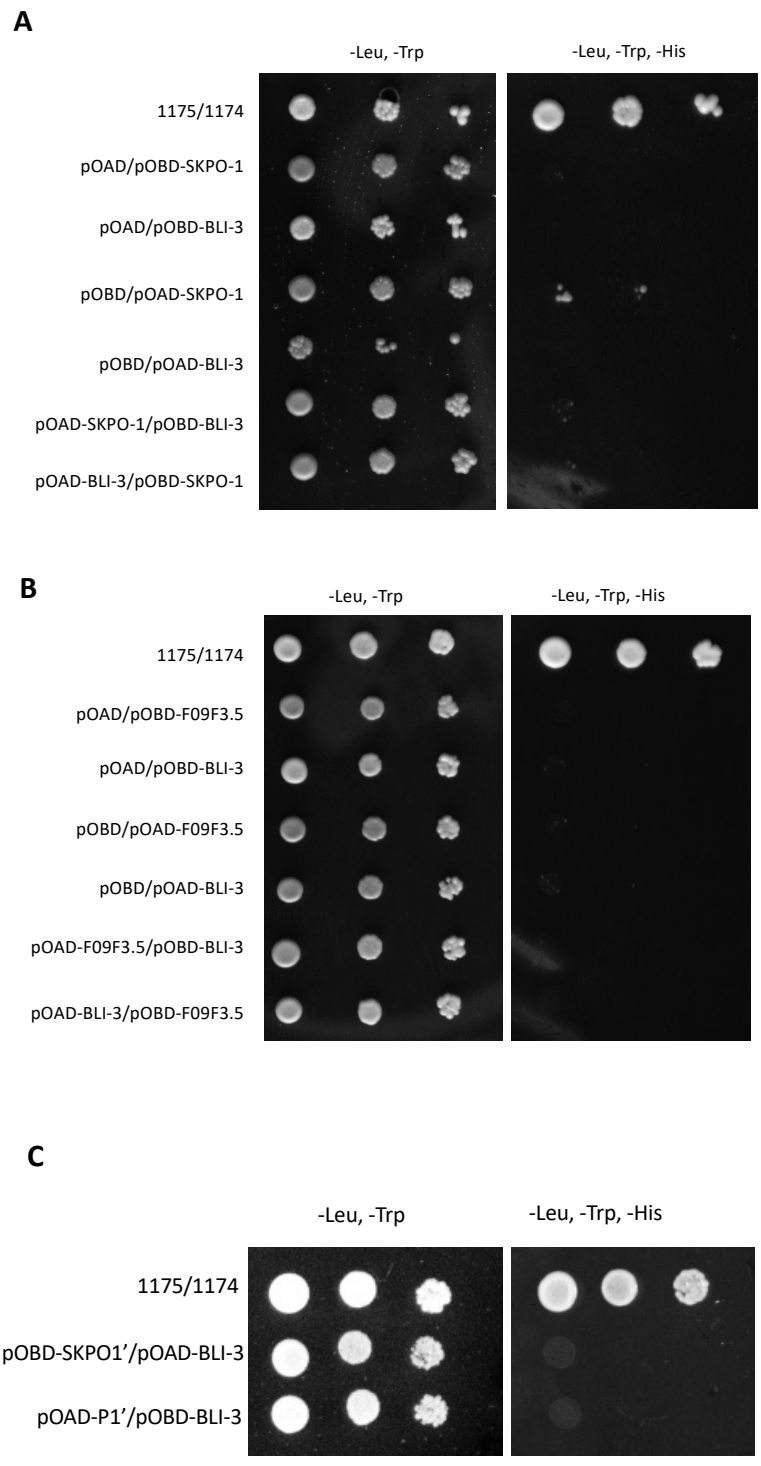

Figure 6.1 No interaction between BLI-3 and the two peroxidases (HPX-2 and SKPO-1) is detected by Yeast-2-hybrid.

REFERENCES

1. Izydor Apostol, P. F. H., and Philip S. Low. (1989) Rapid Stimulation of an Oxidative Burst during Elicitation of Cultured Plant Cells. *PlantPhysiol* **90**, 109-116

2. Levine, A., Tenhaken, R., Dixon, R., and Lamb, C. (1994) H2O2 from the oxidative burst orchestrates the plant hypersensitive disease resistance response. *Cell* **79**, 583-593

3. Rojas, C., and Mysore, K. S. (2012) Glycolate oxidase is an alternative source for H2O2 production during plant defense responses and functions independently from NADPH oxidase. *Plant signaling & behavior* **7**, 752-755

4. Rojas, C. M., Senthil-Kumar, M., Wang, K., Ryu, C. M., Kaundal, A., and Mysore, K. S. (2012) Glycolate oxidase modulates reactive oxygen species-mediated signal transduction during nonhost resistance in Nicotiana benthamiana and Arabidopsis. *The Plant cell* **24**, 336-352

5. Levine, A., Pennell, R. I., Alvarez, M. E., Palmer, R., and Lamb, C. (1996) Calcium-mediated apoptosis in a plant hypersensitive disease resistance response. *Current biology: CB* **6**, 427-437

6. Dong, W. E. D. a. X. (2004) Systemic Acquired Resistance *Annu. Rev. Phytopathol.* **42**, 185-209

7. Buchon, N., Broderick, N. A., Poidevin, M., Pradervand, S., and Lemaitre, B. (2009) Drosophila Intestinal Response to Bacterial Infection: Activation of Host Defense and Stem Cell Proliferation. *Cell Host & Microbe* **5**, 200-211

8. Wu, S.-C., Liao, C.-W., Pan, R.-L., and Juang, J.-L. (2012) Infection-Induced Intestinal Oxidative Stress Triggers Organ-to-Organ Immunological Communication in Drosophila. *Cell Host & Microbe* **11**, 410-417

9. Niethammer, P., Grabher, C., Look, A. T., and Mitchison, T. J. (2009) A tissue-scale gradient of hydrogen peroxide mediates rapid wound detection in zebrafish. *Nature* **459**, 996-999

10. Schreck, R., Rieber, P., and Baeuerle, P. A. (1991) Reactive oxygen intermediates as apparently widely used messengers in the activation of the NF-kappa B transcription factor and HIV-1. *The EMBO journal* **10**, 2247-2258

11. Lipinski, S., Till, A., Sina, C., Arlt, A., Grasberger, H., Schreiber, S., and Rosenstiel, P. (2009) DUOX2-derived reactive oxygen species are effectors of NOD2-mediated antibacterial responses. *Journal of cell science* **122**, 3522-3530

12. Klebanoff, S. J., Kettle, A. J., Rosen, H., Winterbourn, C. C., and Nauseef, W. M. (2013) Myeloperoxidase: a front-line defender against phagocytosed microorganisms. *Journal of leukocyte biology* **93**, 185-198

13. Chapman, A. L., Hampton, M. B., Senthilmohan, R., Winterbourn, C. C., and Kettle, A. J. (2002) Chlorination of bacterial and neutrophil proteins during phagocytosis and killing of Staphylococcus aureus. *The Journal of biological chemistry* **277**, 9757-9762

14. Rosen, H., Crowley, J. R., and Heinecke, J. W. (2002) Human neutrophils use the myeloperoxidase-hydrogen peroxide-chloride system to chlorinate but not nitrate bacterial proteins during phagocytosis. *The Journal of biological chemistry* **277**, 30463-30468

15. Gerson, C., Sabater, J., Scuri, M., Torbati, A., Coffey, R., Abraham, J. W., Lauredo, I., Forteza, R., Wanner, A., Salathe, M., Abraham, W. M., and Conner, G. E. (2000) The lactoperoxidase system functions in bacterial clearance of airways. *American journal of respiratory cell and molecular biology* **22**, 665-671

16. Geiszt, M., Witta, J., Baffi, J., Lekstrom, K., and Leto, T. L. (2003) Dual oxidases represent novel hydrogen peroxide sources supporting mucosal surface host defense. *Faseb J* **17**, 1502-1504

17. Forteza, R., Salathe, M., Miot, F., and Conner, G. E. (2005) Regulated hydrogen peroxide production by Duox in human airway epithelial cells. *American journal of respiratory cell and molecular biology* **32**, 462-469

18. Conner, G. E., Salathe, M., and Forteza, R. (2002) Lactoperoxidase and hydrogen peroxide metabolism in the airway. *American journal of respiratory and critical care medicine* **166**, S57-61

19. Rada, B., and Leto, T. L. (2010) Characterization of hydrogen peroxide production by Duox in bronchial epithelial cells exposed to Pseudomonas aeruginosa. *FEBS letters* **584**, 917-922

20. Moskwa, P., Lorentzen, D., Excoffon, K. J., Zabner, J., McCray, P. B., Jr., Nauseef, W. M., Dupuy, C., and Banfi, B. (2007) A novel host defense system of airways is defective in cystic fibrosis. *American journal of respiratory and critical care medicine* **175**, 174-183

21. Bedard, K., and Krause, K. H. (2007) The NOX family of ROS-generating NADPH oxidases: physiology and pathophysiology. *Physiological reviews* **87**, 245-313

22. Lambeth, J. D. (2004) NOX enzymes and the biology of reactive oxygen. *Nature reviews. Immunology* **4**, 181-189

23. Lambeth, J. D., and Neish, A. S. (2014) Nox enzymes and new thinking on reactive oxygen: a double-edged sword revisited. *Annual review of pathology* **9**, 119-145

24. Jackson, S. H., Gallin, J. I., and Holland, S. M. (1995) The p47phox mouse knock-out model of chronic granulomatous disease. *The Journal of experimental medicine* **182**, 751-758

25. Krause, K. H. (2004) Tissue distribution and putative physiological function of NOX family NADPH oxidases. *Japanese journal of infectious diseases* **57**, S28-29

26. Anh, N. T., Nishitani, M., Harada, S., Yamaguchi, M., and Kamei, K. (2011) Essential role of Duox in stabilization of Drosophila wing. *The Journal of biological chemistry* **286**, 33244-33251

27. Kumar, S., Molina-Cruz, A., Gupta, L., Rodrigues, J., and Barillas-Mury, C. (2010) A peroxidase/dual oxidase system modulates midgut epithelial immunity in Anopheles gambiae. *Science (New York, N.Y.)* **327**, 1644-1648

28. Edens, W. A., Sharling, L., Cheng, G., Shapira, R., Kinkade, J. M., Lee, T., Edens, H. A., Tang, X., Sullards, C., Flaherty, D. B., Benian, G. M., and Lambeth, J. D. (2001) Tyrosine cross-linking of extracellular matrix is catalyzed by Duox, a multidomain oxidase/peroxidase with homology to the phagocyte oxidase subunit gp91phox. *J Cell Biol* **154**, 879-891

29. Thein, M. C., Winter, A. D., Stepek, G., McCormack, G., Stapleton, G., Johnstone, I. L., and Page, A. P. (2009) Combined extracellular matrix cross-linking activity of the peroxidase MLT-7 and the dual oxidase BLI-3 is critical for post-embryonic viability in Caenorhabditis elegans. *The Journal of biological chemistry* **284**, 17549-17563

30. Page, A. P., and Johnstone, I. L. (2007) The cuticle. *WormBook : the online review of C. elegans biology*, 1-15

31. Ewald, C. Y. (2018) Redox Signaling of NADPH Oxidases Regulates Oxidative Stress Responses, Immunity and Aging. *Antioxidants (Basel, Switzerland)* **7**

32. Zamocky, M., Hofbauer, S., Schaffner, I., Gasselhuber, B., Nicolussi, A., Soudi, M., Pirker, K. F., Furtmuller, P. G., and Obinger, C. (2015) Independent evolution of four heme peroxidase superfamilies. *Archives of biochemistry and biophysics* **574**, 108-119

33. Colas, C., and Ortiz de Montellano, P. R. (2003) Autocatalytic radical reactions in physiological prosthetic heme modification. *Chemical reviews* **103**, 2305-2332

34. Finzel, B. C., Poulos, T. L., and Kraut, J. (1984) Crystal structure of yeast cytochrome c peroxidase refined at 1.7-A resolution. *The Journal of biological chemistry* **259**, 13027-13036

35. Gajhede, M., Schuller, D. J., Henriksen, A., Smith, A. T., and Poulos, T. L. (1997) Crystal structure of horseradish peroxidase C at 2.15 A resolution. *Nature structural biology* **4**, 1032-1038

36. Meitzler, J. L., Brandman, R., and Ortiz de Montellano, P. R. (2010) Perturbed heme binding is responsible for the blistering phenotype associated with mutations in the Caenorhabditis elegans dual oxidase 1 (DUOX1) peroxidase domain. *The Journal of biological chemistry* **285**, 40991-41000

37. Harman, D. (2003) The free radical theory of aging. *Antioxidants & redox signaling* **5**, 557-561

38. Dan Dunn, J., Alvarez, L. A., Zhang, X., and Soldati, T. (2015) Reactive oxygen species and mitochondria: A nexus of cellular homeostasis. *Redox biology* **6**, 472-485

39. Pinegin, B., Vorobjeva, N., Pashenkov, M., and Chernyak, B. (2018) The role of mitochondrial ROS in antibacterial immunity. *Journal of cellular physiology* **233**, 3745-3754

40. Yee, C., Yang, W., and Hekimi, S. (2014) The intrinsic apoptosis pathway mediates the pro-longevity response to mitochondrial ROS in C. elegans. *Cell* **157**, 897-909

41. Xu, S., and Chisholm, A. D. (2014) C. elegans epidermal wounding induces a mitochondrial ROS burst that promotes wound repair. *Developmental cell* **31**, 48-60

42. West, A. P., Brodsky, I. E., Rahner, C., Woo, D. K., Erdjument-Bromage, H., Tempst, P., Walsh, M. C., Choi, Y., Shadel, G. S., and Ghosh, S. (2011) TLR signalling augments macrophage bactericidal activity through mitochondrial ROS. *Nature* **472**, 476-480

43. Geng, J., Sun, X., Wang, P., Zhang, S., Wang, X., Wu, H., Hong, L., Xie, C., Li, X., Zhao, H., Liu, Q., Jiang, M., Chen, Q., Zhang, J., Li, Y., Song, S., Wang, H. R., Zhou, R., Johnson, R. L., Chien, K. Y., Lin, S. C., Han, J., Avruch, J., Chen, L., and Zhou, D. (2015) Kinases Mst1 and Mst2 positively regulate phagocytic induction of reactive oxygen species and bactericidal activity. *Nature immunology* **16**, 1142-1152

44. West, A. P., Shadel, G. S., and Ghosh, S. (2011) Mitochondria in innate immune responses. *Nature reviews. Immunology* **11**, 389-402

45. Dharmawardhane, S., and Bokoch, G. M. (1997) Rho GTPases and leukocyte cytoskeletal regulation. *Current opinion in hematology* **4**, 12-18

46. Williams, D. A., Tao, W., Yang, F., Kim, C., Gu, Y., Mansfield, P., Levine, J. E., Petryniak, B., Derrow, C. W., Harris, C., Jia, B., Zheng, Y., Ambruso, D. R., Lowe, J. B., Atkinson, S. J., Dinauer, M. C., and Boxer, L. (2000) Dominant negative mutation of the hematopoietic-specific Rho GTPase, Rac2, is associated with a human phagocyte immunodeficiency. *Blood* **96**, 1646-1654

47. Sulston, J. E., Schierenberg, E., White, J. G., and Thomson, J. N. (1983) The embryonic cell lineage of the nematode Caenorhabditis elegans. *Developmental biology* **100**, 64-119

48. Ellis, H. M., and Horvitz, H. R. (1986) Genetic control of programmed cell death in the nematode C. elegans. *Cell* **44**, 817-829

49. Brenner, S. (1974) The genetics of Caenorhabditis elegans. *Genetics* **77**, 71-94

50. Jiang, H., and Wang, D. (2018) The Microbial Zoo in the C. elegans Intestine: Bacteria, Fungi and Viruses. *Viruses* **10**

51. Pukkila-Worley, R. A., F.M.; Mylonakis. (2011) Candida albicans infection of Caenorhabditis elegans induces antifungal immune defenses

. *PLoS pathogens*, e1002074

52. Tang, R. J., Breger, J., Idnurm, A., Gerik, K. J., Lodge, J. K., Heitman, J., Calderwood, S. B., and Mylonakis, E. (2005) Cryptococcus neoformans gene involved in mammalian pathogenesis identified by a Caenorhabditis elegans progeny-based approach. *Infection and immunity* **73**, 8219-8225

53. Mylonakis, E., Ausubel, F. M., Perfect, J. R., Heitman, J., and Calderwood, S. B. (2002) Killing of *Caenorhabditis elegans* by *Cryptococcus neoformans* as a model of yeast pathogenesis. *Proceedings of the National Academy of Sciences of the United States of America* **99**, 15675-15680

54. Jansson, H. B. (1994) Adhesion of conidia of *Drechmeria coniospora* to *Caenorhabditis elegans* wild type and mutants. *Journal of nematology* **26**, 430-435

55. Mahajan-Miklos, S., Tan, M. W., Rahme, L. G., and Ausubel, F. M. (1999) Molecular mechanisms of bacterial virulence elucidated using a *Pseudomonas aeruginosa-Caenorhabditis elegans* pathogenesis model. *Cell* **96**, 47-56

56. Tan, M. W., Mahajan-Miklos, S., and Ausubel, F. M. (1999) Killing of *Caenorhabditis elegans* by *Pseudomonas aeruginosa* used to model mammalian

bacterial pathogenesis. *Proceedings of the National Academy of Sciences of the United States of America* **96**, 715-720

57. Youn, M., Lee, K. M., Kim, S. H., Lim, J., Yoon, J. W., and Park, S. (2013) Escherichia coli O157:H7 LPS O-side chains and pO157 are required for killing Caenorhabditis elegans. *Biochemical and biophysical research communications* **436**, 388-393

58. Wei, J. Z., Hale, K., Carta, L., Platzer, E., Wong, C., Fang, S. C., and Aroian, R. V. (2003) *Bacillus thuringiensis* crystal proteins that target nematodes. *Proceedings of the National Academy of Sciences of the United States of America* **100**, 2760-2765

59. Sifri, C. D., Begun, J., Ausubel, F. M., and Calderwood, S. B. (2003) *Caenorhabditis elegans* as a model host for *Staphylococcus aureus* pathogenesis. *Infection and immunity* **71**, 2208-2217

60. Jansen, W. T., Bolm, M., Balling, R., Chhatwal, G. S., and Schnabel, R. (2002) Hydrogen peroxide-mediated killing of *Caenorhabditis elegans* by *Streptococcus pyogenes*. *Infection and immunity* **70**, 5202-5207

61. Garsin, D. A., Villanueva, J. M., Begun, J., Kim, D. H., Sifri, C. D., Calderwood, S. B., Ruvkun, G., and Ausubel, F. M. (2003) Long-lived *C. elegans daf-2* mutants are resistant to bacterial pathogens. *Science (New York, N.Y.)* **300**, 1921

62. Garsin, D. A., Sifri, C. D., Mylonakis, E., Qin, X., Singh, K. V., Murray, B. E., Calderwood, S. B., and Ausubel, F. M. (2001) A simple model host for identifying Gram-positive virulence factors. *Proceedings of the National Academy of Sciences of the United States of America* **98**, 10892-10897

63. Sifri, C. D., Mylonakis, E., Singh, K. V., Qin, X., Garsin, D. A., Murray, B. E., Ausubel, F. M., and Calderwood, S. B. (2002) Virulence effect of Enterococcus faecalis protease genes and the quorum-sensing locus fsr in Caenorhabditis elegans and mice. *Infection and immunity* **70**, 5647-5650

64. Moy, T. I., Ball, A. R., Anklesaria, Z., Casadei, G., Lewis, K., and Ausubel, F. M. (2006) Identification of novel antimicrobials using a live-animal infection model. *Proceedings of the National Academy of Sciences of the United States of America* **103**, 10414-10419

65. Xu, A., Shi, G., Liu, F., and Ge, B. (2013) Caenorhabditis elegans mom-4 is required for the activation of the p38 MAPK signaling pathway in the response to Pseudomonas aeruginosa infection. *Protein & cell* **4**, 53-61

66. Powell, J. R., Kim, D. H., and Ausubel, F. M. (2009) The G protein-coupled receptor FSHR-1 is required for the Caenorhabditis elegans innate immune response. *Proceedings of the National Academy of Sciences of the United States of America* **106**, 2782-2787

67. Estes, K. A., Dunbar, T. L., Powell, J. R., Ausubel, F. M., and Troemel, E. R. (2010) bZIP transcription factor zip-2 mediates an early response to Pseudomonas aeruginosa infection in Caenorhabditis elegans. *Proceedings of the National Academy of Sciences of the United States of America* **107**, 2153-2158

68. Aballay, A., Drenkard, E., Hilbun, L. R., and Ausubel, F. M. (2003) Caenorhabditis elegans innate immune response triggered by Salmonella enterica requires intact LPS and is mediated by a MAPK signaling pathway. *Current biology : CB* **13**, 47-52

69. Bae, T., Banger, A. K., Wallace, A., Glass, E. M., Aslund, F., Schneewind, O., and Missiakas, D. M. (2004) Staphylococcus aureus virulence genes identified by bursa aurealis mutagenesis and nematode killing. *Proceedings of the National Academy of Sciences of the United States of America* **101**, 12312-12317

70. Broadway, M. M., Rogers, E. A., Chang, C., Huang, I. H., Dwivedi, P., Yildirim, S., Schmitt, M. P., Das, A., and Ton-That, H. (2013) Pilus gene pool variation and the virulence of Corynebacterium diphtheriae clinical isolates during infection of a nematode. *Journal of bacteriology* **195**, 3774-3783

71. Kim, D. H., Feinbaum, R., Alloing, G., Emerson, F. E., Garsin, D. A., Inoue, H., Tanaka-Hino, M., Hisamoto, N., Matsumoto, K., Tan, M. W., and Ausubel, F. M. (2002) A conserved p38 MAP kinase pathway in *Caenorhabditis elegans* innate immunity. *Science (New York, N.Y.)* **297**, 623-626

72. Garsin, D. A., Frank, K. L., Silanpaa, J., Ausubel, F. M., Hartke, A., Shankar, N., and Murray, B. E. (2014) Pathogenesis and Models of Enterococcal Infection. In *Enterococci: From Commensals to Leading Causes of Drug Resistant Infection* (Gilmore, M. S., Clewell, D. B., Ike, Y., and Shankar, N., eds), Boston

73. Medzhitov, R., and Janeway, C. A., Jr. (1998) An ancient system of host defense. *Current opinion in immunology* **10**, 12-15

74. Seong, S. Y., and Matzinger, P. (2004) Hydrophobicity: an ancient damage-associated molecular pattern that initiates innate immune responses. *Nature reviews. Immunology* **4**, 469-478

75. Matzinger, P. (2002) The danger model: a renewed sense of self. *Science (New York, N.Y.)* **296**, 301-305

76. Brandt, J. P., and Ringstad, N. (2015) Toll-like Receptor Signaling Promotes Development and Function of Sensory Neurons Required for a C. elegans Pathogen-Avoidance Behavior. *Current biology : CB* **25**, 2228-2237

77. Kurz, C. L., and Ewbank, J. J. (2003) Caenorhabditis elegans: an emerging genetic model for the study of innate immunity. *Nature reviews. Genetics* **4**, 380-390

78. Pukkila-Worley, R., Peleg, A. Y., Tampakakis, E., and Mylonakis, E. (2009) Candida albicans hyphal formation and virulence assessed using a Caenorhabditis elegans infection model. *Eukaryot Cell* **8**, 1750-1758

79. Yuen, G. J., and Ausubel, F. M. (2018) Both live and dead Enterococci activate Caenorhabditis elegans host defense via immune and stress pathways. *Virulence* **9**, 683-699

80. Miller, E. V., Grandi, L. N., Giannini, J. A., Robinson, J. D., and Powell, J. R. (2015) The Conserved G-Protein Coupled Receptor FSHR-1 Regulates Protective Host Responses to Infection and Oxidative Stress. *PloS one* **10**, e0137403

81. Pujol, N., Zugasti, O., Wong, D., Couillault, C., Kurz, C. L., Schulenburg, H., and Ewbank, J. J. (2008) Anti-fungal innate immunity in C. elegans is enhanced by evolutionary diversification of antimicrobial peptides. *PLoS pathogens* **4**, e1000105

82. Pujol, N., Cypowyj, S., Ziegler, K., Millet, A., Astrain, A., Goncharov, A., Jin, Y., Chisholm, A. D., and Ewbank, J. J. (2008) Distinct innate immune responses to infection and wounding in the C. elegans epidermis. *Current biology : CB* **18**, 481-489

83. Bischof, L. J., Kao, C. Y., Los, F. C., Gonzalez, M. R., Shen, Z., Briggs, S. P., van der Goot, F. G., and Aroian, R. V. (2008) Activation of the unfolded protein response is required for defenses against bacterial pore-forming toxin in vivo. *PLoS pathogens* **4**, e1000176

84. Zugasti, O., Bose, N., Squiban, B., Belougne, J., Kurz, C. L., Schroeder, F. C., Pujol, N., and Ewbank, J. J. (2014) Activation of a G protein-coupled receptor by its endogenous ligand triggers the innate immune response of Caenorhabditis elegans. *Nature immunology* **15**, 833-838

85. Posas, F., and Saito, H. (1997) Osmotic activation of the HOG MAPK pathway via Ste11p MAPKKK: scaffold role of Pbs2p MAPKK. *Science (New York, N.Y.)* **276**, 1702-1705

86. Huang, G., Shi, L. Z., and Chi, H. (2009) Regulation of JNK and p38 MAPK in the immune system: signal integration, propagation and termination. *Cytokine* **48**, 161-169

87. Keshet, Y., and Seger, R. (2010) The MAP kinase signaling cascades: a system of hundreds of components regulates a diverse array of physiological functions. *Methods in molecular biology (Clifton, N.J.)* **661**, 3-38

88. Troemel, E. R., Chu, S. W., Reinke, V., Lee, S. S., Ausubel, F. M., and Kim, D. H. (2006) p38 MAPK Regulates Expression of Immune Response Genes and Contributes to Longevity in C. elegans. *PLoS genetics* **in press**

89. Shivers, R. P., Pagano, D. J., Kooistra, T., Richardson, C. E., Reddy, K. C., Whitney, J. K., Kamanzi, O., Matsumoto, K., Hisamoto, N., and Kim, D. H. (2010) Phosphorylation of the conserved transcription factor ATF-7 by PMK-1 p38 MAPK regulates innate immunity in Caenorhabditis elegans. *PLoS genetics* **6**, e1000892

90. Kim, D. H., Liberati, N. T., Mizuno, T., Inoue, H., Hisamoto, N., Matsumoto, K., and Ausubel, F. M. (2004) Integration of Caenorhabditis elegans MAPK pathways mediating immunity and stress resistance by MEK-1 MAPK kinase and VHP-1 MAPK phosphatase. *Proceedings of the National Academy of Sciences of the United States of America* **101**, 10990-10994

91. Wolkow, C. A., Kimura, K. D., Lee, M. S., and Ruvkun, G. (2000) Regulation of *C. elegans* life-span by insulinlike signaling in the nervous system. *Science (New York, N.Y.)* **290**, 147-150

92. Antebi, A. (2007) Genetics of aging in Caenorhabditis elegans. *PLoS genetics* **3**, 1565-1571

93. Banyai, L., and Patthy, L. (1998) Amoebapore homologs of *Caenorhabditis elegans*. *Biochimica et biophysica acta* **1429**, 259-264

94. Kato, Y., Aizawa, T., Hoshino, H., Kawano, K., Nitta, K., and Zhang, H. (2002) abf-1 and abf-2, ASABF-type antimicrobial peptide genes in *Caenorhabditis elegans*. *Biochemical Journal* **361**, 221-230

95. Mallo, G. V., Kurz, C. L., Couillault, C., Pujol, N., Granjeaud, S., Kohara, Y., and Ewbank, J. J. (2002) Inducible Antibacterial Defense System in *C. elegans*. *Current biology : CB* **12**, 1209-1214

96. Simonsen, K. T., Gallego, S. F., Faergeman, N. J., and Kallipolitis, B. H. (2012) Strength in numbers: "Omics" studies of C. elegans innate immunity. *Virulence* **3**, 477-484

97. Miltsch, S. M., Seeberger, P. H., and Lepenies, B. (2014) The C-type lectin-like domain containing proteins Clec-39 and Clec-49 are crucial for Caenorhabditis elegans immunity against Serratia marcescens infection. *Developmental and comparative immunology* **45**, 67-73

98. Chavez, V., Mohri-Shiomi, A., Maadani, A., Vega, L. A., and Garsin, D. A. (2007) Oxidative stress enzymes are required for DAF-16-mediated immunity due to generation of reactive oxygen species by Caenorhabditis elegans. *Genetics* **176**, 1567-1577

99. Chavez, V., Mohri-Shiomi, A., and Garsin, D. A. (2009) Ce-Duox1/BLI-3 generates reactive oxygen species as a protective innate immune mechanism in Caenorhabditis elegans. *Infection and immunity* **77**, 4983-4989

100. van der Hoeven, R., Cruz, M. R., Chavez, V., and Garsin, D. A. (2015) Localization of the Dual Oxidase BLI-3 and Characterization of Its NADPH Oxidase Domain during Infection of Caenorhabditis elegans. *PloS one* **10**, e0124091

101. van der Hoeven, R., McCallum, K. C., Cruz, M. R., and Garsin, D. A. (2011) Ce-Duox1/BLI-3 Generated Reactive Oxygen Species Trigger Protective SKN-1 Activity via p38 MAPK Signaling during Infection in C. elegans. *PLoS pathogens* **7**, e1002453

102. Tiller, G. R., and Garsin, D. A. (2014) The SKPO-1 Peroxidase Functions in the Hypodermis to Protect Caenorhabditis elegans From Bacterial Infection. *Genetics* **197**, 515-526

103. Hoeven, R., McCallum, K. C., Cruz, M. R., and Garsin, D. A. (2011) Ce-Duox1/BLI-3 generated reactive oxygen species trigger protective SKN-1 activity via p38 MAPK signaling during infection in C. elegans. *PLoS pathogens* **7**, e1002453

104. Hope, I. A. (1999) *C. elegans A Practical Approach*, Oxford University Press, Oxford

105. Ward, J. D. (2015) Rapid and precise engineering of the Caenorhabditis elegans genome with lethal mutation co-conversion and inactivation of NHEJ repair. *Genetics* **199**, 363-377

106. Kage-Nakadai, E., Kobuna, H., Funatsu, O., Otori, M., Gengyo-Ando, K., Yoshina, S., Hori, S., and Mitani, S. (2012) Single/low-copy integration of transgenes in Caenorhabditis elegans using an ultraviolet trimethylpsoralen method. *BMC Biotechnol* **12**, 1

107. Powell, J. R., and Ausubel, F. M. (2008) Models of Caenorhabditis elegans infection by bacterial and fungal pathogens. *Methods in molecular biology (Clifton, N.J.)* **415**, 403-427

108. Cruz, M. R., Graham, C. E., Gagliano, B. C., Lorenz, M. C., and Garsin, D. A. (2013) Enterococcus faecalis inhibits hyphal morphogenesis and virulence of Candida albicans. *Infection and immunity* **81**, 189-200

109. Tiller, G. R., and Garsin, D. A. (2014) Of Worms and Men: HLH-30 and TFEB Regulate Tolerance to Infection. *Immunity* **40**, 857-858

110. Moribe, H., Yochem, J., Yamada, H., Tabuse, Y., Fujimoto, T., and Mekada, E. (2004) Tetraspanin protein (TSP-15) is required for epidermal integrity in Caenorhabditis elegans. *Journal of cell science* **117**, 5209-5220

111. Trapnell, C., Pachter, L., and Salzberg, S. L. (2009) TopHat: discovering splice junctions with RNA-Seq. *Bioinformatics* **25**, 1105-1111

112. Trapnell, C., Williams, B. A., Pertea, G., Mortazavi, A., Kwan, G., van Baren, M. J., Salzberg, S. L., Wold, B. J., and Pachter, L. (2010) Transcript assembly and quantification by RNA-Seq reveals unannotated transcripts and isoform switching during cell differentiation. *Nature biotechnology* **28**, 511-515

113. Huang, D. W., Sherman, B. T., Tan, Q., Collins, J. R., Alvord, W. G., Roayaei, J., Stephens, R., Baseler, M. W., Lane, H. C., and Lempicki, R. A. (2007) The DAVID Gene Functional Classification Tool: a novel biological module-centric algorithm to functionally analyze large gene lists. *Genome Biol* **8**, R183

114. Dunny, G. M., Brown, B. L., and Clewell, D. B. (1978) Induced cell aggregation and mating in *Streptococcus faecalis:* evidence for a bacterial sex pheromone. *Proceedings of the National Academy of Sciences of the United States of America* **75**, 3479-3483

115. Debroy, S., van der Hoeven, R., Singh, K. V., Gao, P., Harvey, B. R., Murray, B. E., and Garsin, D. A. (2012) Development of a genomic site for gene integration and expression in Enterococcus faecalis. *Journal of microbiological methods* **90**, 1-8

116. Rahme, L. G., Stevens, E. J., Wolfort, S. F., Shao, J., Tompkins, R. G., and Ausubel, F. M. (1995) Common virulence factors for bacterial pathogenicity in plants and animals [see comments]. *Science (New York, N.Y.)* **268**, 1899-1902

117. Kirienko, N. V., Kirienko, D. R., Larkins-Ford, J., Wahlby, C., Ruvkun, G., and Ausubel, F. M. (2013) Pseudomonas aeruginosa disrupts Caenorhabditis elegans iron homeostasis, causing a hypoxic response and death. *Cell Host Microbe* **13**, 406-416

118. Hayashi, T., Makino, K., Ohnishi, M., Kurokawa, K., Ishii, K., Yokoyama, K., Han, C. G., Ohtsubo, E., Nakayama, K., Murata, T., Tanaka, M., Tobe, T., Iida, T., Takami, H., Honda, T., Sasakawa, C., Ogasawara, N., Yasunaga, T., Kuhara, S., Shiba, T., Hattori, M., and Shinagawa, H. (2001) Complete genome sequence of enterohemorrhagic *Escherichia coli* O157:H7 and genomic comparison with a laboratory strain K-12. *DNA Res* **8**, 11-22

119. Makino, K., Ishii, K., Yasunaga, T., Hattori, M., Yokoyama, K., Yutsudo, C. H., Kubota, Y., Yamaichi, Y., Iida, T., Yamamoto, K., Honda, T., Han, C. G., Ohtsubo, E., Kasamatsu, M., Hayashi, T., Kuhara, S., and Shinagawa, H. (1998) Complete nucleotide sequences of 93-kb and 3.3-kb plasmids of an enterohemorrhagic Escherichia coli O157:H7 derived from Sakai outbreak. *DNA Res* **5**, 1-9

120. Fonzi, W. A., and Irwin, M. Y. (1993) Isogenic strain construction and gene mapping in Candida albicans. *Genetics* **134**, 717-728

121. Novick, R. P. (1963) ANALYSIS BY TRANSDUCTION OF MUTATIONS AFFECTING PENICILLINASE FORMATION IN STAPHYLOCOCCUS AUREUS. *J Gen Microbiol* **33**, 121-136

122. Hoiseth, S. K., and Stocker, B. A. (1981) Aromatic-dependent Salmonella typhimurium are non-virulent and effective as live vaccines. *Nature* **291**, 238-239

123. Cerdeno-Tarraga, A. M., Efstratiou, A., Dover, L. G., Holden, M. T., Pallen, M., Bentley, S. D., Besra, G. S., Churcher, C., James, K. D., De Zoysa, A., Chillingworth, T., Cronin, A., Dowd, L., Feltwell, T., Hamlin, N., Holroyd, S., Jagels, K., Moule, S., Quail, M. A., Rabbinowitsch, E., Rutherford, K. M., Thomson, N. R., Unwin, L., Whitehead, S., Barrell, B. G., and Parkhill, J. (2003) The complete genome sequence and analysis of Corynebacterium diphtheriae NCTC13129. *Nucleic acids research* **31**, 6516-6523

124. Melo, J. A., and Ruvkun, G. (2012) Inactivation of conserved C. elegans genes engages pathogen- and xenobiotic-associated defenses. *Cell* **149**, 452-466

125. Rada, B., Lekstrom, K., Damian, S., Dupuy, C., and Leto, T. L. (2008) The Pseudomonas toxin pyocyanin inhibits the dual oxidase-based antimicrobial system as it imposes oxidative stress on airway epithelial cells. *Journal of immunology (Baltimore, Md. : 1950)* **181**, 4883-4893

126. Klebanoff, S. J. (2005) Myeloperoxidase: friend and foe. *Journal of leukocyte biology* **77**, 598-625

127. Forteza, R., Salathe, M., Miot, F., Forteza, R., and Conner, G. E. (2005) Regulated hydrogen peroxide production by Duox in human airway epithelial cells. *American journal of respiratory cell and molecular biology* **32**, 462-469

128. Torres, M. A., Jones, J. D., and Dangl, J. L. (2006) Reactive oxygen species signaling in response to pathogens. *Plant physiology* **141**, 373-378

129. McCallum, K. C., and Garsin, D. A. (2016) The Role of Reactive Oxygen Species in Modulating the Caenorhabditis elegans Immune Response. *PLoS pathogens* **12**, e1005923

130. Fraser, A. G., Kamath, R. S., Zipperlen, P., Martinez-Campos, M., Sohrmann, M., and Ahringer, J. (2000) Functional genomic analysis of *C. elegans* chromosome I by systematic RNA interference. *Nature* **408**, 325-330

131. Kamath, R. S., Fraser, A. G., Dong, Y., Poulin, G., Durbin, R., Gotta, M., Kanapin, A., Le Bot, N., Moreno, S., Sohrmann, M., Welchman, D. P., Zipperlen, P., and Ahringer, J. (2003) Systematic functional analysis of the *Caenorhabditis elegans* genome using RNAi. *Nature* **421**, 231-237

132. Garigan, D., Hsu, A. L., Fraser, A. G., Kamath, R. S., Ahringer, J., and Kenyon, C. (2002) Genetic analysis of tissue aging in *Caenorhabditis elegans*: a role for heat-shock factor and bacterial proliferation. *Genetics* **161**, 1101-1112

133. Mello, C. C., Kramer, J. M., Stinchcomb, D., and Ambros, V. (1991) Efficient gene transfer in C.elegans: extrachromosomal maintenance and integration of transforming sequences. *The EMBO journal* **10**, 3959-3970

134. Herndon, L. A., Crocker, C., Hall, D. H., and Altun, Z. (2012) Pharynx Atlas. *Wormatlas*

135. Albertson, D. G., and Thomson, J. N. (1976) The pharynx of Caenorhabditis elegans. *Philosophical transactions of the Royal Society of London. Series B, Biological sciences* **275**, 299-325

136. Hall, D. H., and Hedgecock, E. M. (1991) Kinesin-related gene unc-104 is required for axonal transport of synaptic vesicles in C. elegans. *Cell* **65**, 837-847

137. Kage-Nakadai, E., Kobuna, H., Kimura, M., Gengyo-Ando, K., Inoue, T., Arai, H., and Mitani, S. (2010) Two very long chain fatty acid acyl-CoA synthetase genes, acs-20 and acs-22, have roles in the cuticle surface barrier in Caenorhabditis elegans. *PloS one* **5**, e8857

138. Ortiz de Montellano, P. R. (2008) Mechanism and role of covalent heme binding in the CYP4 family of P450 enzymes and the mammalian peroxidases. *Drug Metab Rev* **40**, 405-426

139. Meitzler, J. L., and Ortiz de Montellano, P. R. (2009) Caenorhabditis elegans and human dual oxidase 1 (DUOX1) "peroxidase" domains: insights into heme

binding and catalytic activity. *The Journal of biological chemistry* **284**, 18634-18643

140. Meitzler, J. L., and Ortiz de Montellano, P. R. (2011) Structural stability and heme binding potential of the truncated human dual oxidase 2 (DUOX2) peroxidase domain. *Archives of biochemistry and biophysics* **512**, 197-203

141. Zamocky, M., Jakopitsch, C., Furtmuller, P. G., Dunand, C., and Obinger, C. (2008) The peroxidase-cyclooxygenase superfamily: Reconstructed evolution of critical enzymes of the innate immune system. *Proteins* **72**, 589-605

142. Stampler, J., Bellei, M., Soudi, M., Gruber, C., Battistuzzi, G., Furtmuller, P. G., and Obinger, C. (2011) Manipulating the proximal triad His-Asn-Arg in human myeloperoxidase. *Archives of biochemistry and biophysics* **516**, 21-28

143. Hunt-Newbury, R., Viveiros, R., Johnsen, R., Mah, A., Anastas, D., Fang, L., Halfnight, E., Lee, D., Lin, J., Lorch, A., McKay, S., Okada, H. M., Pan, J., Schulz, A. K., Tu, D., Wong, K., Zhao, Z., Alexeyenko, A., Burglin, T., Sonnhammer, E., Schnabel, R., Jones, S. J., Marra, M. A., Baillie, D. L., and Moerman, D. G. (2007) High-throughput in vivo analysis of gene expression in Caenorhabditis elegans. *PLoS Biol* **5**, e237

144. McKay, S. J., Johnsen, R., Khattra, J., Asano, J., Baillie, D. L., Chan, S., Dube, N., Fang, L., Goszczynski, B., Ha, E., Halfnight, E., Hollebakken, R., Huang, P., Hung, K., Jensen, V., Jones, S. J., Kai, H., Li, D., Mah, A., Marra, M., McGhee, J., Newbury, R., Pouzyrev, A., Riddle, D. L., Sonnhammer, E., Tian, H., Tu, D., Tyson, J. R., Vatcher, G., Warner, A., Wong, K., Zhao, Z., and Moerman, D. G. (2003) Gene expression profiling of cells, tissues, and developmental stages of the nematode C. elegans. *Cold Spring Harb Symp Quant Biol* **68**, 159-169

145. Silhavy, T. J., Kahne, D., and Walker, S. (2010) The Bacterial Cell Envelope. *Cold Spring Harb Perspect Biol* **2**

146. Celniker, S. E., Dillon, L. A., Gerstein, M. B., Gunsalus, K. C., Henikoff, S., Karpen, G. H., Kellis, M., Lai, E. C., Lieb, J. D., MacAlpine, D. M., Micklem, G., Piano, F., Snyder, M., Stein, L., White, K. P., and Waterston, R. H. (2009) Unlocking the secrets of the genome. *Nature* **459**, 927-930

147. Simmer, F., Moorman, C., van der Linden, A. M., Kuijk, E., van den Berghe, P. V., Kamath, R. S., Fraser, A. G., Ahringer, J., and Plasterk, R. H. (2003) Genome-wide RNAi of C. elegans using the hypersensitive rrf-3 strain reveals novel gene functions. *PLoS Biol* **1**, E12

148. Dodd, W., Tang, L., Lone, J. C., Wimberly, K., Wu, C. W., Consalvo, C., Wright, J. E., Pujol, N., and Choe, K. P. (2018) A Damage Sensor Associated with the

Cuticle Coordinates Three Core Environmental Stress Responses in Caenorhabditis elegans. *Genetics* **208**, 1467-1482

149. O'Rourke, D., Baban, D., Demidova, M., Mott, R., and Hodgkin, J. (2006) Genomic clusters, putative pathogen recognition molecules, and antimicrobial genes are induced by infection of C. elegans with M. nematophilum. *Genome Res* **16**, 1005-1016

150. Schulenburg, H., and Boehnisch, C. (2008) Diversification and adaptive sequence evolution of Caenorhabditis lysozymes (Nematoda: Rhabditidae). *BMC Evol Biol* **8**, 114

151. Kramer, J. M., Johnson, J. J., Edgar, R. S., Basch, C., and Roberts, S. (1988) The sqt-1 gene of C. elegans encodes a collagen critical for organismal morphogenesis. *Cell* **55**, 555-565

152. von Mende, N., Bird, D. M., Albert, P. S., and Riddle, D. L. (1988) dpy-13: a nematode collagen gene that affects body shape. *Cell* **55**, 567-576

153. Johnstone, I. L., Shafi, Y., and Barry, J. D. (1992) Molecular analysis of mutations in the Caenorhabditis elegans collagen gene dpy-7. *The EMBO journal* **11**, 3857-3863

154. Kim, D. H., and Ewbank, J. J. (2018) Signaling in the innate immune response. *WormBook : the online review of C. elegans biology* **2018**, 1-35

155. Rouger, V., Bordet, G., Couillault, C., Monneret, S., Mailfert, S., Ewbank, J. J., Pujol, N., and Marguet, D. (2014) Independent synchronized control and visualization of interactions between living cells and organisms. *Biophysical journal* **106**, 2096-2104

156. Yook, K., and Hodgkin, J. (2007) Mos1 mutagenesis reveals a diversity of mechanisms affecting response of Caenorhabditis elegans to the bacterial pathogen Microbacterium nematophilum. *Genetics* **175**, 681-697

157. Partridge, F. A., Tearle, A. W., Gravato-Nobre, M. J., Schafer, W. R., and Hodgkin, J. (2008) The C. elegans glycosyltransferase BUS-8 has two distinct and essential roles in epidermal morphogenesis. *Developmental biology* **317**, 549-559

158. Palaima, E., Leymarie, N., Stroud, D., Mizanur, R. M., Hodgkin, J., Gravato-Nobre, M. J., Costello, C. E., and Cipollo, J. F. (2010) The Caenorhabditis elegans bus-2 mutant reveals a new class of O-glycans affecting bacterial resistance. *The Journal of biological chemistry* **285**, 17662-17672

159. Gravato-Nobre, M. J., Stroud, D., O'Rourke, D., Darby, C., and Hodgkin, J. (2011) Glycosylation genes expressed in seam cells determine complex surface properties and bacterial adhesion to the cuticle of Caenorhabditis elegans. *Genetics* **187**, 141-155

160. Cipollo, J. F., Awad, A. M., Costello, C. E., and Hirschberg, C. B. (2004) srf-3, a mutant of Caenorhabditis elegans, resistant to bacterial infection and to biofilm binding, is deficient in glycoconjugates. *The Journal of biological chemistry* **279**, 52893-52903

161. Drace, K., McLaughlin, S., and Darby, C. (2009) Caenorhabditis elegans BAH-1 is a DUF23 protein expressed in seam cells and required for microbial biofilm binding to the cuticle. *PloS one* **4**, e6741

162. Labrousse, A., Chauvet, S., Couillault, C., Kurz, C. L., and Ewbank, J. J. (2000) *Caenorhabditis elegans* is a model host for *Salmonella typhimurium*. *Current Biology* **10**, 1543-1545

163. Stampler, J., Bellei, M., Soudi, M., Gruber, C., Battistuzzi, G., Furtmüller, P. G., and Obinger, C. (2011) Manipulating the proximal triad His–Asn–Arg in human myeloperoxidase. *Archives of biochemistry and biophysics* **516**, 21-28

164. Zhang, Y., Li, W., Li, L., Li, Y., Fu, R., Zhu, Y., Li, J., Zhou, Y., Xiong, S., and Zhang, H. (2015) Structural damage in the C. elegans epidermis causes release of STA-2 and induction of an innate immune response. *Immunity* **42**, 309-320

165. Hiatt, S. M., Shyu, Y. J., Duren, H. M., and Hu, C. D. (2008) Bimolecular fluorescence complementation (BiFC) analysis of protein interactions in Caenorhabditis elegans. *Methods* **45**, 185-191

166. Meitzler, J. L., Hinde, S., Banfi, B., Nauseef, W. M., and Ortiz de Montellano, P. R. (2013) Conserved cysteine residues provide a protein-protein interaction surface in dual oxidase (DUOX) proteins. *The Journal of biological chemistry* **288**, 7147-7157

Vita

Yi Liu was born in Changsha, Hunan, China, the daughter of Tiehui Liu and Junqiang Chen. After graduated from the High School Attached to Hunan Normal University, Yi was

admitted to the Honors Program of Biological Science at Huazhong Agricultural University in Wuhan, China. She worked as an undergraduate researcher at the National Key Laboratory of Microbiology during her junior and senior years and received the degree of Bachelor of Science in June 2008. She then went to Auburn University, Alabama and obtained her Master of Science in 2011. After that, she joined UTHealth at Houston first as a research scientist then as a graduate student in the Microbiology and Molecular Genetics program and joined Dr. Danielle Garsin's laboratory in August 2015.

Permanent address:

3225 Seneca Landing Ln

Pearland, Texas, 77584